

*J. Bruce Gemmell*

CONFIDENTIAL

---

**Studies of VHMS-related alteration:  
geochemical and mineralogical vectors  
to ore**

---

**Field Guide  
Mount Windsor Volcanics, Queensland**

presented by

**Mark Doyle, Holger Paulick, Wally Herrmann,  
Thomas Monecke and Bruce Gemmell**

**CODES-SRC  
University of Tasmania  
May, 1998**

*J. Bruce Gemmell*

CONFIDENTIAL

---

**Studies of VHMS-related alteration:  
geochemical and mineralogical vectors  
to ore**

---

**Field Guide  
Mount Windsor Volcanics, Queensland**

presented by

**Mark Doyle, Holger Paulick, Wally Herrmann,  
Thomas Monecke and Bruce Gemmell**

**CODES-SRC  
University of Tasmania  
May, 1998**

---

## Acknowledgments

---

This research has been supported by the following companies and organisations:

Aberfoyle Resources Limited  
Copper Mines of Tasmania  
Denehurst Limited  
Mineral Resources Tasmania  
Normandy Exploration  
Pasminco Exploration  
Queensland Metals Corporation Limited  
RGC Exploration  
Rio Tinto Exploration

We are grateful to the industry sponsors and AMIRA for their support and contributions to discussions on different aspects of the research. In particular, we thank Aberfoyle Resources Limited and RGC Exploration for allowing studies to be completed at Liontown, Highway-Reward, Snake Oil, Thalanga and Waterloo. Research at Thalanga, Highway-Reward and Waterloo formed part of ARC/Industry funded Ph.D research by Holger Paulick, Mark Doyle and Thomas Monecke. These authors thank Prof. Ross Large, Dr Jocelyn McPhie, Dr Joe Stolz and Dr Bruce Gemmell for their advice and guidance over the duration of the project. Thanks to Ed Dronseika (Aberfoyle), Mike Cawood, Haydon Hadlow, Colin Kendall and Craig Miller (RGC) for assistance during the studies.

We are grateful to AMIRA, Leanne Carr, Craig Miller, Jason Grace and Geoff Phillips for help in organising the field excursion. The production skills of June Pongratz are gratefully acknowledged. Thanks also to Nilar Hlaing and Mike Blake for printing and compiling the guide.

## Table of Contents

Acknowledgments .....	i
Table of contents .....	ii

### PART 1: INTRODUCTION — Mark Doyle

Regional geological setting .....	1
The Seventy Mile Range Group .....	1
Puddler Creek Formation.....	5
Mount Windsor Formation.....	5
Trooper Creek Formation.....	6
Rollston Range Formation.....	7
Age relationships.....	7
Metamorphic grade.....	10
Regional deformation and structure.....	10
Tectonic setting of the Mount Windsor Subprovince .....	10
VHMS deposits in the Seventy Mile Range Group .....	11
Summary .....	11

### PART 2: TOPICS TO BE ADDRESSED — Mark Doyle

Interpreting timing relationships of alteration in volcanic rocks.....	14
Textural evolution of volcanic rocks.....	14
Textural heterogeneity of lavas and intrusions .....	17
Effect of lithofacies on mineralisation and alteration processes.....	19
Exhalation and sub-seafloor replacement in mineral deposition .....	19
Summary of problems and topics.....	24

### PART 3: FIELD GUIDE

#### DAY 1: HYDROTHERMAL ALTERATION OF COHERENT LAVAS AND INTRUSIONS IN THE HOST SUCCESSION OF THE THALANGA VHMS DEPOSIT — Holger Paulick, Wally Herrmann

Stop 1. Thalanga Mine.....	27
Stop 2. Ironstones in the Thalanga West 45 area.....	55

**DAY 2: IRONSTONES; MASSIVE SULFIDE MINERALISATION HOSTED BY LAVAS AND  
INTRUSIONS AT HIGHWAY-REWARD — Mark Doyle, Jason Grace**

Stop 3. Trooper Creek prospect ironstone lenses.....	57
Stop 4. A shoaling volcano-sedimentary succession .....	57
Stop 4.1. Lithofacies associations.....	57
Stop 4.2. Ironstone lenses and associated alteration .....	61
Stop 5. Ironstone lenses and associated alteration .....	61
Stop 5. Regional hematite alteration .....	64
Stop 6. Highway-Reward Mine .....	64
Stop 7. Highway-Reward VHMS deposit .....	65
Stop 7.1. DDH REM 560 and REW 805: Lavas and intrusions.....	65
Stop 7.2. DDH REW 805: The enclosing facies.....	67
Stop 7.3. A syn-sedimentary intrusion-dominated volcanic centre.....	71
Stop 7.4. DDH REM 560: Massive pyrite-chalcopyrite pipes .....	73
Stop 7.5. DDH REM 116: Replacement of peperite.....	74
Stop 7.6. DDH HMO 60: Assessing a sub-seafloor vs. seafloor origin .....	74
Stop 7.7. DDH HMO 89: Stratabound pyrite-sphalerite-barite.....	74
Stop 7.8. DDH HMO 47: Sphalerite-pyrite mineralisation .....	75
Stop 7.9. DDH REM 154: Footwall quartz-sericite-pyrite zone .....	75
Stop 7.10. DDH REM 154 and 116: Chlorite-sericite±quartz zone.....	75
Stop 7.11. DDH HMO 41: Chlorite±anhydrite zone.....	75
Stop 7.12. DDH REW 140: Hanging wall quartz-sericite alteration.....	75
Stop 7.13. DDH REW 805: Regional diagenetic alteration.....	76
Stop 7.14. Core display: modification of primary volcanic textures.....	76

**DAY 3 MASSIVE SULFIDE MINERALISATION HOSTED BY PUMICE BRECCIA UNITS  
— Mark Doyle, Craig Miller, Thomas Monecke, Bruce Gemmell**

Stop 8. Lione town mine site.....	81
Stop 9. Lione town core store .....	81
Stop 9.1. DDH LDD 128: Stratigraphy/lithofacies.....	81
Stop 9.2. DDH LLD 128: Stratiform lodes.....	81
Stop 9.3. DDH LLD 114: Carbonate.....	86
Stop 9.4. DDH LLD 101 and 114: Carrington lode.....	86
Stop 9.5. DDH LLD 114: chlorite-sericite alteration .....	86
Stop 9.6. DDH LLD 114: nodular quartz>sericite-chlorite alteration.....	86
Stop 9.7. DDH LLD 128: patchy sericite-chlorite>quartz alteration.....	87
Stop 9.8. DDH LLD 128: muscovite geochemistry.....	87

---

Stop 9.9. DDH CGD 001: Cougartown ("distal" alteration types).....	87
Stop 10. RGC Exploration core yard, Charters Towers .....	89
Stop 10. Orion prospect.....	89
Stop 10.1. DDH ORDD 1: Regional diagenetic alteration.....	89
Stop 10.2. Snake Oil prospect, DDH SODD 1 and 2 .....	89
Stop 10.3. Waterloo prospect, DDH WTDD 5, 9A, 16, 22, 27 .....	81
REFERENCES.....	113

## PART 1: INTRODUCTION — Mark Doyle

### Regional geological setting

The Mount Windsor Subprovince (Henderson, 1980) in northern Queensland, Australia is part of the Tasman Fold Belt. The Tasman Fold Belt was an active orogenic region from Cambrian to Cretaceous time. In Queensland, the Tasman Fold Belt comprises the Hodgkinson-Broken River Fold Belt in the north, the Thomson Fold Belt in the central part, and the New England Fold Belt to the south (Fig. 1). Murray (1986, 1990) and Wellman (1995) consider the Mount Windsor Subprovince to be part of the Thomson Fold Belt.

The Mount Windsor Subprovince comprises the remnants of a formerly extensive Cambrian to Early Ordovician volcano-sedimentary terrain. The subprovince forms an approximate east-west belt extending for 165 km from the Leichhardt Range in the east, to near Pentland in the west (Fig. 2). The subprovince has been extensively intruded along its northern margin by the Ordovician to Permian Ravenswood Batholith and Lolworth Igneous Complex, and is overlain by the Carboniferous Drummond Basin succession to the south (Henderson, 1980, 1986). A discontinuous cover of Tertiary alluvial and ferricrete deposits obscures much of the subprovince.

Together the Mount Windsor Subprovince, Lolworth-Ravenswood Subprovince and the Burdekin Subprovince form the Charters Towers Province (Henderson, 1980, 1986). The Charters Towers Province is separated from the Ordovician Broken River Province to the north by the Clarke River Fault (Fig. 1; Murray, 1986). The Lolworth-Ravenswood Subprovince occupies a central position in the Charters Towers Province and includes the Running River and Argentine Metamorphics to the north, the Cape River Beds in the west of the province, and the Charters Towers Metamorphics in its central segment. Devonian to Early Carboniferous marine and continentally-derived sedimentary successions of the Burdekin Subprovince on-lap the northern margin of the Lolworth-Ravenswood Subprovince (Henderson, 1980).

The Balcooma Metamorphics, 250 km north of the Mount Windsor Subprovince, comprise volcano-sedimentary units of similar age to the Mount Windsor Subprovince and also host massive sulfide mineralisation (Fig. 1; Huston et al., 1992). The two belts have been correlated although the former is metamorphosed to a higher (amphibolite) grade (Henderson, 1986; Withnall et al., 1991). Volcano-sedimentary sequences at the southern end of the Tasman Fold Belt in western Tasmania (Mount Read Volcanics) and in the western part of the Lachlan Fold Belt also show similarities with the Mount Windsor Subprovince and host many world class massive sulfide deposits (Henderson, 1986; Withnall et al., 1991).

### The Seventy Mile Range Group

The volcanic and sedimentary rocks of the Mount Windsor Subprovince are assigned to the Seventy Mile Range Group (Henderson, 1986). As presently understood, the Seventy Mile Range Group can be subdivided into four conformable formations: the Puddler Creek Formation, Mount Windsor Volcanics, the Trooper Creek Formation and the Rollston Range Formation (Figs. 2–3; Henderson, 1986; Berry et al., 1992). Type sections and fossil localities for each of the formations were presented by Henderson (1983, 1986) and Berry et al. (1992) reassessed the distribution and character of the component lithofacies. The word 'Mount Windsor Volcanics' has often been used as an informal name for the Seventy Mile Range Group (e.g. Stolz, 1995), and is now unworkable as a formation name. In order to avoid confusion, the 'Mount Windsor Volcanics' of Henderson (1986) was renamed the Mount Windsor Formation by Doyle (1997b).

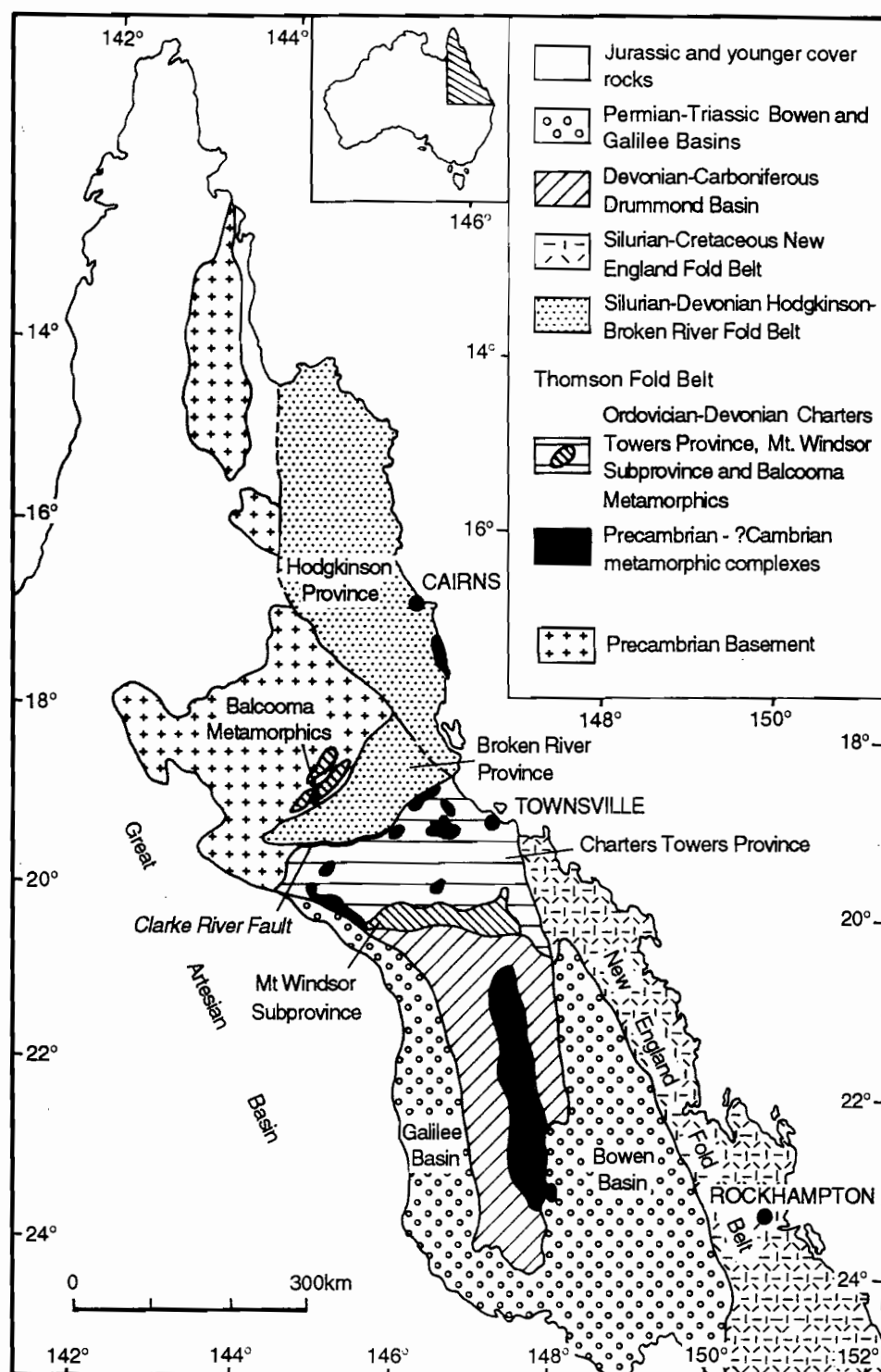


Figure 1. Simplified geological map of northern Queensland showing the distribution of elements in the Tasman Fold Belt and major Cambrian-Devonian structural blocks and provinces. Based on Murray (1990), Stolz (1995) and Withnall et al., (1987).



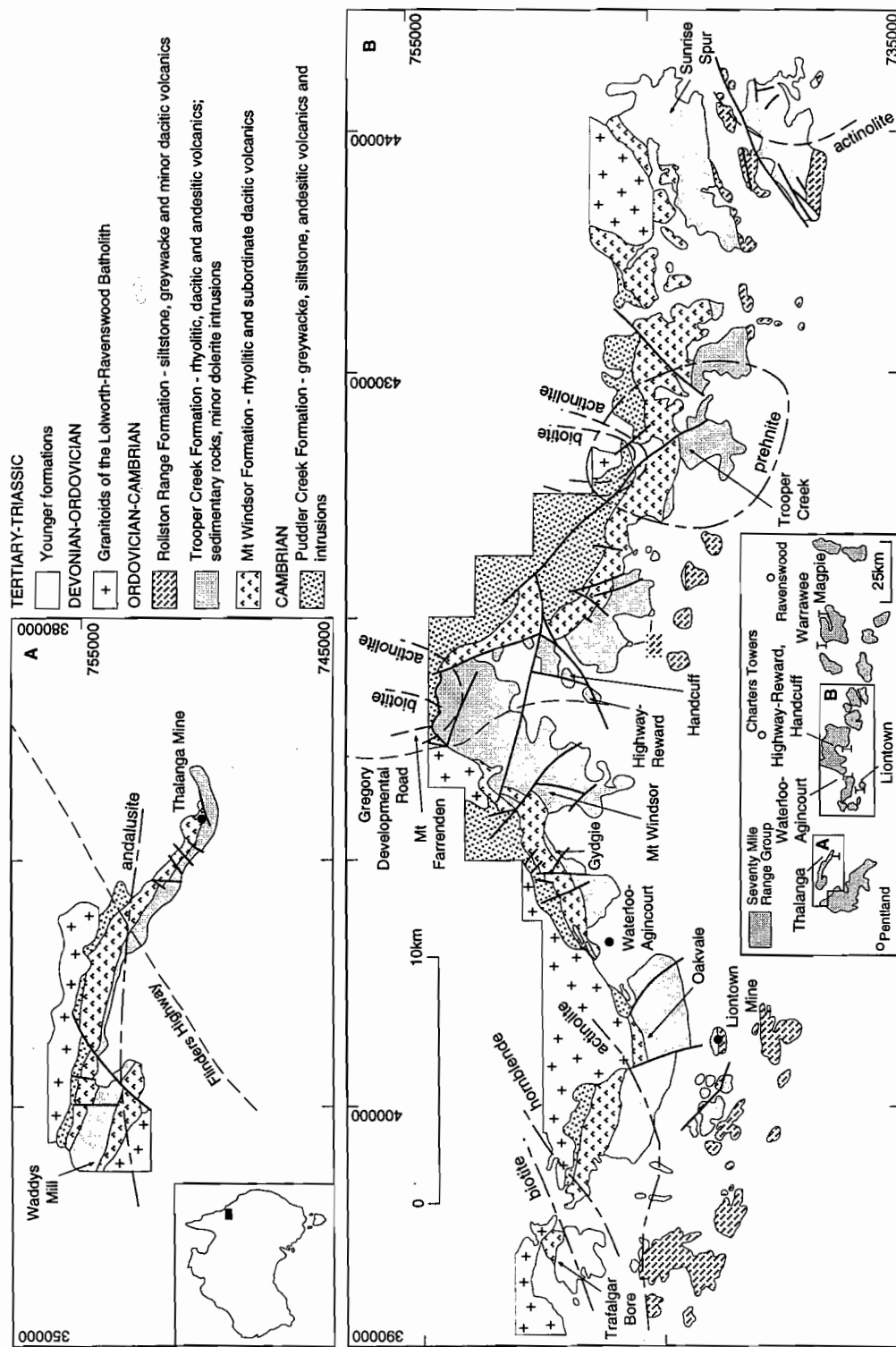


Figure 2: Simplified geological map of the Seventy Mile Range Group between Waddys Mill and Sunrise Spur. The distribution of major geological formations, significant mineral deposits, and locations discussed in the text are illustrated. Modified after Berry et al. (1992).

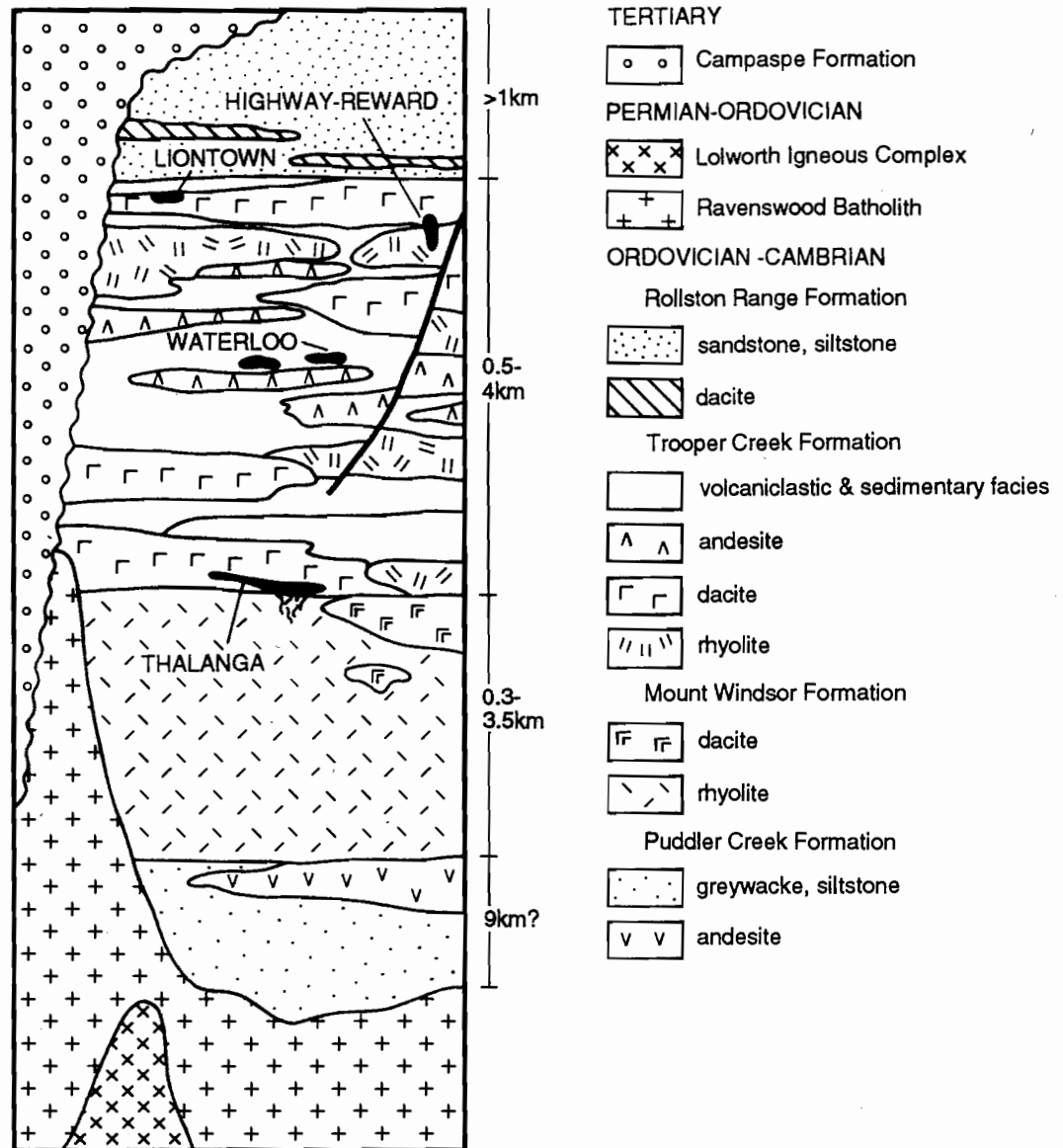


Figure 3. Generalised stratigraphic column for the Seventy Mile Range Group between Waddys Mill and Sunrise Spur. The location of the main massive sulfide deposits is also shown. Modified after Large (1991).

The Seventy Mile Range Group comprises a relatively thick volcano-sedimentary succession (possibly in excess of 12 km; Henderson, 1986). The true thickness of the succession is poorly constrained, due to structural complexities in the Puddler Creek Formation. However, as noted by Stolz (1995), such a thickness may not be unrealistic as more than 10 km of sediments and volcanics have accumulated in the northern Okinawa Trough since the Miocene (Letouzey and Kimura, 1985).

#### Puddler Creek Formation

The oldest exposed part of the Seventy Mile Range Group is the Puddler Creek Formation, a mixed volcanic and sedimentary succession dominated by poorly sorted, quartz- and lithic-rich sandstone, greywacke and siltstone (Fig. 2; Henderson, 1986; Berry et al., 1992; Doyle, 1997b). Sandstone beds are generally massive, locally graded, and range from 5 cm to 2.5 m thick (Henderson, 1986). The largely continentally-derived sedimentary component includes quartz, feldspar, phyllite grains, polycrystalline quartz and detrital mica (Henderson, 1986; Doyle, 1997b). Andesitic lavas frequently dominate the upper 500 m of the formation (Berry et al., 1992). The lavas record intermittent volcanism prior to eruption of the overlying Mount Windsor Formation (Stolz, 1991; Berry et al., 1992). The lithofacies associations are consistent with a submarine depositional setting, most probably below storm wave base.

Mafic dykes and sills become abundant towards the top of the Puddler Creek Formation but do not intrude younger formations. The intrusions are dolerite (Henderson, 1986) and microdiorite (Hartley et al., 1989) and have compositions similar to those of mafic lavas at the top of the formation (Berry et al., 1992). Quartz- and quartz-feldspar-phyric rhyolitic dykes and sills cut across the mafic intrusions (Henderson, 1986) and are interpreted to be feeders to volcanic units in the overlying Mount Windsor Formation and Trooper Creek Formation (Berry et al., 1992). Hartley et al. (1989) considered the mafic and silicic dykes to be similar to dykes that intrude the Charters Towers Metamorphics in the Lolworth-Ravenswood Subprovince.

The base of the formation is not exposed due to widespread granite intrusions of the Ravenswood Batholith. The maximum apparent thickness of the succession is 9 km, assuming no structural repetition (Henderson, 1986; Berry et al., 1992). Contacts between the Puddler Creek Formation and the Mount Windsor Formation are sharp and conformable (Berry et al., 1992) or faulted (Doyle, 1997b).

#### Mount Windsor Formation

The Mount Windsor Formation comprises a thick sequence of rhyolitic volcanic rocks with minor dacite and rare andesite (Henderson, 1986; Berry et al., 1992; Doyle, 1997b). Sedimentary rocks are absent except at the base of the formation. Massive coherent and flow-banded rhyolite and autoclastic breccia form lavas and domes which are mostly 100-150 m thick (Berry et al., 1992). The feeder dykes for the extrusive units have not been identified. However, mapping of the unit boundaries suggests that many lavas probably extended less than a few kilometres from their vents (Doyle, 1997b). The paucity of intervening volcano-sedimentary units implies that the lavas were erupted rapidly from adjacent vents or from fissures, and probably constructed significant topography that strongly influenced sedimentation patterns.

The lavas and intrusions yield little unambiguous information about the depositional setting. Hyaloclastite associated with the lavas provides evidence for emplacement in a subaqueous environment. At Mount Windsor, the Mount Windsor Formation includes resedimented volcanoclastic units interpreted to have been deposited from sediment gravity flows in a submarine environment (Berry et al., 1992). At Thalanga (Fig. 2), VHMS-style mineralisation is partly hosted by volcanoclastic rocks of the Mount Windsor

Formation, suggesting that this part of the Mount Windsor Formation accumulated below storm wave base in a submarine setting (Hill, 1996).

The Mount Windsor Formation forms the core to the Seventy Mile Range and is exposed almost continuously between Sunrise Spur in the east and Waddys Mill in the west. The rhyolitic succession is absent in the area north of Highway-Reward where the Puddler Creek Formation is conformably overlain by the Trooper Creek Formation. The Mount Windsor Formation has a maximum thickness of around 3500 m at Sunrise Spur (Fig. 2) in the eastern part of the subprovince, decreases in thickness to around 1000 m west of Highway-Reward, and is 300-400 m thick at Waddys Mill in the west (Henderson, 1986; Berry et al., 1992; Doyle, 1997b). Henderson (1986) argued that thickening of the Mount Windsor Formation between Highway-Reward and Sunrise Spur indicated an eastern source for the formation. As the lavas and intrusions are proximal to vent, it is more likely that the rhyolitic and dacitic units were erupted from separate intrabasinal vents distributed along the length of the basin, and that volcanic centres in the east were more productive (Doyle, 1997a).

The Mount Windsor Formation and the younger Trooper Creek Formation are often conformable. The contact was defined by Henderson (1986) as the first appearance of dacite or andesite and associated volcanoclastic and sedimentary facies. However, dacite is present in the Mount Windsor Formation complicating the interpretation.

Doyle (1997a) demonstrated that mass-flow deposits in the basal Trooper Creek Formation (Kitchenrock Hill Member) contain rounded clasts of rhyolite, rhyodacite and dacite, which are petrographically and geochemically similar to the Mount Windsor Formation. The clasts were reworked in a high-energy environment (above storm wave base) prior to redeposition, suggesting that the source areas were subaerial to shallow marine. These clasts indicate that parts of the Mount Windsor Formation were subject to significant erosion up until the initial stages of Trooper Creek Formation volcanism. It is likely that while some parts of the contact were being subject to erosion, others were sites of deposition.

### Trooper Creek Formation

The Trooper Creek Formation mainly comprises basaltic, andesitic, dacitic and rhyolitic lavas, intrusions and volcanoclastic rocks, laminated siltstone and mudstone that locally contain graptolite fossils, calcareous metasediment and thin ironstone lenses (Henderson, 1983, 1986; Berry et al., 1992; Doyle, 1997b). The bedforms, graptolites, local intercalated pillow lavas, and peperite and hyaloclastite associated with many lavas and intrusions, collectively suggest a submarine setting (Berry et al., 1992; Doyle, 1994). The Thalanga and Highway-Reward massive sulfide deposits and several other prospects are thought to be part of the Trooper Creek Formation. Andesitic dykes and sills in the Trooper Creek Formation and underlying Mount Windsor Formation may represent feeders for units higher in the succession (Berry et al., 1992).

The recognition of compositional and lithological variations within the Trooper Creek Formation, which are mappable over at least 15 km strike length, prompted a subdivision of the formation into two members, the Kitchenrock Hill Member and the overlying Highway Member (Doyle, 1997a). The Kitchenrock Hill Member comprises volcanoclastic sandstone and breccia units that are typically polymictic and include sub-rounded to well-rounded clasts. In contrast, the Highway Member is dominated by syn-eruptive volcanic breccia to sandstone units, syn-sedimentary intrusions, lavas, and volcanic siltstone. The Kitchenrock Hill Member forms a discontinuous stratigraphic interval overlying rhyolitic and dacitic lavas and intrusions of the Mount Windsor Formation and is well represented in the Kitchenrock Hill area. Variations in thickness and bedding orientation within the Kitchenrock Hill Member probably reflect palaeotopography on the depositional surface of the underlying Mount Windsor

Formation that may have been generated by the lavas and/or syn-depositional growth faults. The Highway Member conformably overlies the Kitchenrock Hill Member. The Highway Member is characterised by rapid lithofacies variations and contains varying proportions of lavas, intrusions, volcanoclastic facies and sedimentary facies. Summary descriptions and interpretations of the twenty principal volcanic and sedimentary facies are given in Table 1. Coherent lithofacies and clasts in the volcanoclastic lithofacies are mostly rhyolitic, dacitic or andesitic in composition but rare basaltic-andesitic examples are present.

The Trooper Creek Formation ranges from 4000 m at Mount Windsor in the central part of the subprovince, to a minimum of 500 m along the Thalanga Range to the west. Abundant lavas, syn-sedimentary intrusions and autoclastic breccia, and thickening of the volcanic sequence at Trafalgar Bore and between Mount Windsor and Highway-Reward suggest proximity to major volcanic centres in these parts of the Trooper Creek Formation (Stolz, 1991; Berry et al., 1992; Doyle, 1994, 1997b). Apparent thickening of the formation in the Sunrise Spur area (Henderson, 1986) and south of Mount Windsor is due to structural repetition (Berry et al., 1992).

The Trooper Creek Formation is conformably and gradationally overlain by the Rollston Range Formation. The transition was defined by Henderson (1986) as the uppermost substantial volcanoclastic unit dominated by pyroclasts.

#### Rollston Range Formation

The Rollston Range Formation is the youngest exposed part of the Mount Windsor Subprovince (Fig. 2) and is composed of a thick (at least 1 km) sequence of sandstone and siltstone units and rare dacitic lavas (Henderson, 1986; Berry et al., 1992) and volcanoclastic units (Doyle, 1997b). Sandstone and siltstone beds are dominated by volcanic components but also contain basement-derived muscovite and phyllite grains. Graptolites and trilobites are known from several locations within the formation and suggest that the base of the formation is older in the west than in the east (Henderson, 1983, 1986). The bedforms and fossils suggest a deep marine depositional environment (Henderson, 1986). The top of the Rollston Range Formation is not exposed, being covered by Tertiary sedimentary formations.

#### Age relationships

An early Ordovician age for the Trooper Creek Formation is well constrained by radiometric dating on zircons ( $468 \pm 5.4$  Ma,  $479.7 \pm 5.6$  Ma; Perkins et al., 1993) and by fossiliferous units within the Trooper Creek Formation and at the base of the Rollston Range Formation (Henderson, 1983). Graptolites and trilobites in the Rollston Range Formation are from the Lancefieldian, Bendigonian and Chewtonian stages of the Early Ordovician epoch. Late Lancefieldian graptolites are the oldest known from the Rollston Range Formation and indicate that the base of the formation is younger in the west than the east. The underlying Mount Windsor Formation and Puddler Creek Formation were interpreted as Late Cambrian by Henderson (1986) on the basis of conformable contacts with lower Ordovician (Lancefieldian) fossiliferous units at the base of the Trooper Creek Formation. Stolz (1995) suggest that the Puddler Creek Formation and Mount Windsor Formation could be of similar age to the Trooper Creek Formation if they were deposited in rapidly subsiding basins. Pb-U dates ( $474.6 \pm 5.1$  Ma and  $479.1 \pm 4.6$  Ma) on zircons from the Mount Windsor Formation (Perkins et al., 1993) are consistent with an early Ordovician age. Wyatt et al. (1971) report a whole-rock isochron Rb-Sr age of  $528 \pm 100$  Ma for the Mount Windsor Formation.

Table 1

Summary of the principal lithofacies in the Trooper Creek Formation. After Doyle (1997b)

Lithofacies	Characteristics	Interpretation
Massive rhyolite to dacite	Aphyric or evenly porphyritic; columnar and tortoise shell jointing; massive or flow banded	Coherent facies of lavas and domes, cryptodomes and syn-sedimentary intrusions
Massive andesite	Aphyric or evenly porphyritic; vesicular (1-15%); massive or flow banded; platy joints	Coherent facies of lava flows and syn-sedimentary intrusions
Basaltic andesite lobes	Close-packed lobes, 5-11 cm in diameter; strongly vesicular cores, glassy margins; inter lobe material is jigsaw-fit, formerly glassy, fragments	Quench fragmented lava. Result of incomplete quenching of lava leaving unfragmented pods of magma which cooled slowly and vesiculated
Basalt to basaltic andesite pillow lava	Close-packed pillow lobes, 10-40 cm in diameter; chilled margins with tiny normal joints (Stolz, 1989; Van Eck, 1994)	Pillowed lava flows emplaced subaqueously (cf. Ballard and Moore, 1977)
Non-stratified rhyolitic to dacitic breccia	Monomictic; poorly sorted; blocky to ragged clasts; clast- to matrix-supported; gradational into coherent facies and/or peperite	Autobreccia and in situ hyaloclastite
Non-stratified andesitic breccia facies	Monomictic; poorly sorted; blocky clasts; some clasts have tiny-normal joints (cf. Yamagishi, 1979); clast supported; gradational into coherent facies	Autobreccia and in situ hyaloclastite
Non-stratified sediment-matrix breccia facies	Rhyolitic to andesitic; blocky, ragged and globular shaped clasts; clast- to matrix-supported; jigsaw-fit texture in matrix-poor breccia; matrix may be siltstone, sandstone or pumice breccia; present along the upper or lower contacts of massive andesite to rhyolite facies; 0.1-1 m thick	Peperite (cf. Busby-Spera and White, 1987; Brooks, 1995)
Stratified, monomictic rhyolitic to dacitic breccia facies	Thick (0.5-11 m), internally massive or graded beds; clast-supported; blocky to elongate jagged clasts; often associated with hyaloclastite, peperite and coherent lava	Gravity-driven collapse and resedimentation of unstable hyaloclastite (cf. Dimroth et al., 1978). Deposits from high-concentration sediment gravity flows
Siltstone-matrix rhyolitic to dacitic breccia	Stratified; polymictic, matrix- to clast-supported; thick (< 7 m); internally massive or normally graded; blocky to ragged clasts locally with jigsaw-fit fabric; siltstone matrix and intraclasts	Gravity-driven collapse of unstable hyaloclastite or peperite from the margins of subaqueous lavas or cryptodomes; deposition from high-concentration sediment gravity flows (? debris flows)
Indurated siltstone-matrix rhyolitic breccia facies	Stratified; polymictic; very poorly sorted; matrix-supported; > 20 m thick; blocky to ragged rhyolite clasts with indurated siltstone rinds; other clasts are indurated siltstone and siltstone intraclasts; sediment matrix	Collapse of unstable peperite from the margins of subaqueous cryptodomes; deposition from debris flows (cf. Hanson and Wilson, 1993)
Graded dacitic to rhyolitic pumice breccia and sandstone	Essentially monomictic; normally graded; non-welded; 1-80 m thick; equant to ragged tube pumice, crystal fragments, shards and sparse angular lithic clasts	Resedimentation of subaerial or shallow submarine pyroclastic pumice into a deeper submarine setting; syn-eruptive; down-slope transport by high-concentration turbidity currents

Table 1 continued

Lithofacies	Characteristics	Interpretation
Stratified crystal-rich volcanic sandstone	Essentially monomictic; massive or weakly normally graded; grain supported; rich in crystal fragments and pumice with lesser shards and lithic clasts; 1-50 m thick	Syn-eruptive; crystal concentration during eruption and transportation; deposition from high-concentration, granular turbidity currents
Quartz eye volcanic breccia and sandstone	Poorly sorted; normally graded; dominantly coarse (to 12 mm) quartz crystals and crystal fragments (up to 60%) and/or lithic clasts (up to 80%); lesser feldspar crystals and pumice; 1-30 m thick (Hill, 1996b)	Syn-eruptive, mass flow resedimentation of crystals, pumice and lithic clasts sourced by: (1) quench fragmentation of a subaqueous lava dome; or (2) explosive eruptions in a shallow subaqueous or subaerial environment (Hill, 1996b)
Planar laminated dacitic pumice breccia	Monomictic; clast-supported; thinly planar laminated; < 5 m thick; probable mantle bedding; non-welded; tube pumice	Water-settled fall in a shallow submarine environment; source of pyroclasts was subaerial or shallow subaqueous
Polymictic lithic-pumice breccia facies	Poorly sorted; matrix-supported; weak normal grading; ~12 m thick; clasts (3 cm-2 m) of siltstone, dacite, ironstone and dacite clasts with indurated siltstone rinds; pumiceous matrix	Gravity-driven collapse of pre-existing unstable peperite, pumice breccia and ironstone; down-slope transport by high-concentration sediment gravity flows (? debris flow); deposited and sourced subaqueously
Graded andesitic scoria breccia	Essentially monomictic; stratified; thin to thick (0.1-40 m), normally graded breccia and sandstone beds; dominantly scoria with 30-50 % vesicles; subordinate poorly-vesicular clasts some with arcuate (quench) fractures	Syn-eruptive resedimentation of pyroclasts from a shallow submarine scoria cone (cf. Lonsdale and Batiza, 1980); deposits from high-particle concentration sediment gravity flows and suspension sedimentation
Cross-stratified andesitic breccia and sandstone	Monomictic, moderately well sorted; high-angle trough cross-bedding; poorly vesicular andesite fragments, and subordinate (5-7 %) scoria fragments; intervals <20 m thick	Resedimentation of pyroclasts into submarine setting from subaqueous to subaerial scoria cone; deposition from traction currents in an above-storm-wave-base environment
Globular clast-rich andesitic breccia	Monomictic, moderately-poorly sorted; massive to normally graded; fragments of bombs supported in a framework of poorly vesicular clasts and minor (10 %) scoria	Near vent pyroclastic deposit; subaqueous to subaerial strombolian eruption; minor down-slope transport
Vitric-crystal-lithic sandstone	Planar, laterally continuous beds; thin (15-70 cm) massive to normally graded crystal-vitric-lithic sandstone and interbedded siltstone; dominantly volcanic; some beds contain non-volcanic detritus	Sandstone beds are deposits from low concentration turbidity currents (Bouma Ta-Te); siltstone predominantly from suspension sedimentation
Massive to laminated siltstone	Laminated or thinly bedded intervals up to 160 m thick; planar, even, continuous beds; in some cases laminae drape small irregularities such as outsize pumice clasts	Predominantly suspension sedimentation; in part water-settled volcanic ash; deposited below storm wave base
Ironstone	Quartz-hematite±magnetite-chlorite-sericite-feldspar-calcite; locally pumiceous; discontinuous lenses (1-160 m long) and pods	Hydrothermal precipitates
Microbialitic ironstone	Microbialites composed of stromatolites, oncolites, pyroclasts and skeletal fragments	In situ stromatolites as thin films, domed biostromes and subspherical bioherms; above-storm-wave-base structures



## Metamorphic grade

The Seventy Mile Range Group has been affected by low to medium grade regional metamorphism (Hutton et al., 1993; Henderson, 1986; Berry et al., 1992). The metamorphic grade is prehnite-pumpellyite facies around Trooper Creek prospect in the east and increases to greenschist facies in the central part of the subprovince near Highway-Reward (Fig. 2; Berry et al., 1992). To the west around Trafalgar Bore and Thalanga, metamorphic grade increases through actinolite, hornblende, biotite and andalusite isograds to amphibolite facies at Waddys Mill. The regional metamorphic assemblage is correlated with deformation event D3 and regional S3 cleavage development (Berry, 1991). In contrast to rocks in the east, the metamorphic assemblage at Waddys Mill is characterised by higher strain, possibly reflecting recrystallisation in response to simultaneous deformation and granitoid emplacement.

In the east, the syn-deformational early regional metamorphic assemblage has been overprinted by hornblende hornfels assemblages which form contact metamorphic aureoles around post-kinematic granitoids of the Lolworth-Ravenswood Batholith (Berry, 1991; Berry et al., 1992). Contact metamorphic aureoles are less prominent in the western part of the subprovince (including the study area) even though post-orogenic granites are common (Fig. 2). Because the regional metamorphic grade was higher in the west, the effects of contact metamorphism were diminished and growth of prograde minerals was restricted to granite margins (Berry, 1991).

## Regional deformation and structure

A complex deformational history is recorded in Seventy Mile Range Group (Henderson, 1986; Laing, 1988; Gregory et al., 1990; Berry, 1989; Berry, 1991; Berry et al., 1992). Many pumiceous rocks preserve relics of an early bedding-parallel foliation (S1), which is defined by compacted, phyllosilicate-altered pumice. S1 is interpreted as a diagenetic compaction fabric or early tectonic fabric, and has not previously been recognised in the subprovince. The foliation is similar to that documented in other massive sulfide districts (e.g. Allen and Cas, 1990; McPhie et al., 1993; Allen et al., 1996b). The structural nomenclature of Berry et al. (1992) has been modified to include the S1 foliation. Three main deformations are recognised in the Seventy Mile Range Group between Waddys Mill and Sunrise Spur (Fig. 2; Berry et al., 1992). The first (D2) comprises thrusts (now wrench faults) and associated F2 folds and cleavage (S2). These structures are overprinted by the regional S3 cleavage and upright east-west F3 folds associated with D3. A second strong cleavage (S4) has been recognised in the subprovince but is only locally developed (Berry et al., 1992). S4 often grades with increasing intensity into D4 faults. F4 folds are locally developed.

## Tectonic setting of the Mount Windsor Subprovince

Models for the tectonic evolution of the Seventy Mile Range Group were presented by Henderson (1986) and Stolz (1994, 1995). Henderson (1986) interpreted the Seventy Mile Range Group as the fill of a Cambro-Ordovician back-arc basin, which developed on stretched Precambrian continental lithosphere west of a continental margin volcanic arc. Nd isotopic studies by Stolz (1995) supported this interpretation and suggested that the volcanic rocks were derived by partial melting of the older crust. The thickness of the calc-alkaline volcanic and sedimentary succession (possibly greater than 12 km; Henderson, 1986) suggests syn-depositional basin subsidence accompanied accumulation (Stolz, 1995). Quartz-rich micaceous sedimentary rocks of the Puddler Creek Formation are interpreted to comprise sediment derived from erosion of a Precambrian source on the attenuated Late Proterozoic to Lower Precambrian margin of northeastern Australia (Stolz, 1995).



During the early Cambrian, westerly dipping subduction of oceanic crust was initiated beneath the passive margin (Stolz, 1995). Modification of the mantle wedge by dehydration of the subducting slab initiated continental margin volcanism (Stolz, 1995). Extension of this arc, possibly due to trench retreat, subsequently initiated the development of a back-arc basin. Rapid accumulation of Puddler Creek Formation sediments within the subsiding basin preceded the eruption of a small volume of basalt and andesite (Stolz, 1995). The increased thermal gradient is interpreted to have generated voluminous crustal melts which were subsequently erupted as the Mount Windsor Formation rhyolite and dacite (Henderson, 1986; Stolz, 1995). This phase of magmatism was complete prior to initiation of Trooper Creek Formation volcanism from mantle sources variably modified by subduction.

Volcanism subsided during the early Ordovician and deposition of the Rollston Range Formation proceeded mostly by reworking of older Trooper Creek Formation volcanoclastic material. The formation may also contain detritus sourced from an active arc (Henderson, 1986; Stolz, 1995).

The orientation of the arc and adjacent back arc basin is equivocal. Henderson (1986) argued that the arc and back-arc basin were oriented north-south between the palaeosubduction zone to the west and a continental province to the east. Within the Puddler Creek Formation, an increase in volcanic components compared with continentally derived sediment moving from west to east supports Henderson's (1986) model. The current east-west orientation of the Seventy Mile Range Group was regarded by Henderson (1986) as the result of disruption and folding during emplacement of the Ravenswood Batholith. However, observations from the Puddler Creek Formation are also consistent with a northeast-southwest-oriented arc that was aligned parallel to the Precambrian cratonic margin (Stolz, 1995).

### **VHMS deposits in the Seventy Mile Range Group**

There are two significant volcanic-hosted massive sulfide (VHMS) deposits (Thalanga, Highway-Rewards) in the Seventy Mile Range Group and several small prospects (Fig. 2; Liontown, Waterloo, Agincourt, Gydgie, and Snake Oil). Berry et al. (1992) provided a synthesis of the current understanding of deposits in the subprovince (Table 2). Mineralisation at Thalanga, Liontown, Snake Oil and many smaller occurrences is mostly as stratiform sulfide lenses which are typically zinc-rich but contain little copper. At Highway-Reward, small stratabound pyrite-sphalerite-galena-barite lenses occur above the sub-vertical Reward pyrite pipe. Disseminated and vein-style Pb-Zn-Ba mineralisation also occurs in hydrothermally-altered rhyolite and dacite at the margins of the pipes.

There is a strong stratigraphic control on mineralisation in the Seventy Mile Range Group. The Thalanga deposit occurs within the Trooper Creek Formation at the contact with the underlying Mount Windsor Formation. The remaining VHMS deposits and prospects, including Highway-Reward, Snake Oil, Liontown, Cougartown, Orion and Waterloo are part of the Trooper Creek Formation (Table 2).

### **Summary**

Volcanic and sedimentary rocks within the Late Cambrian to Early Ordovician Mount Windsor Subprovince, northern Queensland, form the Seventy Mile Range Group (Henderson, 1986). The Seventy Mile Range Group comprises the four major formations: the Puddler Creek Formation, Mount Windsor Formation, Trooper Creek Formation and the Rollston Range Formation. Doyle (1997a) subdivided the Trooper Creek Formation into two members, the Kitchenrock Hill Member and overlying Highway Member, on the basis of compositional and lithofacies variations which primarily reflect changing provenance. The Thalanga and Highway-Reward VHMS

Table 2: Characteristics of volcanic-hosted massive sulfide deposits in the Seventy Mile Range Group (Summarised from Berry et al., 1992; Doyle, 1994; Huston et al., 1995; Beams and Dronseika, 1995).

	Grade and tonnage	Geometry	Ore mineralogy	Host lithologies	Stratigraphic position
Thalanga	primary 7.5 m.t. @ 1.6% Cu, 9.3% Zn, 3% Pb, 77 g/t Ag, 0.4 g/t Au  supergene 0.667 m.t. @ 5.8% Cu, 8.3% Zn, 2.1% Pb, 83 g/t Ag, 1.7 g/t Au  oxide 0.184 m.t. @ 96 g/t Ag, 0.8 g/t Au (proved or probable)	stratiform sheet	sphalerite, pyrite, galena, chalcopyrite; minor magnetite, tetrahedrite, arsenopyrite	Hanging wall dacitic lavas and volcaniclastic units, minor andesite  Ore Horizon quartz- and feldspar-phyric rhyolite, crystal-rich sandstone and polymictic volcaniclastic beds  Footwall rhyolitic lavas and volcaniclastic units	Within the Trooper Creek Formation at the contact with the underlying Mount Windsor Formation
Reward	primary 0.2 m.t. @ 3.5% Cu, 13 g/t Ag, 1 g/t Au  supergene 0.3 m.t. @ 11.6% Cu, 21 g/t Ag, 1.8 g/t Au  oxide 0.1 m.t. @ 33 g/t Ag, 6.49 g/t Au	pyrite (Cu-Au) pipe with marginal stratabound Pb- Zn lenses	pyrite, chalcopyrite, sphalerite, galena; minor electrum, tennantite; trace electrum	dacitic to rhyolitic lavas, syn- sedimentary intrusions, pumice breccia-sandstone, siltstone, polymictic breccia	Upper Trooper Creek Formation
Highway	primary 1.2 m.t. @ 5.5% Cu, 6.5 g/t Ag, 1.2 g/t Au  oxide 0.07 m.t. @ 6.04 g/t Au	pyrite (Cu-Au) pipe	pyrite, chalcopyrite, sphalerite, galena; minor electrum, tennantite	dacitic to rhyolitic lavas, syn- sedimentary intrusions, pumice breccia-sandstone, siltstone, polymictic breccia	Upper Trooper Creek Formation
Handcuff	primary 1 m.t. @ 0.4% Cu, 0.2% Pb, 7.4% Zn, 8.8 g/t Ag, 0.2 g/t Au (inferred)	veins, lenses	sphalerite, pyrite; minor chalcopyrite, galena	dacitic to rhyolitic lavas, syn- sedimentary intrusions, pumice breccia-sandstone, siltstone	Central Trooper Creek Formation
Liontown	primary 2 m.t. @ 0.5% Cu, 6.6% Zn, 2.3% Pb, 50 g/t Ag, 0.9 g/t Au	tabular lenses, pods and disseminated sulfides	sphalerite, pyrite; minor chalcopyrite, galena	Hanging wall dacitic pumice breccia, syn- sedimentary sills  Ore horizon tuffaceous siltstone  Footwall carbonaceous shale, dacitic pumice- crystal breccia-sandstone, dacitic and rhyolitic lavas/intrusions	Contact between the Rollston Range Formation and underlying Trooper Creek Formation
Waterloo	primary 0.372 m.t. @ 3.8% Cu, 19.7% Zn, 2.8% Pb, 94 g/t Ag, 2.0 g/t Au (inferred)	lenses	sphalerite, pyrite, chalcopyrite; minor galena, tennantite	Hanging wall greywacke, argillite, chert; felsic volcaniclastic rocks  Footwall schist, andesitic lavas and volcaniclastic units; rhyolitic volcaniclastic units	Central Trooper Creek Formation
Agincourt	—	disseminated; barite lenses	sphalerite, pyrite, galena, chalcopyrite; minor tennantite	Hanging wall andesitic-dacitic volcaniclastic rocks and lavas; lesser sandstone-siltstone  Footwall andesitic and rhyolitic lavas and volcaniclastic beds; schist	Central Trooper Creek Formation
Warrawee	—	multiple lenses	sphalerite, galena, chalcopyrite	felsic tuffaceous siltstone; rhyodacitic sill	Trooper Creek Formation
Magpie	primary 0.25 m.t. @ 2% Cu, 15% Zn, 2% Pb, 30 g/t Ag, 1 g/t Au (inferred)	stacked lenses	sphalerite, pyrite, chalcopyrite, galena; minor pyrrhotite, magnetite, marcasite	Hanging wall dacitic lavas and volcaniclastic rocks  Footwall sedimentary rocks and intermediate-mafic volcanics	Central Trooper Creek Formation
Snake Oil	—	lenses	sphalerite, galena, pyrite	Hanging wall dacitic-rhyodacitic volcaniclastics and intrusions  Footwall rhyolite	Near contact between Trooper Creek and Rollston Range Formations

deposits and several smaller mineral occurrences (Liontown, Snake Oil and Waterloo) are interpreted to occur within the Trooper Creek Formation.

The Seventy Mile Range Group has been metamorphosed to prehnite-pumpellyite and lower greenschist grade and affected by three main deformation events of equivocal age. The volcanics have been intruded by Ordovician to Permian granitoids of the Ravenswood Batholith and Lolworth Igneous Complex. Contact metamorphic aureoles are locally developed along the margins of the granitoids.

## PART 2: TOPICS TO BE ADDRESSED — Mark Doyle

### Interpreting timing relationships of alteration in volcanic rocks

Alteration is defined as a change in the mineralogy or texture of a rock facilitated by the action of hot or cold aqueous solutions or gases. All volcanic facies in ancient volcanic successions have been altered. These include mineralogical and textural changes resulting from emplacement (hydration, devitrification), diagenetic alteration and compaction, metamorphism and hydrothermal alteration. Each represents an *alteration stage* although the time between each stage may be very short or even overlap and several stages may be unimportant or not affect all parts of a volcanic deposit/rock. Several *steps*, each recorded by a characteristic mineral assemblage, are often involved in forming the alteration texture which characterises each stage.

Determination of the relative roles, timing and significance of each alteration stage in modifying a volcanic rock or facies is dependant on: (1) establishing the regional extent of mineral assemblages; (2) interpreting overprinting relationships of alteration minerals to primary volcanic textures, volcanic facies and intrusive units; (3) relation of alteration minerals and assemblages to tectonic, diagenetic and stylolitic foliations; (4) overprinting relationship between different alteration mineral assemblages; (5) consideration of mineral stability fields; and (6) knowledge of alteration assemblages in comparable modern volcanic successions (e.g. Green Tuff Belt, Japan; Table 3).

In the context of VHMS exploration, the challenge is to distinguish between: (a) regional diagenetic alteration of formerly glassy volcanic facies; (b) "barren" alteration associated with local hydrothermal systems; (c) syn-volcanic hydrothermal alteration concurrent with mineralisation; and (d) regional metamorphic assemblages.

### Textural evolution of volcanic rocks

The textural effects of hydrothermal and diagenetic alteration processes are strongly influenced by the pre-existing volcanic texture that was created by eruption and primary fragmentation, "high" temperature devitrification and hydration. The path of textural evolution varies for different volcanic facies and sometimes, different parts of the one unit (Fig. 4). Textures are enhanced, modified or destroyed during the textural progression. Evaluating the role of hydrothermal and diagenetic alteration in generating the final texture of a rock is dependent on considering the role of earlier processes in generating the texture of a volcanic rock.

#### *Devitrification textures*

Glass is thermodynamically unstable and so will devitrify over time. Devitrification refers to the nucleation and growth of crystalline minerals in glasses at sub-solidus temperatures. High-temperature devitrification of glass accompanies emplacement, and generated spherulites, lithophysae and micropoikilitic texture. Low-temperature devitrification of silicic glass to assemblages of minerals including zeolite, smectite, sericite, chlorite, quartz and feldspar is generally attributed to interaction with syn-volcanic hydrothermal fluids and early to late diagenetic fluids, and can be referred to as hydrothermal and diagenetic alteration.

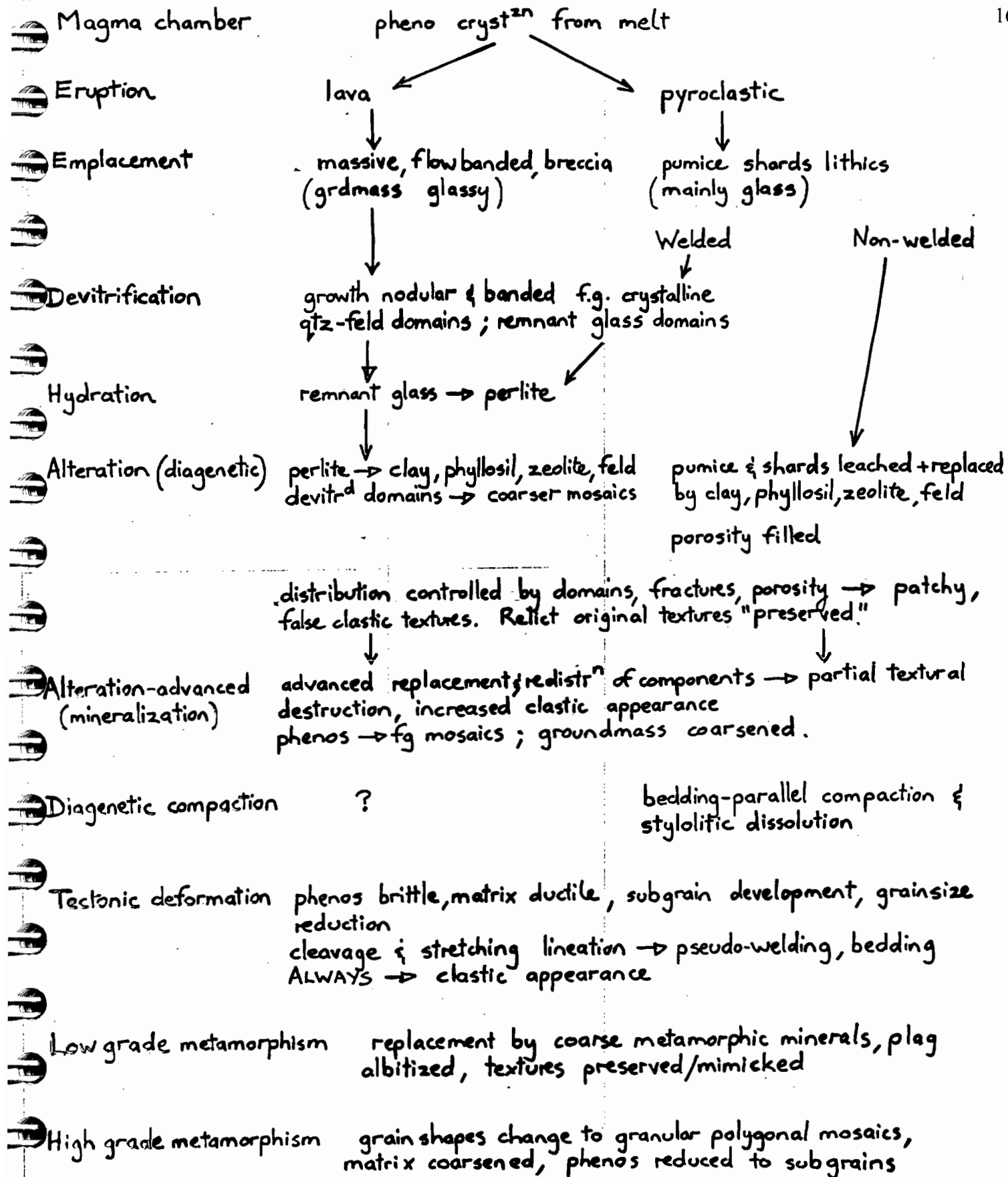
#### *Spherulites and lithophysae*

Spherulites are high-temperature devitrification structures characterised by radially arranged crystal fibres which nucleate from a single point. In originally glassy silicic rocks, crystal fibres comprise alkali feldspar and/or quartz. In mafic rocks, spherulite fibres are plagioclase intergrown with pyroxene. In many formerly glassy rocks, spherulite fibres recrystallise to a quartz-feldspar mosaic during later hydrothermal alteration or metamorphism.

Table 3. Timing relationships of alteration in volcanic rocks (after Allen and Large, 1996)

Relationship	Interpretation
<b>(1) Relationship of alteration to primary volcanic texture</b>	
Alteration truncated by clast margins	Pre-fragmentation
Clasts of different alteration types in same rock	Pre-deposition
Infills primary porosity $\pm$ rims clast margins	Pre-lithification
Rock has relict high-temperature devitrification textures	Post-devitrification
<b>(2) Relation to successive volcanic units/intrusions</b>	
Alteration assemblage cut by younger (less altered) units	Older syn-volcanic/intrusive
Overprints younger rocks	Syn- to post-younger facies
<b>(3) Relation to diagenetic compaction</b>	
Protects primary texture from compaction	Pre-compaction
Overprinted by early diagenetic minerals	Early diagenetic
Overprints late diagenetic minerals	Post diagenesis
<b>(4) Relationship of hydrothermal alteration assemblages</b>	
Overprinted by hydrothermal assemblages	Pre-hydrothermal alteration
Overprinted by early hydrothermal assemblages	Early hydrothermal
<b>(5) Relationship to early stylolitic dissolution foliation</b>	
Overprinted by stylolitic foliation	Pre-dissolution
Overprints stylolitic foliation	Post-dissolution
<b>(6) Relation to tectonic foliations and lineations</b>	
Cut by tectonic foliation	Pre-cleavage
Less deformed than tectonic foliation	Pre- to syn-cleavage
Undeformed	Post-cleavage
<b>(7) Relationship to metamorphic assemblages</b>	
Overprinted by metamorphic assemblage	Pre-metamorphic
Overprints metamorphic assemblage	Post-metamorphic
<b>(8) Regional distribution</b>	
Regionally distributed	Diagenetic or metamorphic
Stratabound in formerly permeable facies	Pre- to syn-lithification
Locus in fractured domain of coherent facies	Post-lithification & fracture
Restricted to faults or shears	Syn- to post-faulting

Fig.4 Textural evolution of volcanic rocks



Lithophysae are spherulites with a central vugh that may be open or lined with chalcedony or agate (Ross and Smith, 1961). Lithophysae begin to grow during emplacement as spherulites nucleate around a vesicle. As crystallisation proceeds, the central vugh expands as volatiles are exsolved. In some cases the lithophysal cavity is partly filled with glass, injected while it was still hot and able to deform plastically. Spherulites and lithophysae often nucleate on phenocrysts, vesicles or flow bands in lava.

#### *Micropoikilitic texture*

Micropoikilitic textures comprises crystals of one mineral that enclose microlites of another mineral. In many cases, feldspar microlites or radiating fibres of feldspar in spherulites are poikilitically enclosed in optically continuous quartz. Micropoikilitic quartz can also occur within former glassy perlitic kernels and sometimes overprints the perlitic fractures (e.g. Bigger and Hanson, 1992). The age relations suggests that micropoikilitic texture develops both during the early devitrification history and after hydration (e.g. Bigger and Hanson, 1992).

#### *Hydration*

Hydration is the diffusion of water into the structure of glass. Strain resulting from the associated volume increase is released by means of perlitic fracturing. Hydration (and so perlitic fracturing) begins after emplacement and may continue long after cooling to surface temperatures. Perlitic fractures are arcuate and concentrically arranged around a non-fractured core. In flow banded rocks, perlitic cracks form rectilinear networks (banded perlite) (Allen, 1988).

### **Textural heterogeneity of coherent lavas and intrusions**

Lavas and intrusions typically comprise coherent and autoclastic facies. They can also display complex internal variations in flow fold attitude, joint patterns, vesicularity, and the effects of crystallisation, devitrification and hydration. Some felsic submarine lavas and intrusions display significant variation in the size and abundance of vesicles. Subaerial lavas can include various arrangements of coarsely vesicular pumice, dense glass and finely vesicular pumice (e.g. Little Glass Mountain, California, Fink, 1980, 1983). Submarine lavas with pumiceous zones and pumiceous hyaloclastite have also been recognised (e.g. Kurokawa, 1992). In strongly altered and deformed volcanic successions, pumiceous lavas/intrusions and associated autoclastic facies can sometimes be difficult to distinguish from pumiceous mass flow deposits.

Sections through lavas and intrusions can also show a textural zonation resulting from devitrification and hydration (e.g. DeRosen-Spence, 1980; Furnes et al., 1980). During emplacement, the outer margins of lavas and intrusions are cooled rapidly to glass (Fig. 5). After emplacement and late in the cooling history of glass, or following cooling to surface temperatures, perlitic cracks sometimes developed in response to hydration of the glass (e.g. Allen, 1988). The interior of the lavas and intrusions often cools slower, resulting in a crystallised and devitrified core (e.g. Bigger and Hanson, 1992). A mixed glassy and devitrified zone outside the core records the progression of devitrification fronts within the lavas and intrusions during cooling. The fronts record the end in growth of spherulites, lithophysae and microlites as temperatures decreased below a critical value for high-temperature devitrification to continue in the cooling glass. The remaining glassy domains experience low-temperature devitrification (hydrothermal and diagenetic alteration) to form finely crystalline mosaics of alteration minerals.

The mineralogical zones developed during emplacement and cooling are important in controlling the distribution of subsequent alteration minerals deposited from hydrothermal and diagenetic fluids (e.g. McPhie et al., 1993; Doyle, 1998b). In cases of moderate to weak alteration, devitrified domains are generally silicified or recrystallise to quartzofeldspathic mosaic. Formerly glassy domains typically alter to smectite, zeolite,

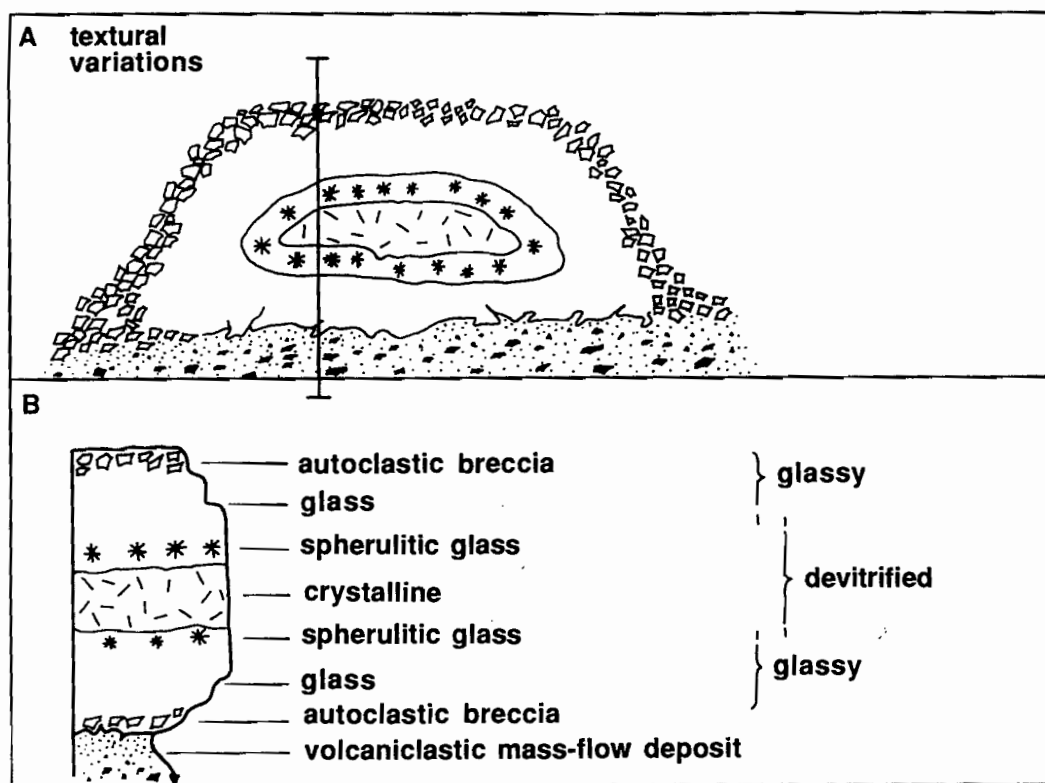


Figure 5. Schematic cross-section through a subaqueous lava flow. (A) The internal textural variations generated during vesiculation, devitrification and flow fragmentation are illustrated. (B) Vertical section through the lava at the position indicated in (A), showing the principal textural zones. After Fink and Manley (1987) and Duffield and Dalrymple (1990).



phyllosilicate minerals or feldspar. In zones of intense hydrothermal alteration, few primary textures may remain and mottled or patchy alteration styles are common.

### **Effect of lithofacies on mineralisation and alteration processes**

The nature of the lithofacies which hydrothermal fluids ascend during their passage to the seafloor strongly influences the distribution, geometry, textures and mineralogy of mineralisation and associated hydrothermal alteration (e.g. Large, 1992; Doyle, 1997a,b). Figure 6 summarises the main attributes of some types of massive sulfide deposits and alteration styles as a function of host lithofacies character and evolution. It does not cover all possible scenarios for VHMS mineralisation, but simply highlights the spectrum of deposit style and alteration halos which may form and their relationship to the enclosing strata and evolution of the depositional centre.

Within relatively impermeable centres, dominated by lavas or intrusions, ascending hydrothermal fluids and circulating connate fluids are likely to be focussed through more porous and permeable units, including faults (e.g. Large, 1992), the fractured glassy margins of lavas and intrusions and resedimented autoclastic units (Doyle, 1997a,b). In cases where volcanic centres are dominated by syn-sedimentary intrusions, the enclosing sediment within several tens of metres of syn-sedimentary sills may be indurated, metamorphosed to low grades, and less porous than the enclosing strata. The reduction in porosity accompanying intrusion is a mechanism for generating even more efficient, focused, hydrothermal fluid discharge. In lava- or intrusion-dominated volcanic centres, well-focussed fluid flow gives rise to lens- or pipe-shaped massive sulfide deposits and well developed, zoned, alteration pipes (Fig. 6). Hydrothermal fluids can exhale onto the seafloor to form a seafloor massive sulfide deposit (e.g. Hellyer). In the presence of a relatively impermeable barrier (e.g. indurated sediment, massive crystalline/devitrified lava), hydrothermal fluid flow may be impeded and sub-seafloor sulfide deposition proceeds by replacement and infiltration of the enclosing strata (e.g. Doyle, 1997b). The fractured, glassy, porous and permeable parts of lavas and shallow intrusions and volcanoclastic deposits are often preferentially replaced (e.g. Highway-Reward; Doyle, 1997a,b).

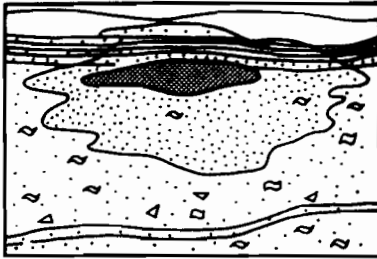
Other massive sulfide deposits are hosted by sequences dominated by pumiceous mass flow deposits (e.g. Khin Zaw and Large, 1992; Allen, 1994; Allen et al., 1996) water-settled fall (e.g. Allen et al., 1997b) or turbidites (e.g. Bodon and Valenta, 1995) (Fig. 6). The originally highly porous, permeable, water saturated and glassy nature of these lithofacies caused hydrothermal fluids to be poorly focussed. Ascending hydrothermal permeate through the substrate to produce widespread strata-bound alteration zones and lens- or sheet-style massive sulfide mineralisation (cf. Large, 1992). In many cases, sulfide deposition is interpreted to have commenced at the interface between the ascending hydrothermal fluid and overlying cold, seawater-saturated strata (e.g. Allen et al., 1996) forming sub-seafloor replacement massive sulfide mineralisation (e.g. Hercules, Khin Zaw and Large, 1992; Rosebery (Allen, 1994), Liontown (Miller, 1996; Doyle unpub. data).

In VHMS host successions comprising mixtures of relatively poorly porous rocks (e.g. lavas and shallow intrusions) and incompetent, very porous deposits (e.g. pumiceous units), a variety of mineralisation types and alteration styles may develop in close proximity (e.g. Highway-Reward, Doyle, 1997a,b).

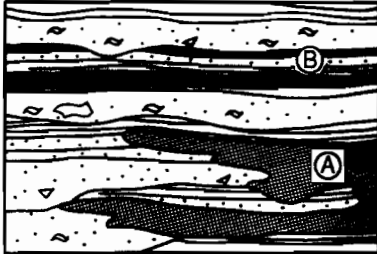
### **Exhalation and sub-seafloor replacement in mineral deposition**

Sub-seafloor sulfide accumulation by open space filling and replacement of volcanic and sedimentary facies is increasingly being recognised as important in the genesis of VHMS deposits. Doyle (1997b) critically assessed the criteria for evaluating the role of seafloor

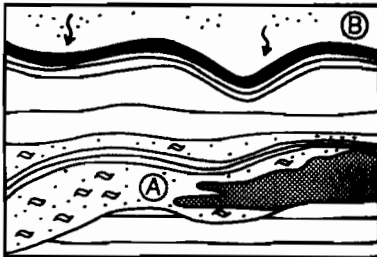
## mass-flow deposits



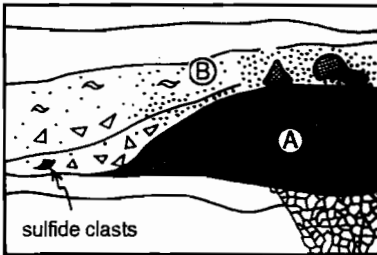
## turbidites &amp; siltstone



## water-settled fall



## burial by mass-flows



## sulfide clasts

pumice

lithic

intraclast

sand and finer

enclosing strata

infiltration &amp; replacement ore

seafloor massive sulfide

stringer veins

strong hydrothermal alteration

- Sub-seafloor replacement of rapidly emplaced mass-flow deposits(s)
- Host commonly syn-eruptive & pumiceous

(e.g. Rosebery, Allen, 1994; South Hercules, Khin Zaw & Large, 1995; Lontown, Miller, 1996; Långdal & Långsete, Allen et al., 1997b)

- Ⓐ Sub-seafloor sulfide replacement front within rapidly emplaced units

- Ⓐ + Ⓑ Synchronous sedimentation & sulfide precipitation both above & below the seafloor

(e.g. Currawong, Bodon & Valenta, 1995; Ansil, Galley et al., 1995)

- Ⓐ Sub-seafloor replacement of a single rapidly emplaced unit  
(e.g. Renström, Allen et al., 1997b)

- Ⓐ + Ⓑ Synchronous sedimentation & massive sulfide deposition by replacement, infiltration & exhalation

- Ⓐ Seafloor massive sulfide

- Ⓐ + Ⓑ Burial; replacement of volcanoclastic deposits during ongoing hydrothermal activity  
(e.g. Que River, Large et al., 1988)

Figure 6. Schematic representation of various scenarios in which massive sulfide deposits may form and the morphology of the alteration halo associate with each. (Doyle, 1997a,b).

syn-sedimentary sill

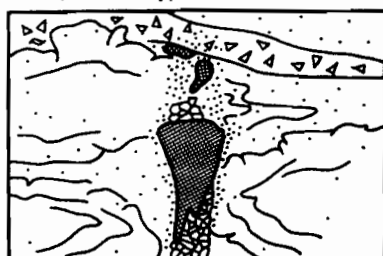


- Ⓐ Ponding of hydrothermal fluids beneath a syn-sedimentary sill. Sub-seafloor replacement of the sill margin & host

- Ⓑ Ascending fluids form a stacked system

(e.g. Rosebery, Allen, 1994)

lavas, sills &amp; cryptodomes

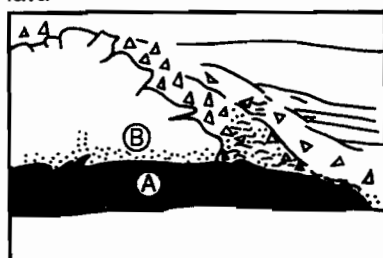


- Sub-seafloor replacement within a discordant alteration envelope

- Stacked massive sulfide pipes & stratiform lenses

(e.g. Highway-Reward)

lava



- Ⓐ Seafloor massive sulfide mineralisation

- Ⓑ Burial by lavas. Hanging wall alteration develops during continued hydrothermal activity. May form a stacked system

(e.g. Fukazawa, Sato et al., 1979)

lava



- Ⓐ Seafloor massive sulfide

- Ⓑ Replacement of in situ & resedimented autoclastic breccia units

□ pumice

□ lithic

□ sand and finer

□ autoclastic breccia

□ resedimented autoclastic breccia

□ glassy lava - intrusion

□ enclosing strata

□ infiltration & replacement ore

□ seafloor massive sulfide

□ stringer veins

□ strong hydrothermal alteration

Figure 6 continued. Cartoon showing the various circumstances under which massive sulfide mineralisation may develop and the alteration halo associated with each. In these examples the host succession also includes lavas and intrusions.

massive sulfide deposition and sub-seafloor replacement in mineral deposition. The following discussion is taken from Doyle (1997b) and a paper in preparation.

Studies of ancient VHMS deposits suggest that there are interdependent criteria for evaluating the role of sub-seafloor replacement during syn-genetic sulfide (or other minerals) deposition: (1) presence of precursor particles or relic coherent facies within the massive sulfide; (2) facies characteristics indicating that mineralisation post-dates deposition of the host; (3) identification of syn-depositional replacement fronts; (4) discordance with the enclosing host lithofacies; and (5) the presence of hanging wall alteration zones with footwall affinities. In most cases, more than a one criterion is required to demonstrate a seafloor or sub-seafloor origin for the mineralisation.

### *1. The presence of precursor particles or coherent facies*

Volcanic and sedimentary particles can sometimes be preserved within massive sulfide mineralisation. The particles may be partially or completely replaced by sulfide minerals, or are altered and contain disseminated sulfides (e.g. Bodon and Valenta, 1995; Galley et al., 1995). Fragment types, shape, composition and texture help constrain the particle forming mechanism and, when combined with the lithofacies character (bedforms, geometry, internal organization), can be used to establish the character (porosity, permeability) of the precursor lithofacies and mechanisms of sulfide accumulation. Considered alone, precursor particles are consistent with either sub-seafloor replacement or synchronous sedimentation and sulfide precipitation.

In some VHMS deposits, the matrix of autoclastic breccia is replaced by sulfides (e.g. Galley et al., 1995), or the massive sulfide contains segments or patches of strongly altered, mineralized coherent igneous rock (e.g. Highway-Reward). Parts of the massive sulfide mineralisation contained within relic coherent facies or autoclastic breccia can only have formed by replacement and infiltration. Where emplacement as a lava or intrusion cannot be proven, it remains possible that the igneous component was resedimented onto seafloor massive sulfide or sourced from the subsurface environment and transported with the hydrothermal fluid (e.g. Humphris et al., 1995).

### *2. Evidence for rapid emplacement of the host facies*

This criterion involves a genetic interpretation of the host, with particular attention to transport and depositional mechanisms and the nature and position of contacts between the host rock and mineralisation. Massive sulfide mineralisation which is hosted by rapidly or mass-flow emplaced units can only have formed by replacement and impregnation (Allen, 1994; Allen et al., 1996). Most often the host will be a lava or intrusion and associated autoclastic breccia (e.g. Zierenberg et al., 1988), or syn-eruptive pumiceous mass-flow deposit (e.g. Allen, 1994; Khin Zaw and Large, 1992). Parts of some sub-seafloor replacement style massive sulfide deposits are hosted by thinly bedded volcano-sedimentary units rather than a single thick depositional unit (e.g. Bodon and Valenta, 1995; Galley et al., 1995). In these, the possibility remains that sedimentation was synchronous with hydrothermal activity and that precipitation of sulfides occurred at, above, and below the seafloor over the life of the hydrothermal system.

The rate of sediment accumulation will determine the relative importance of seafloor and sub-seafloor processes in massive sulfide accumulation. If sedimentation surpasses sulfide precipitation at the seafloor, then sub-seafloor replacement will become important. Growth rates for sulfide mounds are poorly constrained. Chimneys on mounds can grow 8 to 30 cm per day (Goldfarb et al., 1983; Hekinian et al., 1983). Although a single typical black smoker chimney produces around 250 tonnes of sulfide per annum, much of this is dispersed by currents and incorporated into distal sediments (Scott, 1992). Sulfide precipitation at seafloor mounds may be intermittent and separated by long periods dominated by ambient sedimentation (e.g. Rona et al., 1993). Regional sedimentation rates for oceanic spreading centers are generally low (e.g. 1.8 cm/kyr, TAG, Scott et al., 1978), whereas in back arc basin settings sedimentation can be rapid (e.g. Taylor et al.,

1991). In the Sumisu Rift of the Izu-Bonin island arc, sediments accumulated at between 90 mm/kyr and 6 m/kyr from 0.1 to 1 Ma (Taylor et al., 1991). The basin fill includes hemipelagic sediment and voluminous volcanoclastic turbidites sourced from arc volcanoes (Nishimura and Murakami, 1988). Volcanism, especially explosive volcanism, has the potential to release large volumes volcanoclastic detritus into submarine settings (e.g. Cas and Wright, 1991; McPhie and Allen, 1992). Burial of sulfide mounds by volcanoclastic mass flows or lavas can occur during the life of the hydrothermal system, interrupting or terminating seafloor sulfide deposition (e.g. Haymon et al., 1993). As the hydrothermal system attempts to re-establish a seafloor position, sub-seafloor replacement of the intervening lithofacies by sulfide minerals may become important (e.g. Haymon et al., 1993; Humphris et al., 1995).

### *3. Identification of syn-depositional replacement fronts*

Bodon and Valenta (1995) documented primary and tectonic features in the Currawong Zn-Cu-Pb VHMS deposit, Benambra. At the margins of one massive sulfide lens there are replacement fronts passing from the various ores into sandstone beds. Intercalated siltstone laminae are not replaced. A thin quartz-sericite alteration halo extends out from the margins of the sulfide lenses into relic sandstone beds and provides critical evidence for replacement of a pre-existing lithology. Galley et al. (1995) identified similar replacement fronts in the Ansil VHMS deposit, Canada. Alteration intensity increases towards contacts between the massive sulfide lens and tuffaceous host rocks, and beds can be traced into the massive sulfide. At South Hercules (Khin Zaw and Large, 1992) and Lione town (Doyle, unpub. data, 1997), massive sphalerite mineralisation often passes out through a zone of altered host rock with "spotty" sphalerite ore, into the enclosing pumiceous units. The "spotty" ore records the nucleation of sulfides within the pumiceous host (e.g. Khin Zaw and Large, 1992) and can be considered one type of replacement front. Partially replaced beds and/or clasts are good evidence that bedforms in sulfide can be the product of selective replacement and that these parts of a deposit formed by sub-seafloor replacement of permeable volcano-sedimentary horizons.

### *4. Discordance within the enclosing lithofacies*

Discordance within the enclosing volcano-sedimentary package can provide evidence for replacement of a precursor lithofacies (e.g. Khin Zaw and Large, 1992; Galley et al., 1993). However, progressive burial of the older parts of a growing mound/lens by sedimentation or volcanism concurrent with massive sulfide deposition might generate sharp discordant contacts. Accordingly, the criterion cannot be used alone and requires consideration of the transport and depositional mechanisms of the host lithofacies, and the recognition of the seafloor position(s) at the time of mineralisation.

### *5. Hanging wall alteration zones with footwall affinities*

In seafloor VHMS deposits, the upward termination of intense hydrothermal alteration at the position of stratiform sulfides indicates that the ore-forming hydrothermal activity occurred after emplacement of the footwall rocks and before deposition of the hanging wall rocks. Zones of subtle hanging wall alteration have been reported above mineralized intersections in a number of Australian VHMS deposits (e.g. Mount Chalmers, Large and Both, 1980; Hellyer, Jack, 1989). These are interpreted to record weak hydrothermal activity during deposition of the hanging wall volcano-sedimentary package. In contrast, zones of intense hanging wall alteration suggest that ore-forming hydrothermal activity was continuing during deposition of the hanging wall lithologies or that massive sulfide deposition was entirely sub-seafloor. Given that many volcanic facies are rapidly emplaced, strong hanging wall alteration is entirely plausible even for seafloor exhalative deposits. Burial of seafloor massive sulfide by lavas (e.g. Haymon et al., 1993) or volcanoclastic units can only be discounted by considering the lithofacies character of the host.

### *An assessment of other textures and structures in VHMS deposits*

Chimneys and chimney fragments provide strong evidence for sulfide accumulation at the seafloor (Lydon, 1988b) and have been recognized in ancient deposits (e.g. Oudin and Constantinou, 1984). Fossil tube worms and bivalves in chemolithotrophic communities which colonise modern seafloor sulfide mounds can sometimes be preserved by sulfide minerals and are characteristic of seafloor deposits (Haymon et al., 1984; Oudin and Constantinou, 1984). Few other textures or structures in VHMS deposits have genetic significance in distinguishing seafloor deposits from sub-seafloor deposits. Many massive sulfide textures form through open space filling (e.g. colloform banding, network textures). However, this can include intramound porosity, primary lithological porosity, and/or space formed by fluid-rock-mineral interaction (e.g. dissolution of anhydrite). A critical line of evidence in support of a seafloor origin for VHMS deposits has been the recognition of sedimentary structures within some massive sulfide lenses. Graded bedding, cross bedding, and intercalations of laminated and fragmental ore have been identified in the Kuroko deposits (e.g. Ohmoto and Skinner, 1983) and Australian deposits (e.g. Mount Chalmers, Large and Both, 1980). The recognition of similar structures in sub-seafloor replacement style deposits suggests that selective replacement of clasts in pre-existing lithofacies can form similar structures (e.g. Bodon and Valenta, 1995; Galley et al., 1995). Apparent interbedding of sulfide and sediment can result if more permeable laminae are selectively replaced and fine-grained (impermeable) laminae remain unaffected (Bodon and Valenta, 1995). Breccia ore facies can also form in situ within sulfide mounds by dissolution of anhydrite in the matrix to sulfide patches (e.g. TAG, Humphris et al., 1995). Banded sulfides are a common feature of VHMS deposits. In most cases, it is difficult to determine whether the banding is primary or due to later deformation (e.g. Large et al., 1988).

Iron oxide-silica units ("ironstones") that form the ore equivalent horizon to VHMS deposits can provide evidence for a seafloor position which includes the ore horizon. However, very similar iron-oxide silica units can form by sub-seafloor replacements of pre-existing strata (Doyle, 1996, 1997b). Microaerophilic chemolithotrophic organisms can colonise sub-seafloor sediments and hydrothermal conduits (e.g. Haymon et al., 1993; Doyle, 1996, 1997b) so are not characteristic of a seafloor position. In some cases, the favorable horizon is not represented by a chemical sediment but sulfide-clast bearing mass-flow deposits (e.g. Hercules, Allen and Hunns, 1990; Hellyer, Waters and Wallace, 1992). Mass flows can erode several metres down into the substrate and successive mass flows up to 10's of metres. Sulfide clasts indicate only that massive sulfide accumulation occurred at or near the seafloor.

### **Summary of problems and topics**

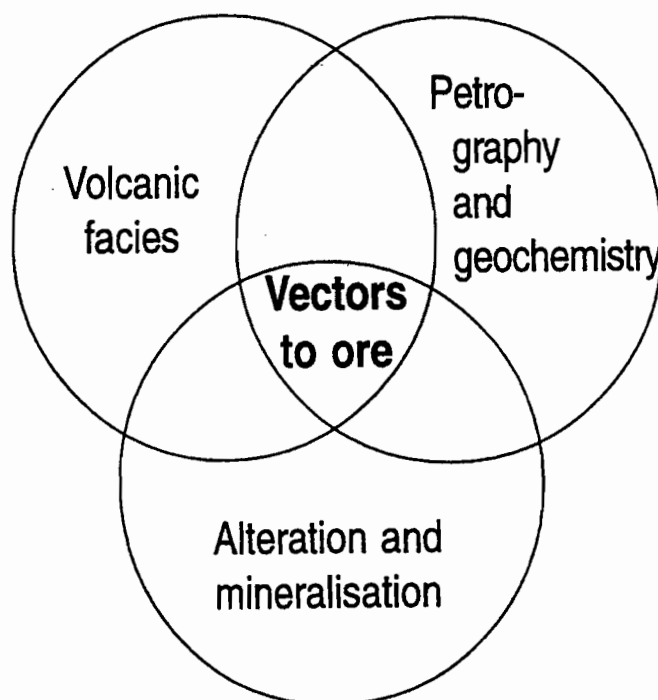
In summary, it is clear that interpreting the significance of alteration in volcanic successions requires consideration of:

- (1) timing relationships of alteration assemblages in volcanic rocks;
- (2) effects of lithofacies on mineralisation and alteration processes;
- (3) role of eruption, emplacement, devitrification and hydration in influencing the distribution and texture of successive alteration assemblages;
- (4) role of sub-seafloor replacement and seafloor deposition during mineral (including sulfide) deposition.

### PART 3: FIELD GUIDE

Interpreting the significance of alteration in volcanic successions requires a multidisciplinary approach incorporating volcanic facies studies, ore deposit research and geochemistry. This approach has been successfully applied in the Mount Windsor Volcanics. Studies within the Mount Windsor Volcanics have focussed on the known mineral deposits and prospects with the aim of identifying proximal and medial vectors to ore.

The primary outcomes of the research to date will be presented over the next three days (Fig. 7). Day 1 will be spent examining the alteration halo associated with the Thalanga VHMS deposit. The character of the pipe-style Cu-Au Highway-Reward deposit will be evaluated during day 2. The facies architecture in the Highway-Reward area contrasts with the shallower water setting implied for the succession at Trooper Creek prospect. This succession hosts barren ironstone lenses that will be a focus of discussions during day 2. On day 3, alteration associated massive sulfide deposits (e.g. Lione town, Snake Oil) hosted by pumice breccia beds will be evaluated. The role of seafloor and sub-seafloor accumulation during massive sulfide deposition will also be addressed.





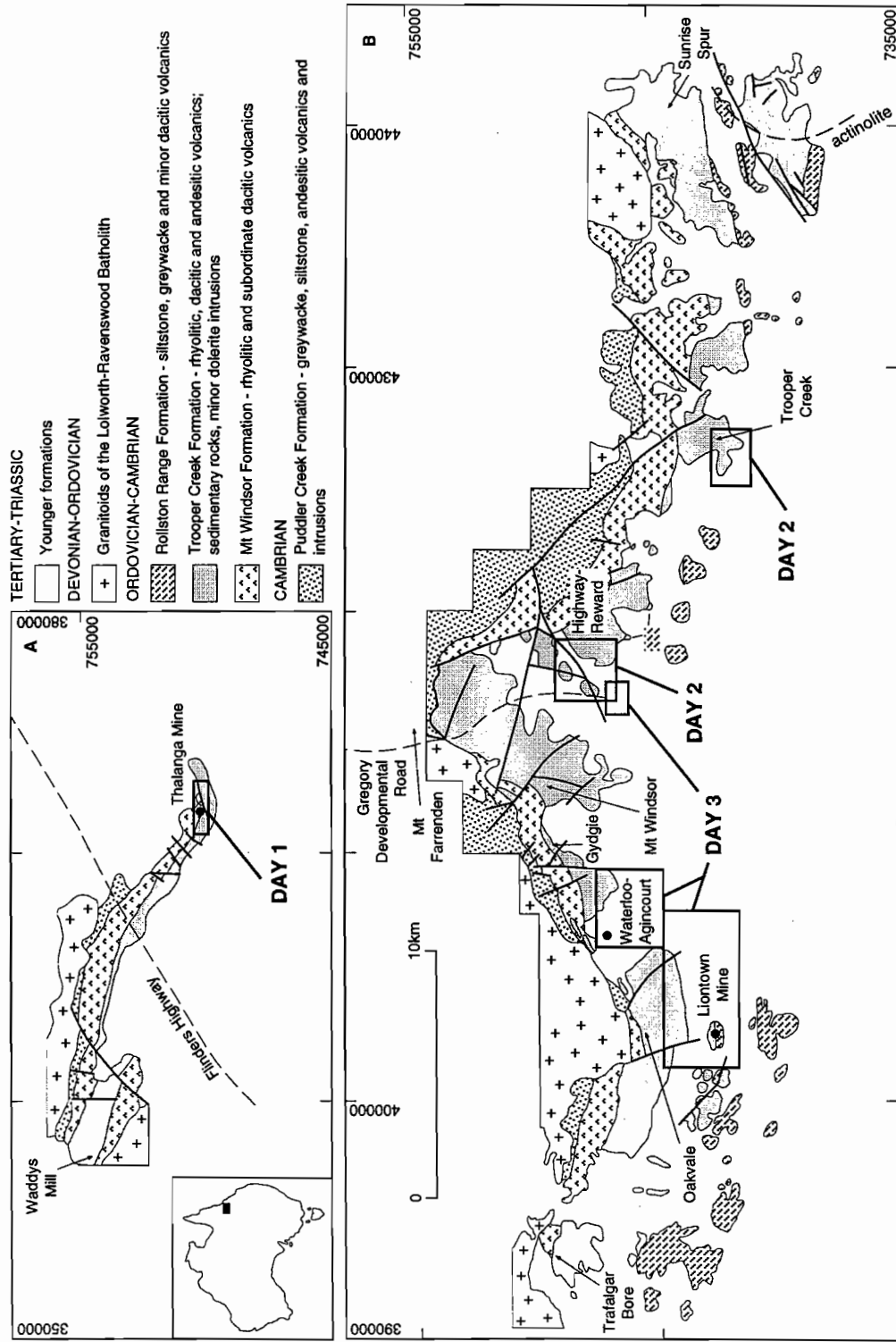


Figure 7: Simplified geological map of the Seventy Mile Range Group between Waddys Mill and Sunrise Spur. The distribution of major geological formations, significant mineral deposits, and locations to be visited during the excursion. Modified after Berry et al. (1992).



## Day 1: Hydrothermal alteration of lavas and intrusions in the host succession of the Thalanga VHMS deposit

Holger Paulick and Walter Herrmann

*Directions:* Drive the Flinders Highway to the east (direction: Mt Isa, Hughenden) for ~ 65 km following the railway line. You will pass a roadhouse called Balfes Creek on the way. The turn off to Thalanga (sealed road) is on your left ~ 10 km beyond Balfes Creek and is indicated by a large white sign (there are also loading facilities close to the railway line on your left). Follow the access road to the mine and park at the car park in front of the offices.

### STOP 1: The Thalanga mine

#### *Regional Setting*

The Thalanga deposit lies near the western end of a 165 km long, E-W trending belt of deformed Cambro-Ordovician marine sediments and volcanics known as the Mt Windsor Subprovince, (Henderson, 1986; Gregory et al., 1990; Berry et al., 1992). The stratigraphic sequence in the Subprovince is grossly conformable with an exposed thickness of up to 10 km. It faces south and comprises the following major formations:

TOP

Name and age	thickness	description and geo-tectonic interpretation
<b>Rollston Range Formation</b> Lower Ordovician (Bendigonian, Chewtonian, Henderson, 1986)	?	Lower Ordovician fossiliferous sandstones, siltstones and cherty siltstones of volcanic provenance; conformably overlie the TCF.
<b>Trooper Creek Formation</b> (TCF) Lower Ordovician (Lancefieldian 2-Lancefieldian 3, Henderson, 1986)	500-4000 m	Basaltic-andesitic, dacitic and rhyolitic volcanics, mass flow volcanoclastic breccias, volcanogenic siltstones and vitric ash units with minor calcareous metasediments and exhalative siliceous ironstones. Magmas generated by melting of a variably subductio modified, sub-arc, mantle wedge and erupted during back arc extension (Stolz, op. cit.).
<b>Mt Windsor Formation</b> (MWF) Lower Ordovician (481 ± 5 Ma and 485 ± 5 Ma; Perkins, 1993)	400-1200 m (max.: 4000 m, Brittania and Sunrise Spur area)	Subaqueously deposited rhyolites dominated by passively extruded thick flows, domes and high level intrusives with subordinate volcanoclastics and mass flow breccias. Isotopic evidence (Stolz, op. cit.) suggests derivation from melting of continental crust.
<b>Puddler Creek Formation</b> ?Cambrian	upto 9000 m ?	Massive to laminated wackes and siltstones of continental and volcanic provenance. Minor basaltic-andesitic volcanics concentrated in the upper few hundred metres. The volcanics have geochemical signatures typical of intraplate volcanism, related to lithospheric thinning and incipient back-arc basin development (Stolz, 1995).

BASE

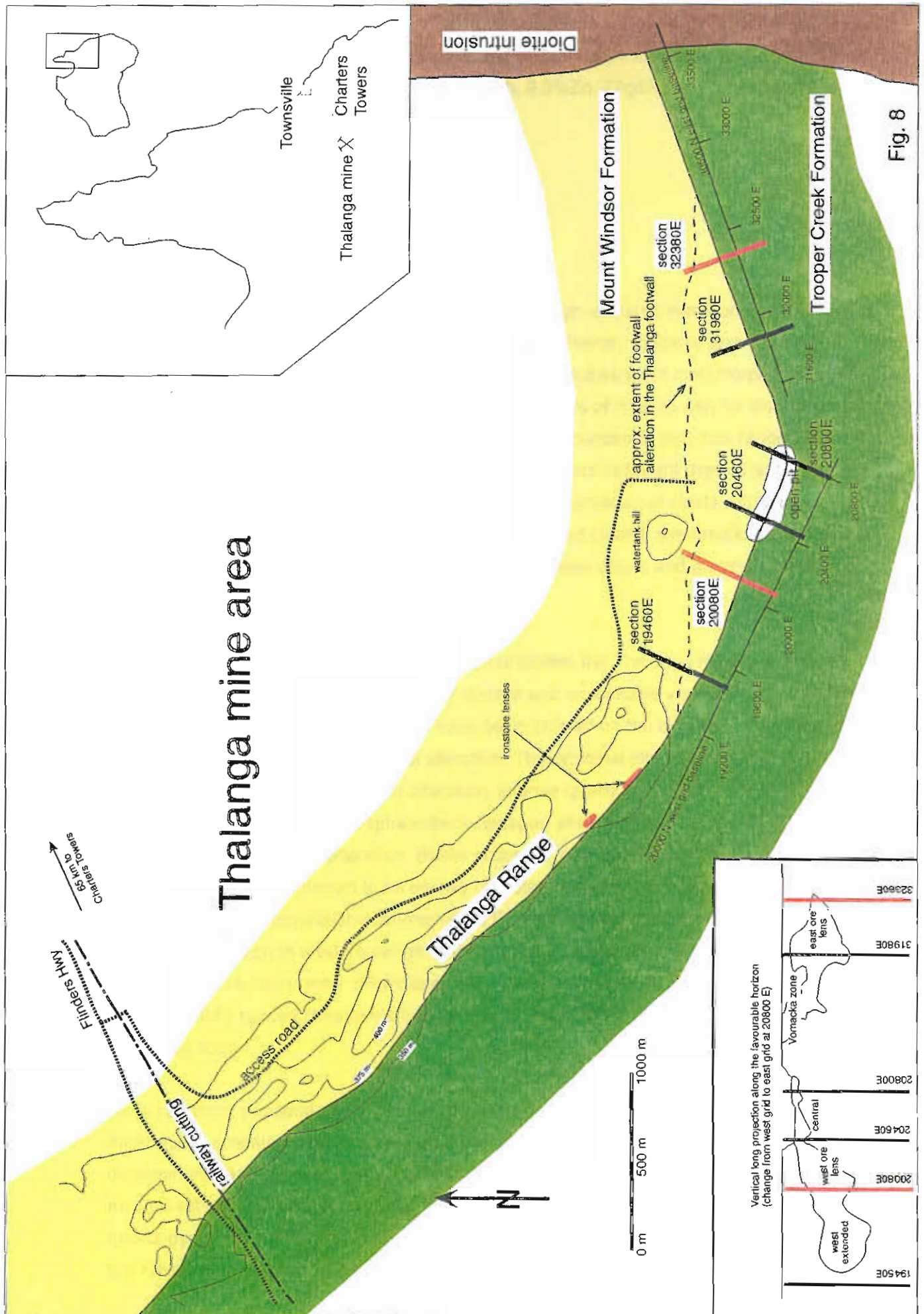
The Subprovince has been deformed by at least one, possibly two, major event/s. The most recognisable, D2, (Berry et al., 1992) appears to have coincided with or closely followed extensive intrusions of early plutonic, gneissic phases of the Ravenswood Granodiorite Complex in about the Mid-Late? Ordovician period. D2 produced relatively low pressure regional metamorphic assemblages, ranging from prehnite grade in the east to upper greenschist andalusite-biotite grade in the west, and a near vertical axial plane penetrative cleavage, S2. The Mt Windsor Subprovince appears to represent a single south facing limb of a large, E-W trending, upright D2 antiform.

A locally developed ENE trending cleavage, S3, exists in association with steep NE to ENE trending faults with south side up displacements which Berry et al., (op. cit.) related to emplacement of unfoliated (post D2) granitoids of Siluro-Devonian age. The post-kinematic granitoid plutons are associated with local contact metamorphic aureoles up to cordierite grade which are most recognisable in the eastern areas where prograde contact metamorphism exceeded the grade of the earlier regional metamorphism.

#### *Ore deposit morphology*

The Thalanga massive sulfide deposit is situated at the foot of the eastern end of a low, north-west trending, strike ridge, flanked to the north, east and south by an extensive peneplain that covers the uneven basement surface with up to 100 m of semi consolidated Tertiary alluvial sediments, known as Campaspe Beds (Fig. 8). Surface exposure in the vicinity of the deposit is poor and most of the geological interpretation is based on observations from RAB/Percussion holes, diamond drill holes and mine development.

The deposit consists of several semi-connected, thin, stratiform lenses of pyrite-sphalerite-galena-chalcopryite with variable gangue assemblages including chlorite, tremolite, carbonate, quartz, barite, magnetite and felsic volcanoclastic materials, lying conformably on a single favourable horizon sandwiched between the near vertically dipping contact of the Mt Windsor Formation (MWF) and the Trooper Creek Formation (TCF). In longitudinal projection (Fig. 8) the sulfide lenses show a semi continuous, broad arcuate distribution, partly attributable to faulting, over a known strike extent of about 3000 m. The maximum vertical dimension is about 400 m and thickness ranges from <1 m to about 25 m with an average of about 5 m. The Central Thalanga lens cropped out in an area of shallow (<2 m) soil cover as an in situ hematite-limonite boxwork gossan which led directly to the discovery in 1975 (Herrmann, 1995). The Western and Eastern sulfide lenses have no surface expression.



The total known mineral resource was estimated at June 1994 as 8.6Mt; consisting of 2.5Mt mined production and 6.1Mt @ 1.6%Cu, 3.0%Pb, 9.3%Zn, 77g/tAg and 0.4g/tAu of in situ resource.

### *Footwall Units*

The footwall rocks consist of massive rhyolite lavas, syn-volcanic intrusions, rhyolitic breccias and monomict rhyolitic gravity flow deposits. Primary volcanic textures are generally obliterated due to hydrothermal alteration and subsequent metamorphism. However, careful textural studies showed that four types of rhyolite can be distinguished based on consistent differences in phenocryst types, abundance and size range (Table 4). Discrimination of true monomict rhyolitic clastic facies from coherent rhyolite with pseudoclastic texture due to alteration relies on the observation of clasts with laminar fabrics in random orientation (eg. rotated, flow laminated clasts), systematic differences in quartz phenocryst abundance and/or size range between clasts and groundmass and normal grading of gravity flow deposits.

A laterally extensive footwall alteration system underlies the Thalanga mineralisation. Alteration is texturally and compositionally diverse and small scale variations are commonly observed in drill core but several types have been defined on the basis of dominant mineral assemblages and general intensity of alteration. The principal alteration types in the footwall are: mottled chlorite-sericite  $\pm$ pyrite alteration, intense quartz-pyrite(-sericite) and chlorite-pyrite alteration, late quartz ( $\pm$  sphalerite $\pm$ K-feldspar) alteration and carbonate-calc-silicate (epidote-zoisite-tremolite) alteration. Biotite occurs in least altered rhyolite as well as in altered rhyolite and is inferred to be entirely of metamorphic origin. Massive to semi-massive assemblages of carbonate-chlorite-tremolite ('CCT') commonly occur within, or close to, the Favourable Horizon in west Thalanga. These rocks, formerly regarded as exhalites, have been recently re-interpreted (Herrmann, 1994) as metamorphosed equivalents of zones of intense, VHMS related chlorite+carbonate alteration formed in rhyolitic volcanoclastics, close to the sea floor.

Semi stratiform proximal zones of intense quartz-pyrite(-sericite) alteration of upto ~50 m thickness are located directly below the mineralisation. They are associated with disseminated and stringer pyrite (5-20%) and minor chalcopyrite-sphalerite (<5%) mineralisation. This stratiform pyritic stringer zone is connected with zones of intense quartz-pyrite(-sericite) or chlorite-pyrite alteration which cross cut the footwall and intercept the Favourable Horizon with a low angle orientation (20 to 50 degrees). At Central and East

Table 4: Rhyolite and dacite types in the Thalanga sequence

name	description	alteration	occurrences
rhyolite type 1	poorly to moderately quartz-feldspar phyric, fine to medium rhyolite phenocrysts: 1 - 5 vol%; $\leq 1 - 2$ mm feldspar phenocrysts pseudomorphed or obliterated in intensely altered areas geochemistry: Ti/Zr: $3.9 \pm 0.4$ Ti/Th: $45 \pm 12$	moderate to strong alteration common	immediate footwall to Thalanga mineralisation in all sections
rhyolite type 2	highly quartz-feldspar phyric medium rhyolite phenocrysts: 7 - 15 vol%; mainly 2-5mm geochemistry: Ti/Zr: $3.9 \pm 0.4$ Ti/Th: $45 \pm 12$	fresh (water tank hill) to weakly altered	in lower part of east and west Thalanga, outcropping at watertank hill
rhyolite type 3	moderately to highly quartz phyric, fine to medium rhyolite (feldspar phenocrysts absent or subordinate in fresh and altered specimen) phenocrysts: 8-15 vol%; $< 1$ to 2 mm geochemistry: Ti/Zr: $3.9 \pm 0.4$ Ti/Th: $45 \pm 12$	fresh to weakly altered, strongly altered in central Thalanga	railway cutting, west Thalanga (TH410), central Thalanga (TH18, TH38)
rhyolite type 4 (previously referred to as QEP = 'Quartz Eye Porphyry' or QFP = 'Quartz Feldspar Porphyry')	very highly quartz-feldspar phyric, coarse rhyolite phenocrysts: 20-25 vol%; mainly 4-8 mm quartz phenocrysts are commonly blue geochemistry: three sub-types of rhyolite type 4 can be defined based on immobile element ratios: type 4a: Ti/Zr: 4 - 5.5      Ti/Th: 30 - 45 type 4b: Ti/Zr: 5.6 - 11.5      Ti/Th: 95 - 155 type 4c: Ti/Zr: 15.7      Ti/Th: 300	unaltered to weakly altered	intrusions within footwall, at Favourable Horizon position, in hangingwall of west Thalanga
dacite type 1	poorly feldspar phyric; fine dacite (or aphyric dacite) phenocrysts: $< 1$ vol%, $< 1$ mm geochemistry: Ti/Zr: $12.4 \pm 0.4$ Ti/Th: $244 \pm 7$	hematite altn, diss. or vein controlled epidote altn, diss. chlorite and biotite, locally minor diss. actinolite	East Thalanga
dacite type 2	moderately feldspar phyric, medium (to fine) dacite phenocrysts: 1-5 vol%; mainly 1-3 mm geochemistry: Ti/Zr: $11.1 \pm 0.9$ Ti/Th: $244 \pm 20$	epidote ( $\pm$ carbonate $\pm$ actinolite) alteration, hematite alteration, diss. chlorite-biotite	West Thalanga, Central Thalanga
dacite type 3	highly feldspar phyric, fine dacite phenocrysts: 8-15 vol%; $\leq 1$ mm geochemistry: Ti/Zr: $18.7 \pm 1.0$ Ti/Th: $390 \pm 30$	epidote alteration, biotite-chlorite alteration	West, Central and East Thalanga



Thalanga, there are close spatial associations between massive sulphide lenses and up dip terminations of pyritic stringer zones at the Favourable Horizon; the stringer zones appear to represent feeder conduits of high fluid flow.

Zones of intense alteration and pyrite veining in the footwall are enclosed by feldspar destructive, mottled chlorite-sericite alteration with 1-4 vol.% disseminated pyrite and locally mild silicification extending up to at least 200 m stratigraphically into the footwall. The mottled chlorite-sericite  $\pm$  pyrite alteration type has a wide range of textures and common endmembers are: pseudoclastic textures with wispy, phyllosilicate-rich domains and lensoidal quartz-rich domains, phyllosilicate-rich rhyolite with pervasive foliation and rhyolite with blotches of chlorite in a quartz-sericite-rich groundmass (Fig. 9). These different textures are probably the result of the combined effects of heterogeneous devitrification during and after rhyolite emplacement, domainal alteration, and deformation associated with metamorphism. Zones of mottled chlorite-sericite  $\pm$  pyrite alteration have been overprinted by later massive white quartz ( $\pm$  sphalerite) alteration. Resulting textures include patchy white quartz domains, white siliceous 'network-shaped' domains ('pseudomatrix') or massive white quartz (drill core intervals of upto 20 m length) with remnant domains of muscovite-biotite-chlorite (Fig. 9).

The distribution of coherent and volcanoclastic facies in cross section was interpreted from drill core logging and it appears that zones of intense alteration are not confined to volcanoclastic facies. This indicates that permeability contrast between coherent and volcanoclastic facies was not a major factor controlling hydrothermal fluid flow and associated development of alteration zones.

Immobile element ratios of variably altered rhyolite indicate substantial uniformity of primary compositions in footwall rhyolitic rocks (Herrmann, 1994, Paulick, 1997, and Paulick, 1998).

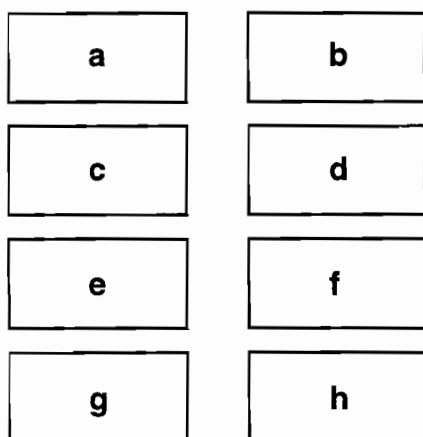
#### *Favourable Horizon*

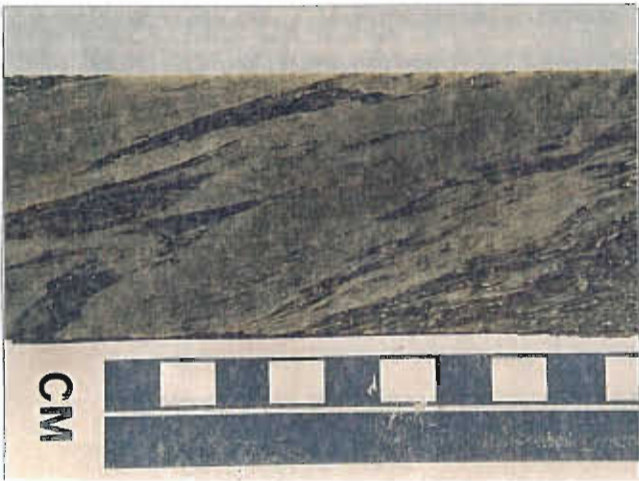
The Thalanga Favourable Horizon in the mine area is occupied by a unit ranging up to a few tens of metres thickness which is comprised of variable assemblages of:

- Massive sulphides (pyrite+sphalerite+galena $\pm$ chalcopyrite $\pm$ magnetite $\pm$ pyrrhotite).
- Semi massive disseminated to patchy sulphides (dominantly sphalerite, galena & chalcopyrite) in a gangue of carbonate-tremolite-chlorite (in West Thalanga) or distinctive bluish quartz crystal rich volcanoclastic materials (typical in East Thalanga).
- Sulphide poor carbonate-tremolite-chlorite rocks which are almost ubiquitous in West Thalanga but of minor proportion elsewhere. Formerly termed "exhalites" they have been

Fig. 9 Some typical textures of variably altered rhyolite from the Thalanga footwall

- a) least altered rhyolite with quartz and feldspar phenocrysts (sample TH394-43.90)
- b) foliated rhyolite with chlorite-sericite±pyrite alteration (sample TH394-114.0, section 32380E)
- c) rhyolite with chlorite-sericite±pyrite alteration and a pseudoclastic texture (sample TH245-224.49, section 20080E)
- d) rhyolite with chlorite-sericite±pyrite alteration and a pseudoclastic texture with blotches of chlorite (sample TH394-293.0, section 32380E)
- e) rhyolite with intense quartz-pyrite-sericite alteration (sample TH394-454.80, section 32380E)
- f) rhyolite with intense chlorite-pyrite alteration (TH85A-383.60, section 31980E)
- g) rhyolite with pseudoclastic texture due to late quartz alteration (apparent matrix) overprinting chlorite-sericite alteration (sample TH247-322.10, section 20080E)
- h) rhyolite with massive, white silicification (late quartz alteration) and remnant sericite-rich domains (sample TH394-197.5)







re-interpreted on the basis of immobile element geochemistry as metamorphosed chlorite-carbonate altered rhyolitic rocks (Herrmann, 1994).

- Massive to semi massive barite usually with some disseminated sulphides, prominent in the up dip fringes of West Thalanga and the West Extended, Vomacka and Far East lenses.
- Minor fine granuloblastic magnetite-quartzite representing metamorphically recrystallised iron-silica exhalites, mainly in the distal or upper fringes of ore lenses and also ~1.5km west of the mine, at the favourable horizon and ~100m above it, in TCF volcanics.
- Relatively non-mineralised coherent coarse quartz-feldspar porphyry (QFP, rhyolite type 4) and coarse-massive to fine-bedded quartz crystal rich volcanics (QEV) variously known as "quartz-eye" tuff/sandstone/porphyry.

Massive, pyritic sulphide lenses and carbonate-tremolite-chlorite associated semi-massive mineralisation are mainly located close to the footwall contact and overlain by QEV and QFP. A close temporal relationship between sulphide forming hydrothermal circulation and QEV-QFP emplacement is implied by the occasional presence of reworked sulphide clasts, local footwall style alteration and lenses of semi massive sulphide, barite and magnetite quartzite within QEV breccias. Peperitic contact relationships indicating that QFP was intruded as coherent sills and lava tongues into wet, non-lithified, QEV volcanics. Thick, coherent QFP is negatively correlated with ore.

### *Hangingwall Units*

Over most of the deposit, the hangingwall is defined by unmineralised and relatively unaltered feldspar phyric to aphyric coherent dacite and associated volcanoclastic facies conformably overlying the QEV/QFP unit of the Favourable Horizon or in direct contact with massive sulphides. Consistent variation in feldspar phenocryst abundance and size range can be used to define 3 types of dacite (Table 4). To the west, dacite type 2 and type 3 are the principal lithofacies in the hangingwall whereas dacite type 1 is dominant in east Thalanga. Top contacts are generally depositional except for dacite type 3 which has intrusive top contacts.

In Central and West Thalanga, the hangingwall sequence includes one or more thick units of andesite which are semi conformable, massive, and appear to be sills. Volcanoclastic sediments of mostly dacitic derivation, including lithic mass flow breccias, sandstones and massive to laminated siltstones interbedded with feldspar crystal-rich turbidites, are a minor component of the hangingwall sequence in the mine area but increase in proportion westward.

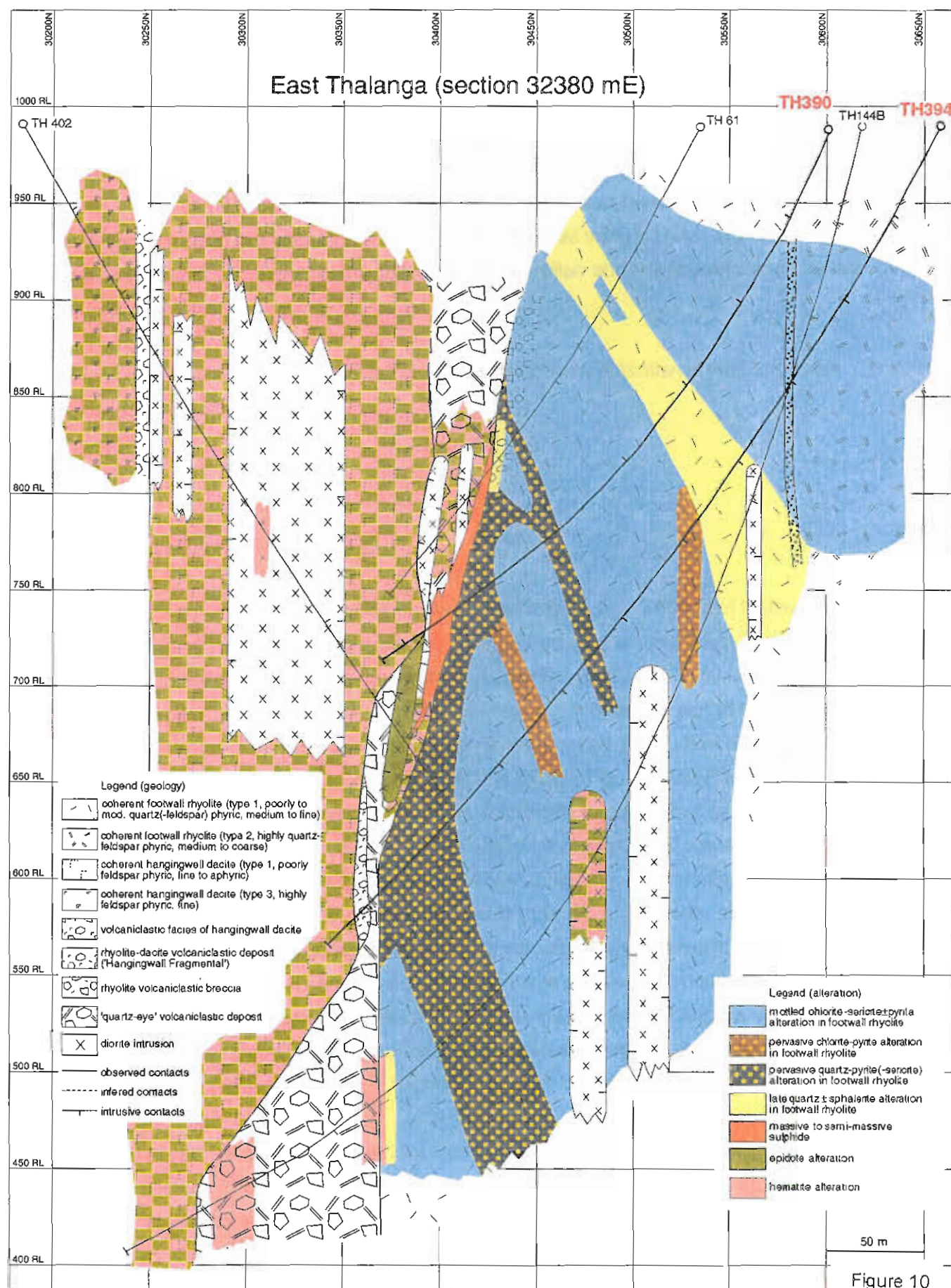
A distinctive volcanoclastic sandstone/breccia known as "Hangingwall Fragmental" (HWF) forms a thin basal unit of the hangingwall sequence in the Vomacka to East Thalanga area. It is interpreted as a dacite-rhyolite gravity flow deposit characterised by coarse, matrix supported, clasts of aphyric dacite and sparse feldspar and quartz crystals in a foliated sericitic matrix.

Alteration of hangingwall dacite is generally patchy or fracture controlled and typical assemblages are epidote+quartz+carbonate±chlorite±actinolite without significant sulphides. Pink hematite staining of feldspar phenocrysts and groundmass domains is ubiquitous. Geochemical data show that most of the dacite was affected by Na-metasomatism (albite alteration, cf. Paulick, 1997) which, however, lacks a reliable textural expression in hand specimen. Post tectonic diorite intrusions show similar epidote+quartz veining and hematite alteration and therefore hangingwall alteration may be largely unrelated to the mineralising hydrothermal system.

#### *East Thalanga (section 32380 E)*

In the east Thalanga section 32380 E (Fig. 8) about 400 m of footwall and hangingwall stratigraphy were intercepted by exploration diamond drilling (Fig. 10). This section contains some economic mineralisation representing the fringes of the east Thalanga ore lens. In the footwall, rhyolite type 2 (highly quartz-feldspar phyric, medium to coarse phenocrysts) with a depositional top contact occurs below rhyolite type 1 (moderately quartz(-feldspar) phyric, fine to medium phenocrysts). In this section rhyolitic volcanoclastic facies is subordinate and it appears that most of the footwall is coherent. The hangingwall consists dominantly of coherent aphyric to poorly feldspar phyric, fine dacite lava (type 1) which is overlain by coherent facies of highly feldspar phyric, fine dacite (type 3). The Favourable Horizon in section 32380E consists of locally mineralised massive to normal graded 'quartz-eye' volcanoclastics and minor rhyolite-dacite gravity flow deposits (Hangingwall Fragmental). Massive, unfoliated diorite intrusions with chilled margins are common in section 32380E and occur in the footwall, the hangingwall and the Favourable Horizon.

Alteration of footwall rhyolites shows a well developed zonal pattern in section 32380 E with a general increase in alteration intensity approaching the mineralised part of the Favourable Horizon. A broad mottled chlorite-sericite±pyrite zone envelopes zones of intense quartz-pyrite-sericite and chlorite-pyrite alteration and was locally overprinted by late quartz alteration. An up to 50 m thick zone of quartz-pyrite alteration underlies the mineralised part of the Favourable Horizon and extends down dip for at least 100 m beyond the massive



sulphides. The hangingwall dacites commonly show patchy to vein controlled epidote and hematite alteration which also occurs in some parts of the 'quartz-eye' volcanoclastic facies in the Favourable Horizon and in diorite intrusions.

Drill core of diamond drill hole (DDH) TH394 shows the progressive increase in alteration intensity from least altered rhyolite type 2 through to strongly quartz-pyrite altered rhyolite type 1 close to the Favourable Horizon (Fig. 11). Various textural endmembers of the mottled chlorite-sericite±pyrite alteration are present in TH394 as well as zones of pyrite veining associated with quartz-pyrite and chlorite-pyrite alteration and zones overprinted by late quartz alteration.

Diamond drill hole TH390 intercepted massive sulphide mineralisation in the Favourable Horizon up dip from TH394.

#### *West Thalanga (section 20080 E)*

Cores from several exploration diamond drill holes expose about 500 m of footwall and hangingwall stratigraphy on cross section 20080 E through the main West Thalanga ore lens (Fig. 12). In the footwall, highly porphyritic rhyolite (type 2) is overlain by less porphyritic rhyolite (type 1). Rhyolite type 1 is mainly coherent in the down dip part of the section whereas monomict rhyolite breccia (typically normal graded gravity flow deposits) are common in the up dip part (cf. graphic log of DDH TH247; Fig. 13). The Favourable Horizon contains massive to semi-massive sulphides dominantly in calcareous gangue, zones of carbonate-chlorite-tremolite 'pseudoexhalite' and minor 'quartz-eye' volcanoclastic sandstone (cf. graphic log of underground hole: W2011NED42; Fig. 14). The hangingwall consists of a series of moderately feldspar phyric dacite lavas (type 2), a stratiform, highly feldspar phyric dacite intrusion (type 3) and stratiform andesite intrusions. The interpretation of intrusive emplacement is based on examination of top contacts and the observation of displaced rhyolitic breccia and 'quartz eye' volcanoclastic sandstone into the hangingwall. A normal fault, which offsets the Favourable Horizon to the south, was interpreted based on the arrangement of lithological units in the down dip parts of the section.

A zone of intense quartz-pyrite-sericite alteration underlies the massive sulphides in section 20080 E which extends ~ 10 to 50 m into the footwall and ~ 100 m down dip beyond economic mineralisation. Stratigraphically below this zone of intense alteration the footwall alteration is mainly of the mottled chlorite-sericite±pyrite type and a gradation into least altered rhyolite at about 200 m below the mineralisation can be observed in the up dip part of the section (Fig. 13). In the down dip part, zones of disseminated carbonate-zoisite-epidote-



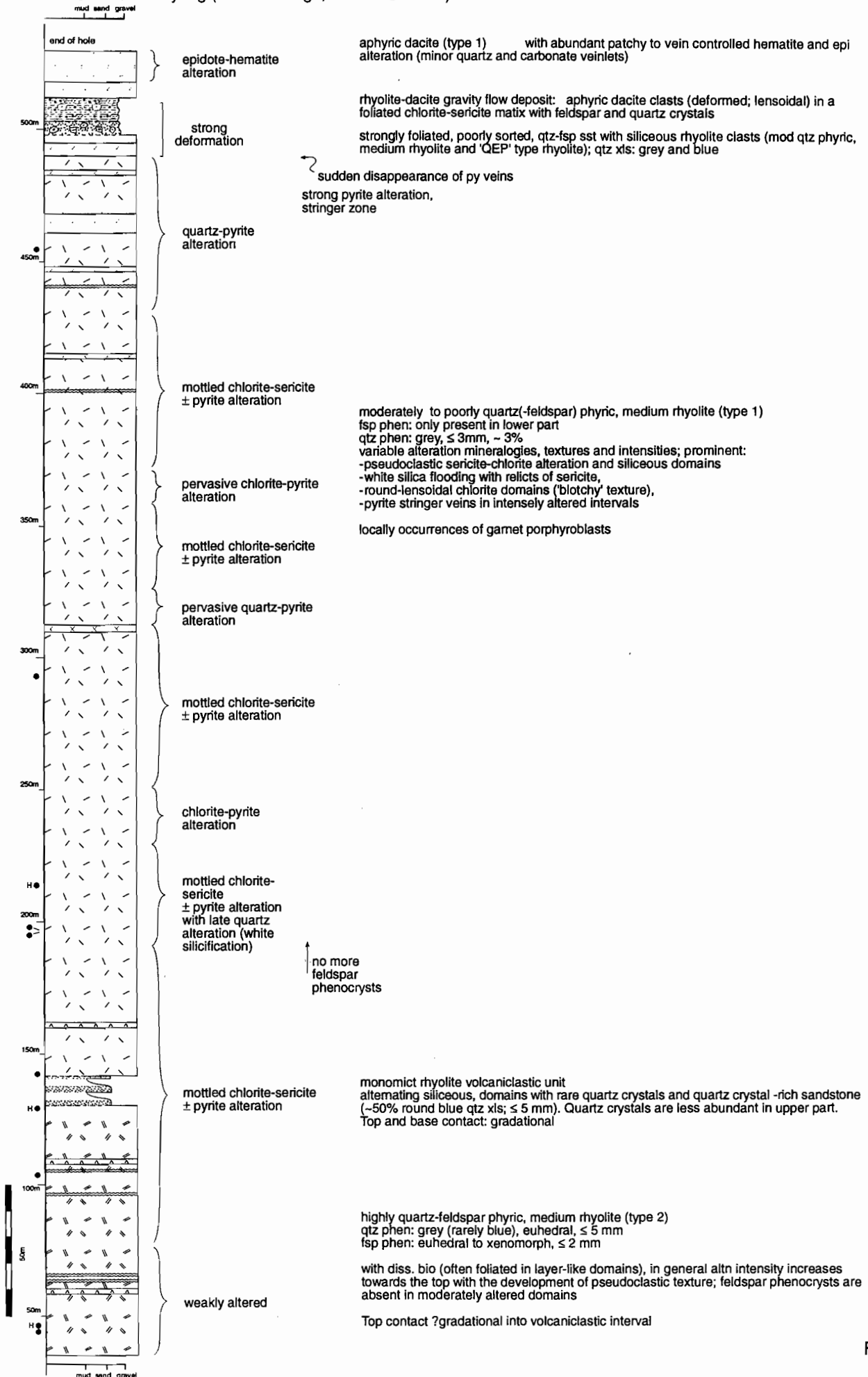


Figure 11

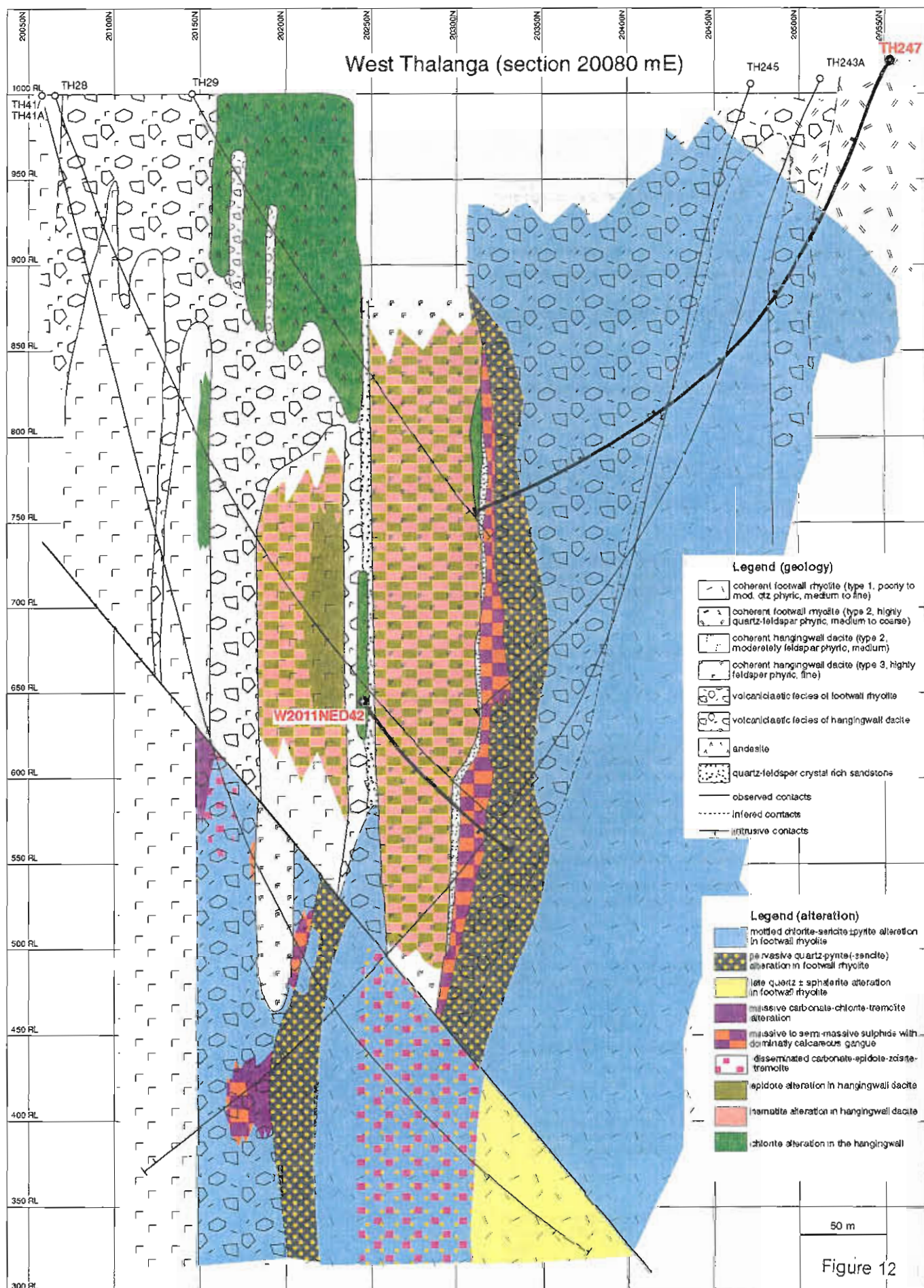


Figure 12

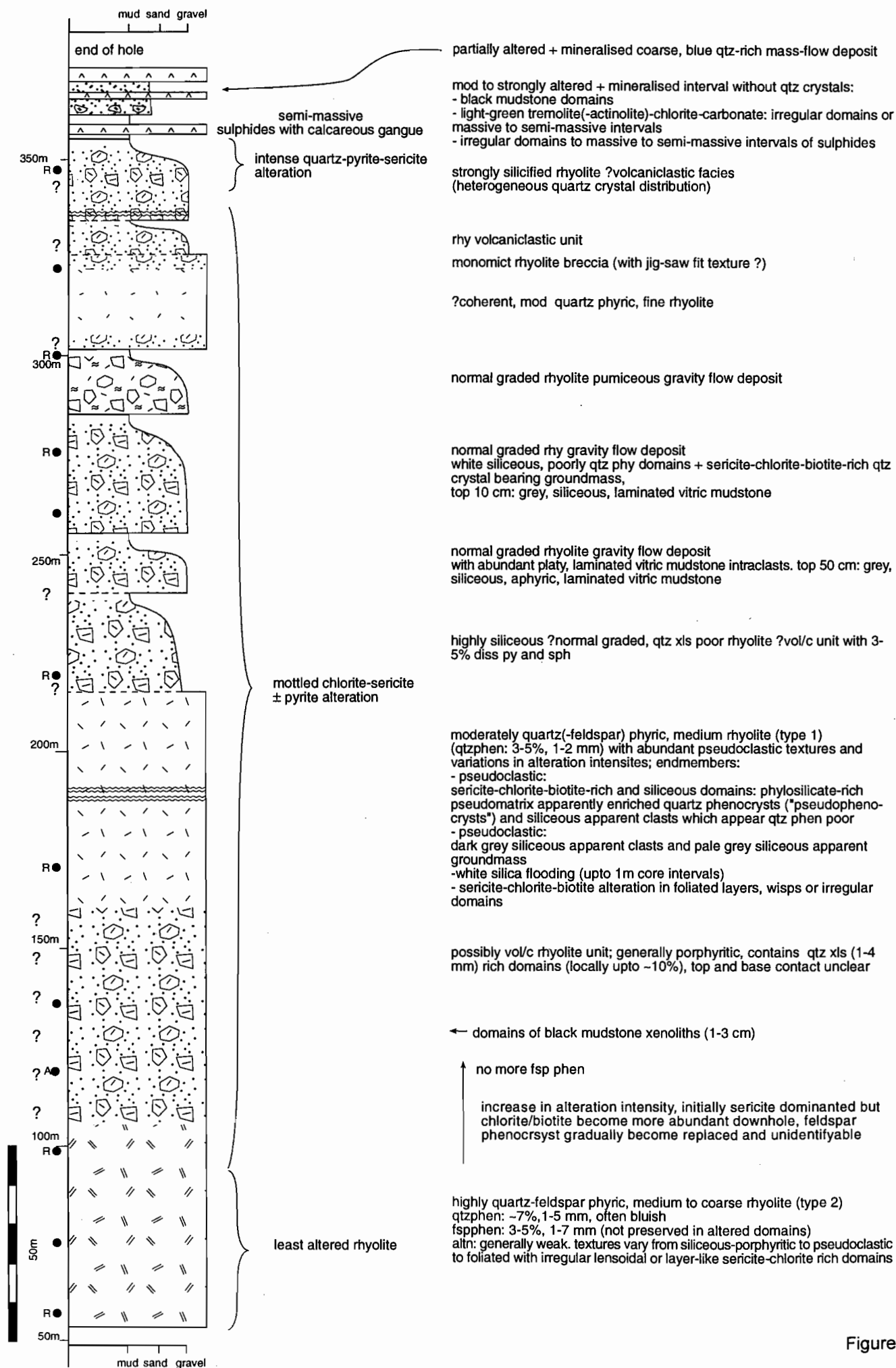
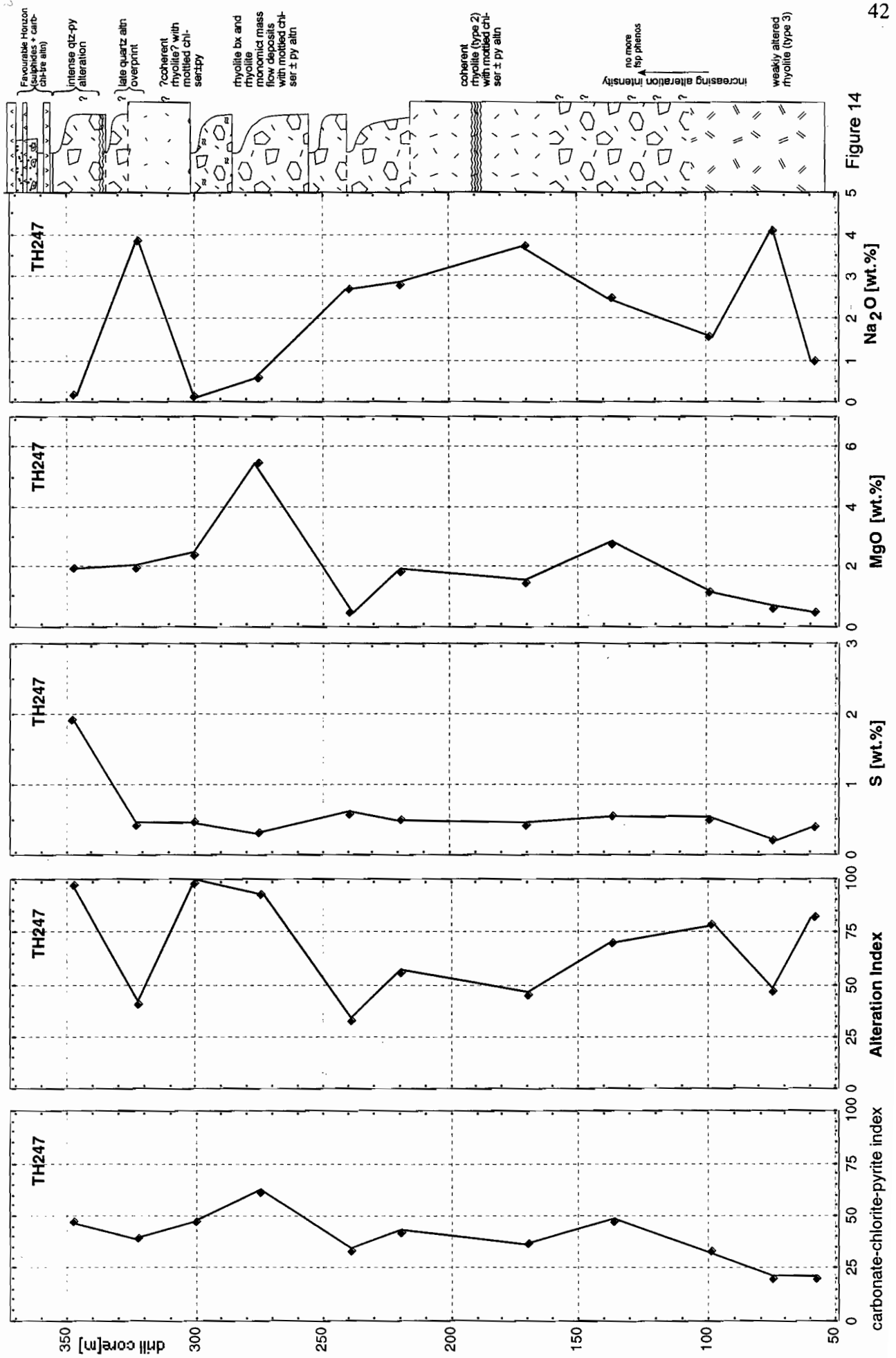
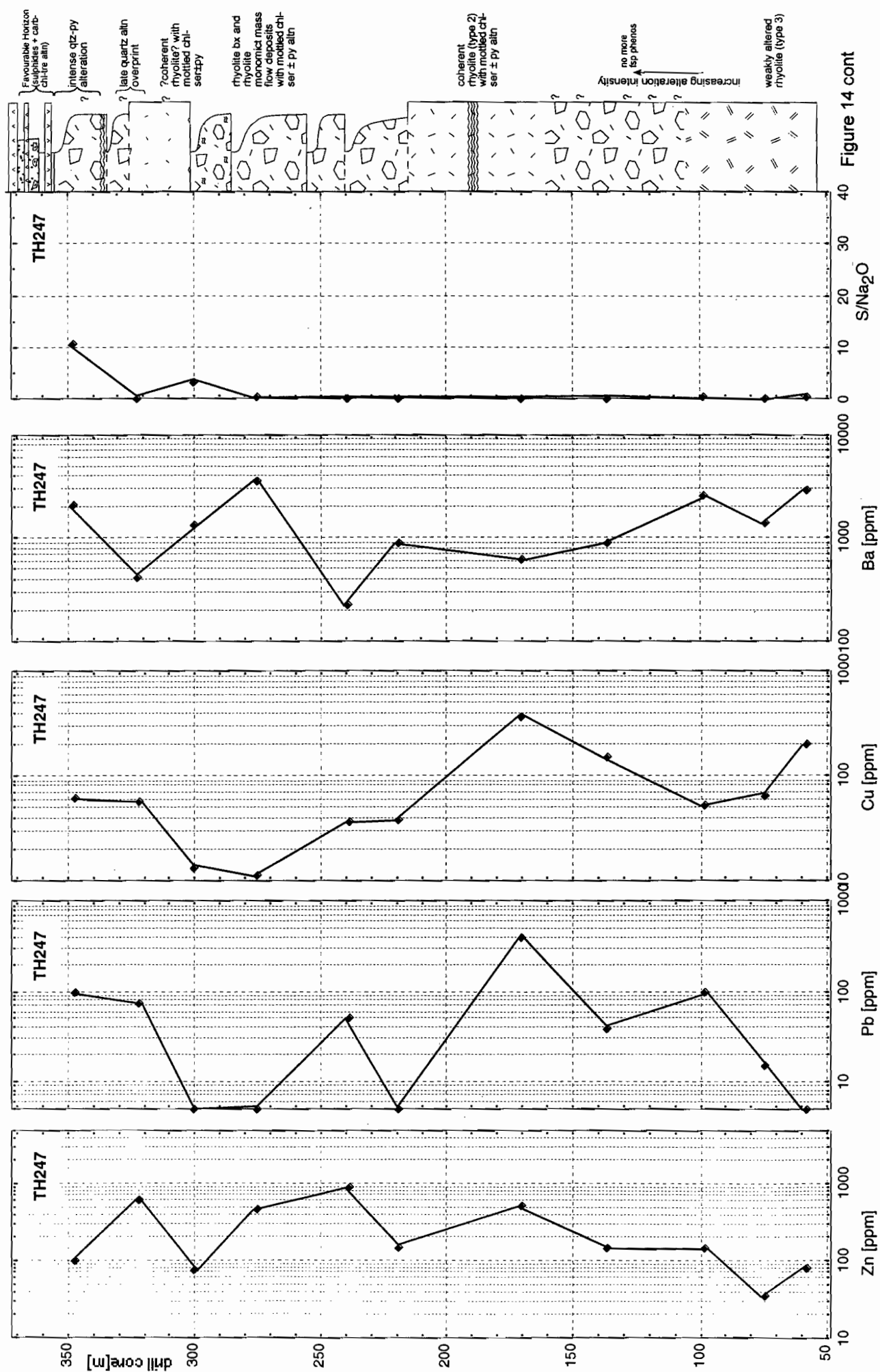
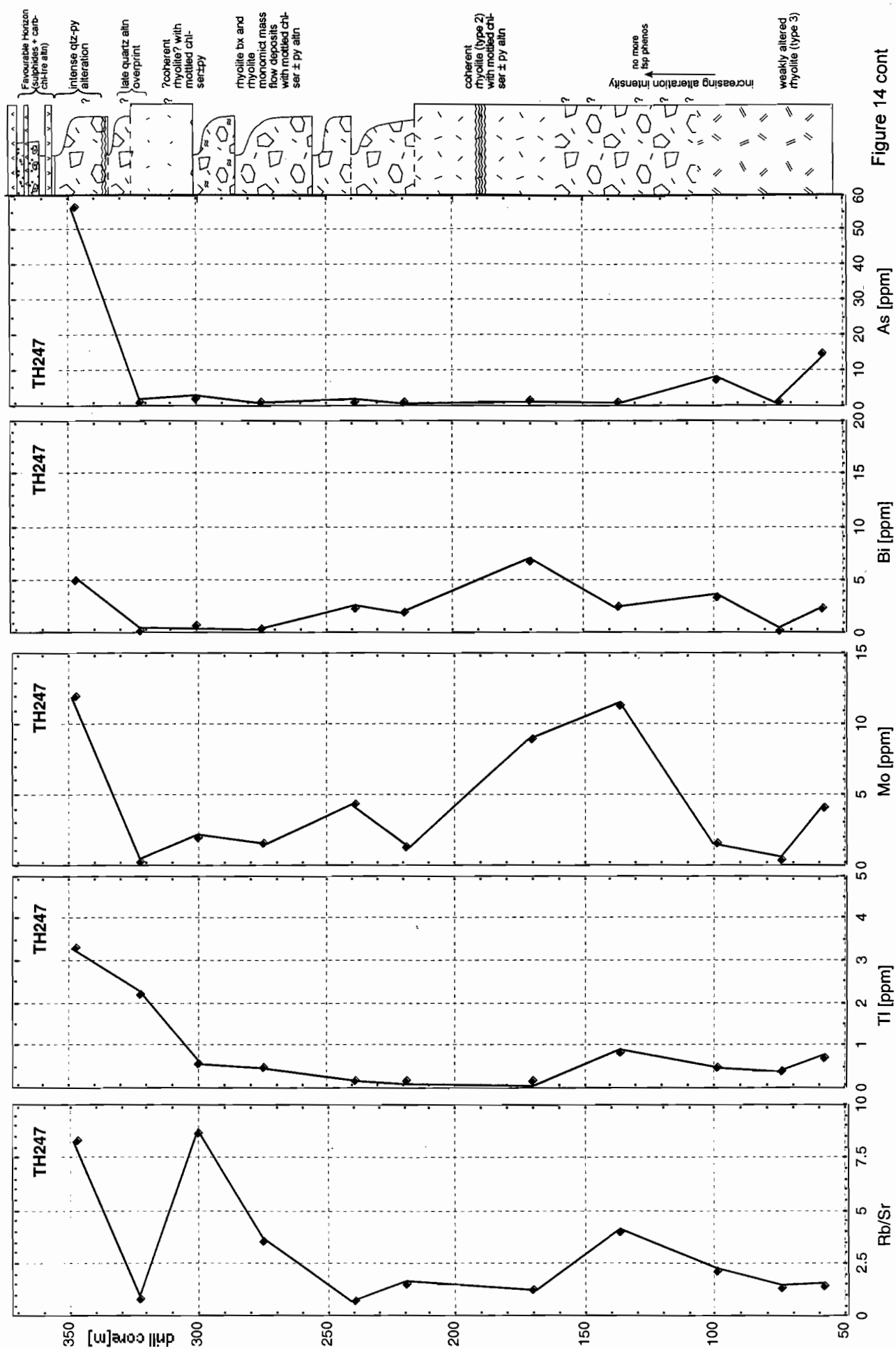


Figure 13









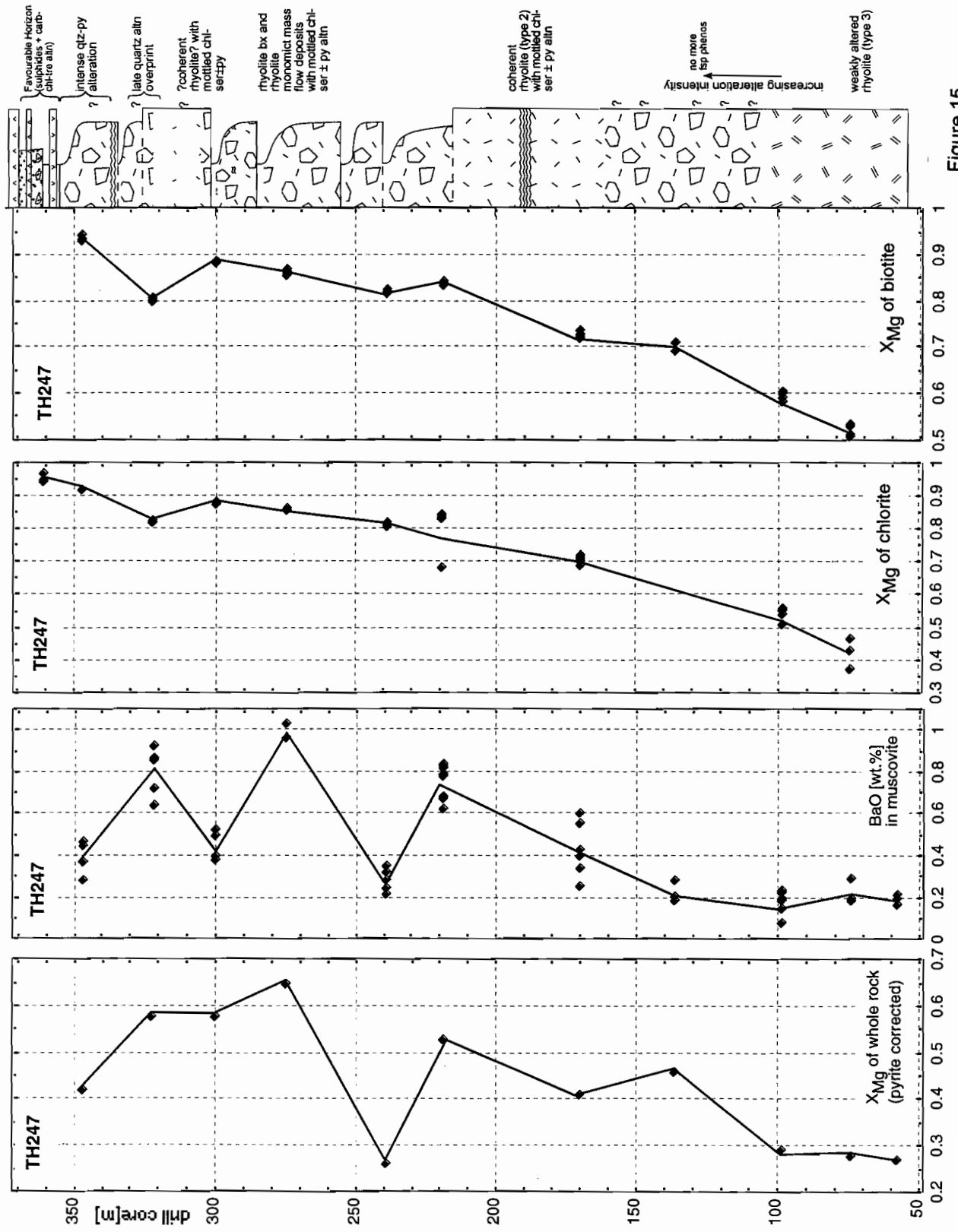


Figure 15

tremolite and late quartz alteration occur. Dacites in the hangingwall are generally fresh or epidote-hematite altered. Chlorite-dominated alteration in the hangingwall is mainly confined to andesites corresponding to their mafic geochemical composition.

Geochemical analyses of samples from DDH TH247 show some general compositional changes which are characteristic ore proximity indicators at Thalanga (Fig. 14). A decrease in  $\text{Na}_2\text{O}$  concentration and increase in  $\text{MgO}$ , Alteration Index and Chlorite-Carbonate-Pyrite Index are common features of moderately altered rhyolite in relatively distal positions to the mineralisation. Close to the mineralisation (mainly in the quartz-pyrite-sericite altered rhyolite) pronounced increase in trace elements such as As, Bi, Mo, and Tl can be observed.

The composition of chlorite and biotite of samples from TH247 changes systematically approaching the mineralisation (Fig. 15). In least altered rhyolite, the  $X_{\text{Mg}}$  of chlorite and biotite is relatively low ( $\sim 0.5$ ) and increases steadily to values of 0.85 to 0.95 close to the mineralisation.

The sulphide intersection in W2011NED42 is typical of the West Thalanga ore lens (Fig. 16). In this hole, mineralisation consists of a lower lens of massive pyrite,  $\sim 5\text{m}$  thick, immediately overlying altered footwall rhyolitic volcanoclastics and an upper sphalerite rich massive sulphide lens,  $\sim 2\text{m}$  thick. Quartz-eye volcanoclastic breccia overlying the upper sulphide lens, contains rare clasts of massive pyrite and massive barite consistent with a synvolcanic origin for the sulphide deposit.

The sulphide lenses are separated by  $\sim 8\text{m}$  of variably chlorite, tremolite, dolomite and calcite rich assemblages with patchy minor to semi-massive sulphides. These rocks have extremely Mg, Ca and  $\text{CO}_2$  rich compositions and were originally interpreted as carbonate rich chemical sediments ("exhalites") precipitated on the sea floor from VHMS associated hydrothermal fluids (Fig. 17). However, they have similar immobile element characteristics to footwall rhyolites (Fig. 18) which strongly supports the interpretation that they originated as chlorite+carbonate altered rhyolitic volcanoclastics, subsequently metamorphosed to tremolite bearing assemblages. Their compositions plot near the top of the AI-CCPI boxplot in fields similar to chlorite+carbonate alteration assemblages closely associated with sulphide ore at Rosebery (Figure 19).

#### *Alteration geochemistry and halo model*

Based on the geometry of the alteration zones interpreted from drill core logging and the study of geochemical data a general model for the hydrothermal system of the Thalanga deposit can be inferred (Fig. 20). The volumetrically dominant alteration type of footwall

Table 5: Geochemistry of samples from DDH TH247

HOLE_ID	TH247	TH247	TH247	TH247	TH247	TH247	TH247	TH247	TH247	TH247	TH247	TH247	TH247	TH247	TH247	TH247	TH247
DEPTH_FRC	57.7	74.5	78.3	75.4	79.5	73.7	75.1	79.6	80.8	65.5	78.0	79.2	322.1	347.2	TH247	TH247	TH247
DEPTH_TO	57.9	74.65	78.3	75.4	79.5	73.7	75.1	79.6	80.8	65.5	78.0	79.2	322.1	347.2	TH247	TH247	TH247
SOURCE	RGC Expl	Paulick (1998)	Paulick (1998)	RGC Expl	Hill (1996)	Paulick (1998)	RGC Expl	RGC Expl	RGC Expl	RGC Expl	RGC Expl	RGC Expl	Paulick (1998)	RGC Expl	Paulick (1998)	RGC Expl	RGC Expl
SAMP_ID	32146	TH247-2	TH247-2	TH247-2	TH247-119	TH247-3	TH247-3	TH247-3	TH247-3	TH247-3	TH247-3	TH247-3	TH247-3	TH247-3	TH247-3	TH247-3	TH247-3
rocktype	rhyolite	rhyolite	rhyolite	rhyolite	rhyolite	rhyolite	rhyolite	rhyolite	rhyolite	rhyolite	rhyolite	rhyolite	rhyolite	rhyolite	rhyolite	rhyolite	rhyolite
[wt.%]																	
SiO2	78.9	78.3	78.3	75.4	79.5	73.7	75.1	79.6	80.8	65.5	78.0	79.2	322.1	347.2	TH247	TH247	TH247
TiO2	0.08	0.11	0.11	0.13	0.13	0.13	0.10	0.08	0.05	0.13	0.12	0.09	322.25	347.35	TH247	TH247	TH247
Al2O3	9.21	11.81	12.50	12.50	10.68	13.31	11.68	10.64	7.73	13.47	12.65	10.70	300.2	347.35	TH247	TH247	TH247
Fe2O3	1.24	1.39	2.69	2.69	2.19	3.13	2.07	1.70	1.47	2.70	1.79	1.50	300.2	347.35	TH247	TH247	TH247
MnO	0.02	0.04	0.05	0.05	0.05	0.10	0.06	0.04	0.02	0.10	0.02	0.06	300.2	347.35	TH247	TH247	TH247
MgO	0.44	0.58	1.12	1.12	1.20	2.77	1.44	1.84	0.46	5.50	2.40	1.98	300.2	347.35	TH247	TH247	TH247
CaO	0.24	0.24	0.15	0.15	0.21	0.32	0.36	0.11	0.15	0.17	0.01	1.07	300.2	347.35	TH247	TH247	TH247
Na2O	0.97	4.06	1.56	1.56	2.10	2.50	3.72	2.78	2.72	0.57	0.15	3.84	300.2	347.35	TH247	TH247	TH247
K2O	5.18	3.25	5.52	5.52	3.63	3.88	1.83	1.90	0.93	4.48	4.34	1.45	300.2	347.35	TH247	TH247	TH247
P2O5	0.01	0.02	0.01	0.01	0.02	0.02	<0.01	<0.01	<0.01	0.01	0.01	0.01	300.2	347.35	TH247	TH247	TH247
LOI		0.71			0.62	2.02							300.2	347.35	TH247	TH247	TH247
S	0.38	0.20	0.51	0.51	0.28	0.56	0.42	0.49	0.57	0.30	0.48	0.41	300.2	347.35	TH247	TH247	TH247
Total	96.67	100.52	99.64	99.64	100.26	101.85	96.78	99.17	94.90	92.93	99.97	100.94	300.2	347.35	TH247	TH247	TH247
[ppm]																	
Ba	2920	1409	2600	2600	2388	902	622	914	225	3530	1370	411	57	61	TH247	TH247	TH247
Cu	197	64	53	53	101	148	360	38	36	11	13	57	73	100	TH247	TH247	TH247
Pb	5	15	100	100	604	39	400	5	50	5	5	73	609	101	TH247	TH247	TH247
Zn	82	36	145	145	101	145	513	146	911	463	75	609	101	56	TH247	TH247	TH247
As	15	1.4	7	7	1.4	1.4	2	<1	1	<1	2	1.4	1.4	56	TH247	TH247	TH247
Bi	2.4	0.2	3.5	3.5	2.5	2.5	6.7	2.0	2.3	0.5	0.7	0.2	0.2	5.1	TH247	TH247	TH247
Mo	4.1	<0.5	1.5	1.5	11.3	11.3	9.0	1.3	4.4	1.5	2.0	0.2	0.2	12.0	TH247	TH247	TH247
Rb	92	72	112	112	72	159	80	77	25	166	157	59	71	21	TH247	TH247	TH247
Sb	1.04	0.04	0.44	0.44	0.15	0.15	<0.2	<0.2	<0.2	<0.2	<0.2	2.32	2.32	1.48	TH247	TH247	TH247
Sr	65	54	51	51	1	40	64	51	33	47	18	71	42	21	TH247	TH247	TH247
Th	9	11	12	12	4	12	12	12	8	13	13	7	7	19	TH247	TH247	TH247
Tl	0.7	0.40	0.5	0.5	0.86	0.86	0.2	0.2	0.2	0.5	0.6	2.2	2.2	3.3	TH247	TH247	TH247
U	3.09	2.92	2.67	2.67		2.93	2.05	3.78	2.02	4.52	3.43	2.2	2.2	4.81	TH247	TH247	TH247
Y		34			25	32						42	42	274	TH247	TH247	TH247
Zr	118	149	172	172	142	164	141	133	89	198	181	143	143	274	TH247	TH247	TH247
Ti/Zr	3.95	4.46	4.42	4.42	3.83	4.50	4.21	3.63	3.51	3.96	4.05	3.83	3.83	3.87	TH247	TH247	TH247
Al/tn Index	82	47	79	79	68	70	45	56	33	93	98	41	41	97	TH247	TH247	TH247
CCP Index	20	20	33	33	36	47	37	42	33	61	47	39	39	47	TH247	TH247	TH247
S/Na2O	0.4	0.05	0.3	0.3	0.1	0.2	0.1	0.2	0.2	0.5	3.2	0.1	0.1	10.6	TH247	TH247	TH247
Rb/Sr	1.4	1.3	2.2	2.2		4.0	1.3	1.5	0.8	3.5	8.7	0.8	0.8	8.3	TH247	TH247	TH247

6  
Table 3: geochemistry of samples from DDH TH394

HOLE_ID	TH394	TH394	TH394	TH394	TH394	TH394	TH394	TH394	TH394	TH394	TH394	TH394	TH394	TH394	TH394	TH394	TH394
DEPTH_FROM	43.8	46.8	47.2	48.8	49.2	50.8	51.2	52.8	53.2	54.8	55.2	56.8	57.2	58.8	59.2	60.8	61.2
DEPTH_TO	44	47.2	47.2	48.8	49.2	50.8	51.2	52.8	53.2	54.8	55.2	56.8	57.2	58.8	59.2	60.8	61.2
SOURCE	Paulick (1998)	Hermann 94	Paulick (1998)	Hermann 94	Paulick (1998)	Hermann 94	Paulick (1998)	Hermann 94	Paulick (1998)	Hermann 94	Paulick (1998)	Hermann 94	Paulick (1998)	Hermann 94	Paulick (1998)	Hermann 94	Paulick (1998)
SAMP_ID	TH394-1	TH394-1	TH394-2	TH394-2	TH394-3	TH394-3	TH394-4	TH394-4	TH394-5	TH394-5	TH394-6	TH394-6	TH394-7	TH394-7	TH394-8	TH394-8	TH394-9
rocktype	rhyolite	rhyolite	rhyolite	rhyolite	rhyolite	rhyolite	rhyolite	rhyolite	rhyolite	rhyolite	rhyolite	rhyolite	rhyolite	rhyolite	rhyolite	rhyolite	rhyolite
[wt.%]																	
SiO <sub>2</sub>	76.4	81.3	72.6	75.9	77.4	78.0	78.2	79.6	78.2	79.6	75.7	75.7	78.8	78.8	75.7	75.7	78.8
TiO <sub>2</sub>	0.11	0.08	0.13	0.11	0.09	0.08	0.08	0.07	0.08	0.07	0.07	0.07	0.05	0.05	0.07	0.07	0.05
Al <sub>2</sub> O <sub>3</sub>	11.90	9.88	14.61	13.00	11.85	11.27	11.70	10.89	11.70	10.89	11.38	11.38	6.60	6.60	11.38	11.38	6.60
Fe <sub>2</sub> O <sub>3</sub>	1.64	1.23	1.83	1.68	1.13	1.40	1.35	1.34	1.35	1.34	5.14	5.14	7.03	7.03	5.14	5.14	7.03
MnO	0.04	0.03	0.03	0.03	0.02	0.04	0.01	0.02	0.04	0.01	0.08	0.08	<0.01	<0.01	0.08	0.08	<0.01
MgO	0.67	0.35	1.53	1.25	0.76	1.43	0.59	0.64	0.59	0.64	2.38	2.38	0.39	0.39	2.38	2.38	0.39
CaO	1.42	0.93	0.33	0.64	0.46	0.25	0.14	0.15	0.25	0.14	<0.01	<0.01	0.03	0.03	<0.01	<0.01	0.03
Na <sub>2</sub> O	2.27	2.03	1.41	2.03	4.79	2.49	2.74	3.32	2.74	3.32	0.21	0.21	0.19	0.19	0.21	0.21	0.19
K <sub>2</sub> O	4.04	3.54	5.09	3.90	1.82	3.09	3.64	2.04	3.64	2.04	2.39	2.39	2.01	2.01	2.39	2.39	2.01
P <sub>2</sub> O <sub>5</sub>	0.02	0.03	0.02	0.02	0.01	0.01	0.01	0.02	0.01	0.02	0.01	0.01	0.01	0.01	0.02	0.01	0.01
LOI	0.60	0.41	1.60	1.07	0.49	1.36	1.29	1.47	1.29	1.47	2.75	2.75	4.43	4.43	2.75	2.75	4.43
S	0.01	0.04	<0.01	<0.01	<0.01	0.49	0.79	0.85	0.79	0.85	0.65	0.65	5.42	5.42	0.65	0.65	5.42
Total	99.15	99.80	99.17	99.66	98.81	99.44	99.79	99.56	99.79	99.56	100.06	100.06	99.54	99.54	100.06	100.06	99.54
[ppm]																	
Ba	1069	726	615	515	329	789	1193	726	1193	726	335	335	256	256	335	335	256
Cu	5	9	3	1	3	22	13	7	22	13	18	18	66	66	18	18	66
Pb	20	5	8	5	14	25	87	37	25	87	11	11	48	48	11	11	48
Zn	49	31	59	54	40	262	316	26	316	26	79	79	45	45	79	79	45
As	<1	<1	<1	<1	<1	4	2	3	4	2	3	3	16	16	3	3	16
Bi	0.6	0.3	0.3	0.3	0.3	0.2	0.6	0.3	0.2	0.6	0.3	0.3	8.4	8.4	0.3	0.3	8.4
Mo	0.8	0.8	<0.5	1.5	<0.5	1.5	1.8	1.4	1.5	1.8	1.4	1.4	2.8	2.8	1.4	1.4	2.8
Rb	111	138	138	55	55	93	82	66	93	82	66	66	60	60	66	66	60
Sb	0.2	0.2	0.2	0.2	0.2	0.2	0.3	0.2	0.2	0.3	0.2	0.2	0.3	0.3	0.2	0.2	0.3
Sr	83	48	48	50	50	34	42	8	34	42	8	8	5	5	8	8	5
Th	12	16	16	14	14	11	14	13	11	14	13	13	7	7	13	13	7
Tl	0.5	0.6	0.6	0.1	0.1	1.9	1.4	0.1	1.9	1.4	0.1	0.1	0.6	0.6	0.1	0.1	0.6
U	2.19	3.1	3.1	2.55	2.55	3.6	3.21	2.21	3.6	3.21	2.21	2.21	1.48	1.48	2.21	2.21	1.48
Y	40	23	46	39	34	38	43	38	38	43	37	37	21	21	37	37	21
Zr	148	135	193	184	139	117	138	128	138	128	131	131	76	76	131	131	76
Ti/Zr	4.45	3.51	4.08	3.66	3.87	4.11	3.52	3.20	3.52	3.20	3.29	3.29	3.96	3.96	3.20	3.29	3.96
Alin Index	56	57	79	66	33	62	59	44	59	44	96	96	92	92	44	96	92
CCP Index	25	21	33	32	21	33	22	26	33	22	73	73	75	75	26	73	75
Si/Na <sub>2</sub> O	0.004	0.02	0.003	0.001	0.001	0.2	0.3	0.3	0.2	0.3	3.0	3.0	27.0	27.0	0.3	3.0	27.0
Rb/Sr	1.3		2.9		1.1	2.7	2.0	8.1	2.0	2.7	8.1	8.1	11.6	11.6	2.0	8.1	11.6



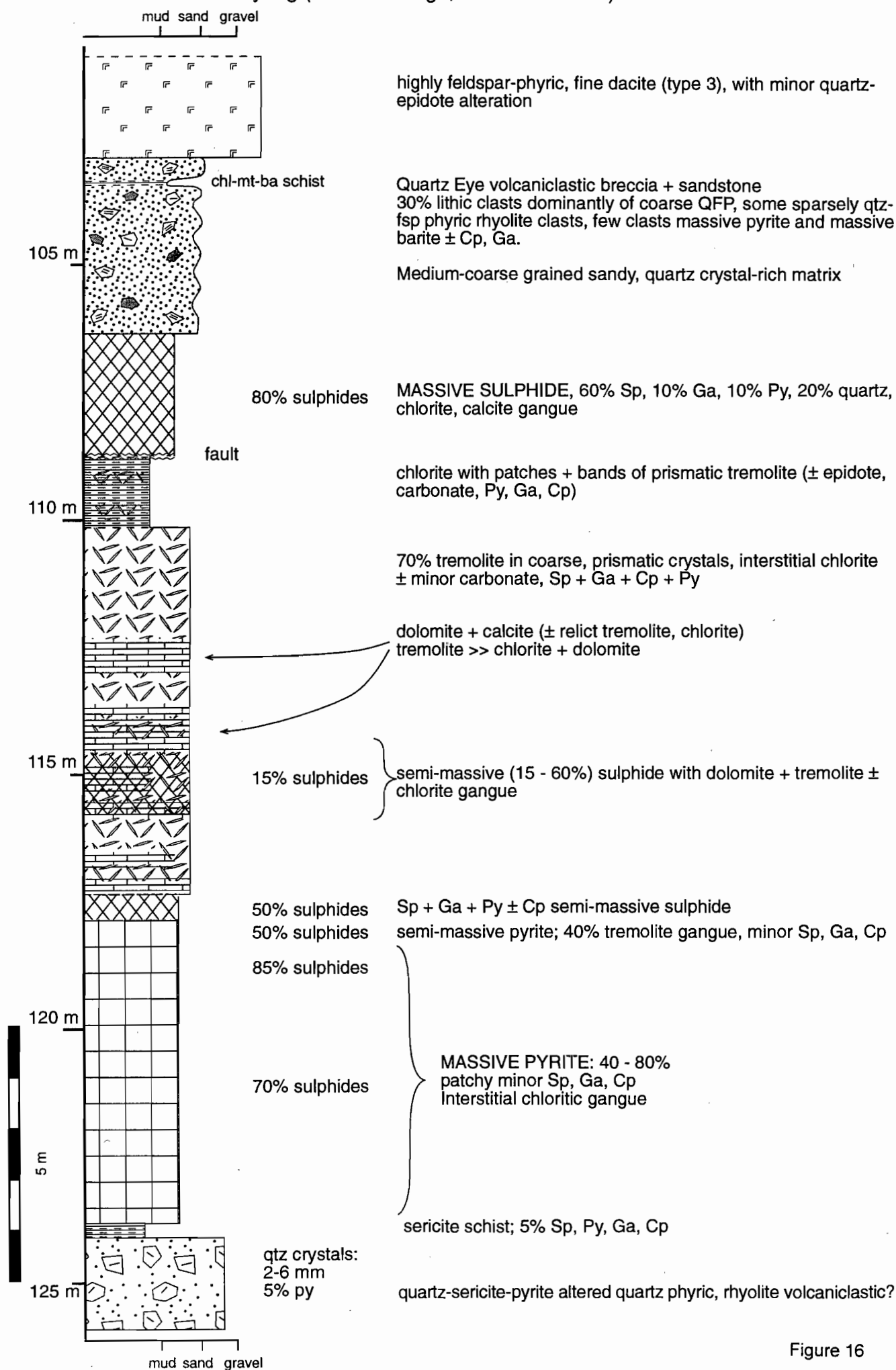


Figure 16

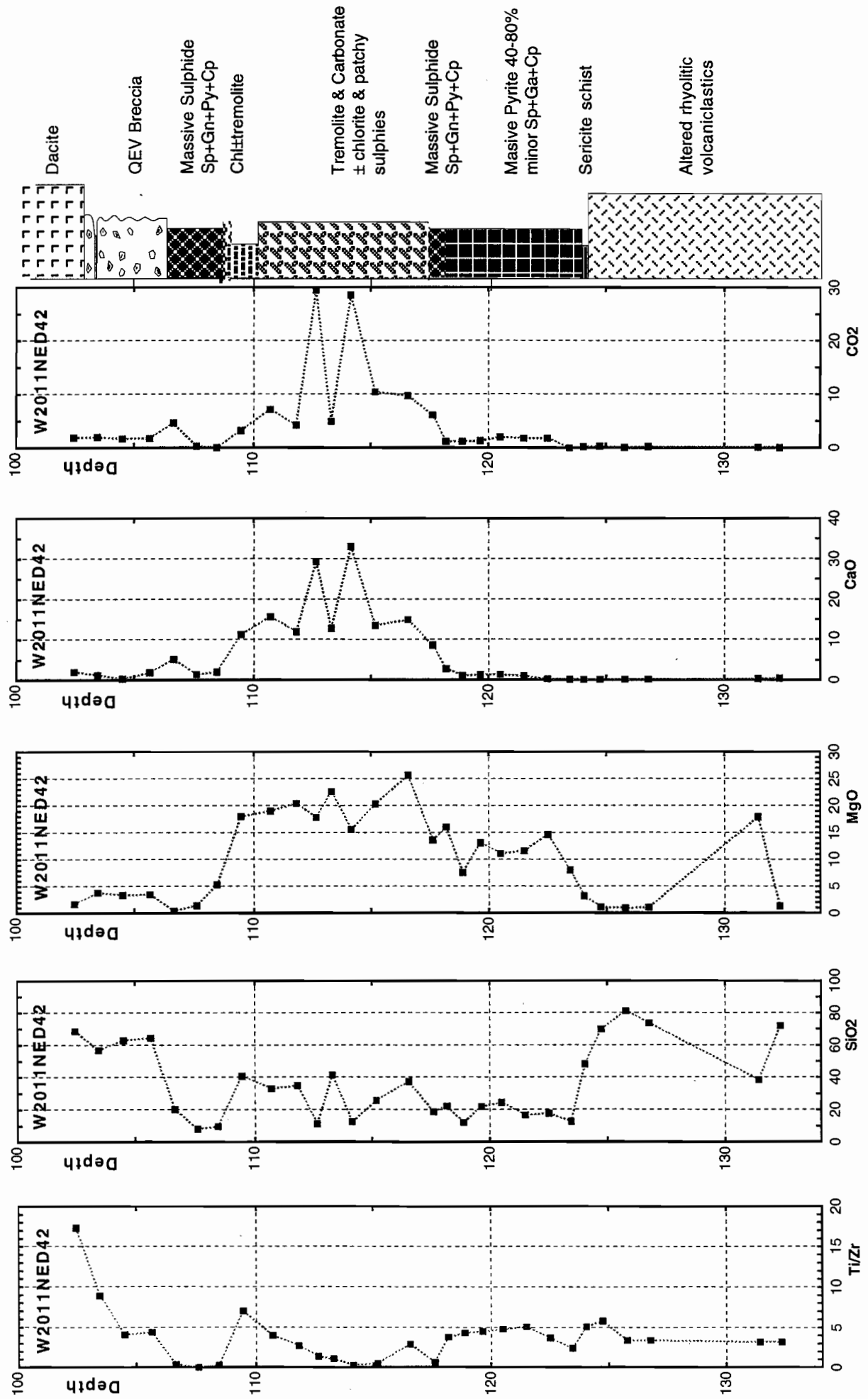


Figure 17 Downhole geochemistry of the favourable horizon intersection in W2011NED42, West Thalanga. All components in wt% (except Ti/Zr)

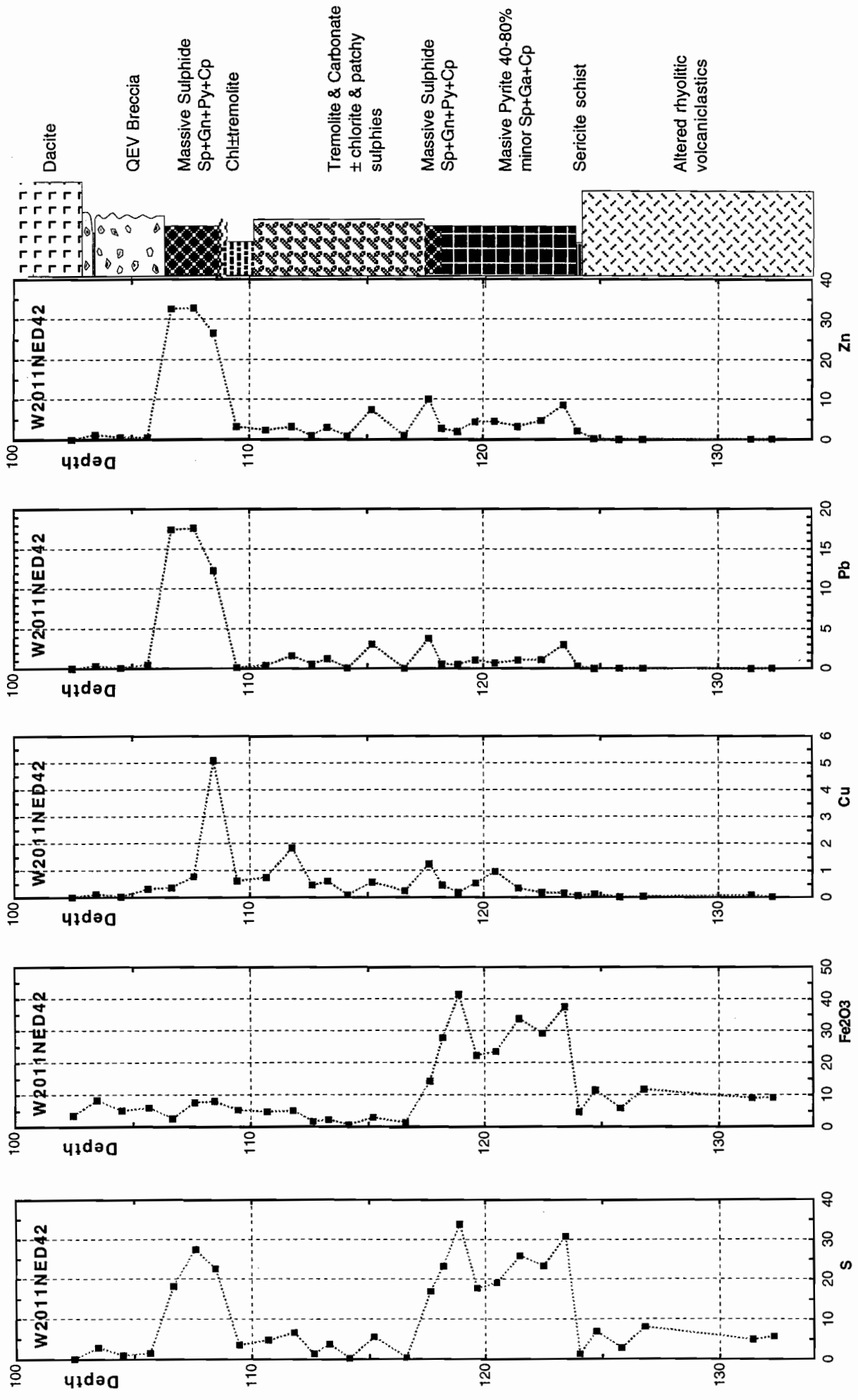


Figure 17 cont Downhole geochemistry of the favourable horizon intersection in W2011NED42, West Thalanga.  
All components in wt% (except Ti/Zr)

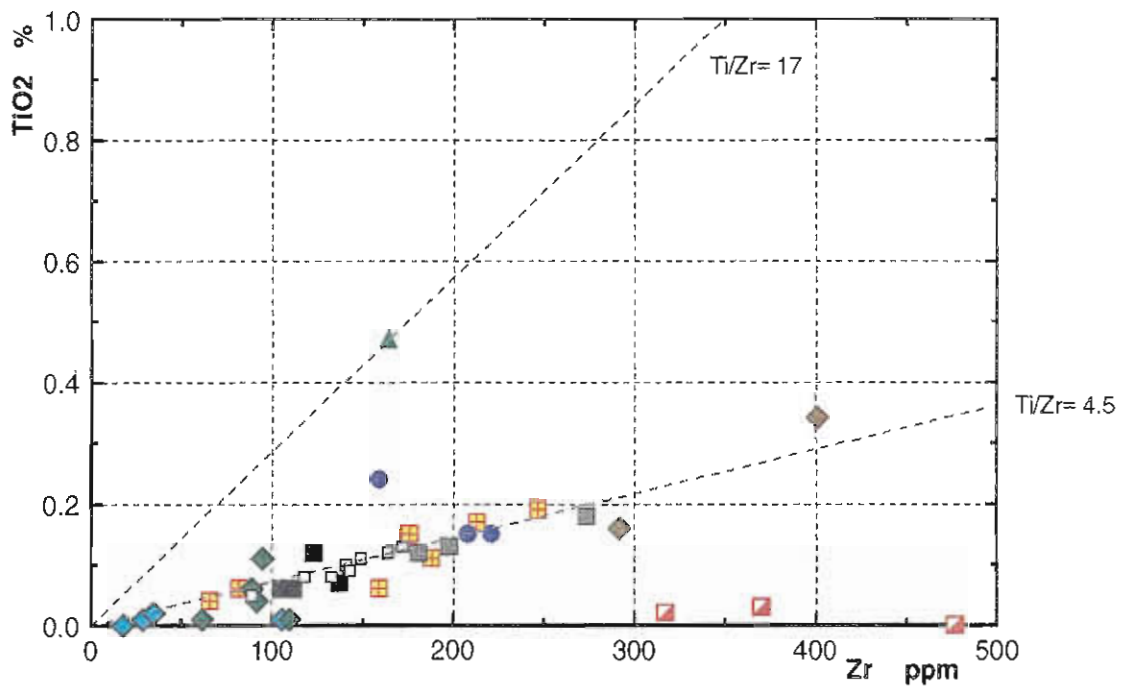


Figure 18 Zr-TiO<sub>2</sub> immobile element plot for samples from drill holes TH247 and W2011NED42, West Thalanga; legend as for Figure 12. The tremolite & carbonate rich pseudoexhalites plot on a linear trend including least altered and altered footwall rhyolites.

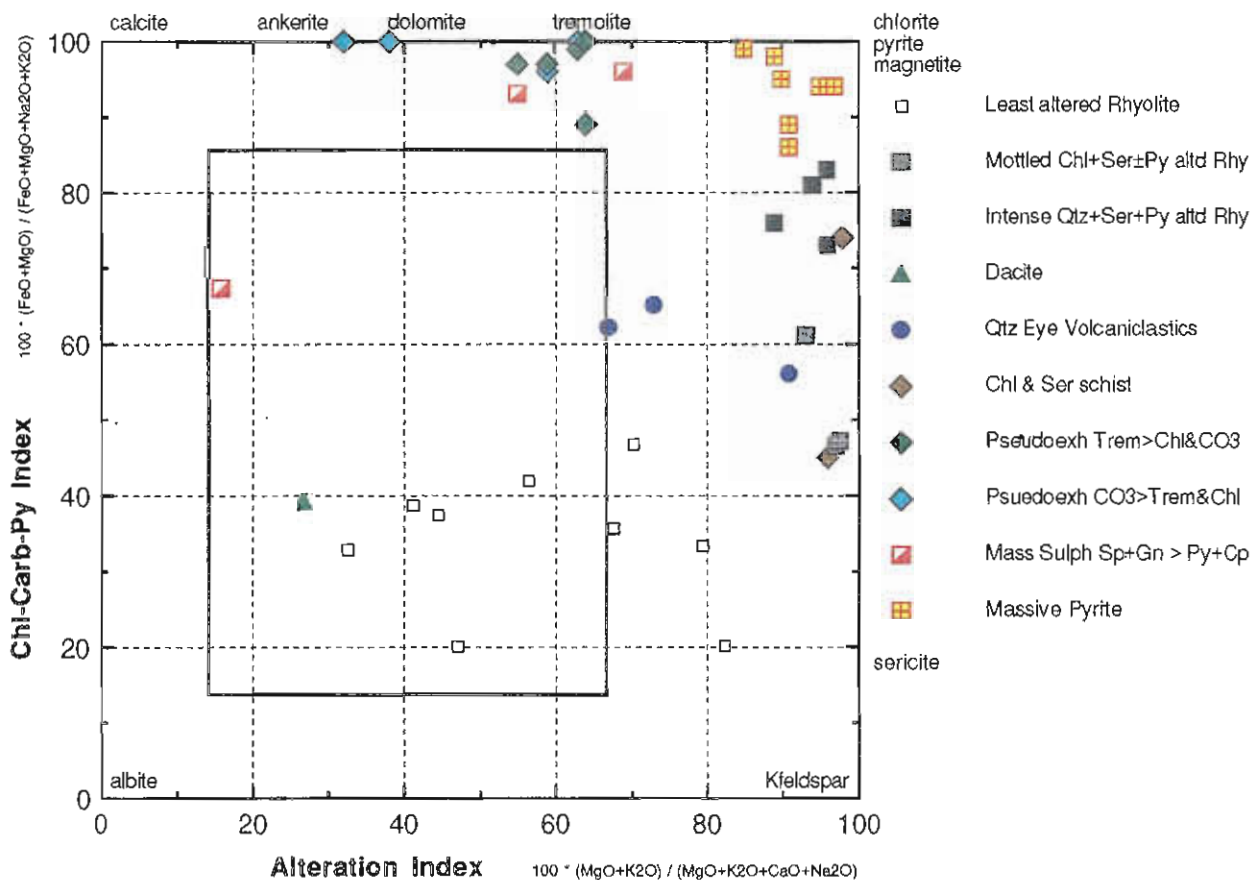


Figure 19 Al-CCPI boxplot for samples from drill holes TH247 and W2011NED42, West Thalanga. The tremolite & carbonate rich pseudoexhalites plot in fields similar to chlorite-carbonate alteration associated with ore lenses at Rosebery.

rhyolite can be characterised as mottled chlorite-sericite±pyrite alteration which was found to have experienced relatively little overall mass change (Paulick, 1998). On average, rhyolite with mottled chlorite-sericite±pyrite alteration has lost Si, Na, Ca and Sr and gained Mg, Ba, S, Pb, Zn and Rb. This style of alteration affected a thick, stratabound zone below the mineralisation which envelops zones of intense chlorite-pyrite alteration in east Thalanga.

Mass balance results (Paulick, 1998) show that chlorite-pyrite alteration is associated with silica, sodium and barium loss and relatively large gains in Mg, Cu and Zn. This suggests that this type of alteration originated from the passage of hot metal and magnesium bearing fluids. Interaction with the rhyolite country rock resulted in the deposition of pyrite, chalcopyrite and sphalerite and the formation of Mg-rich phyllosilicate whereas silica, sodium and barium were leached from the rock. The loss of SiO<sub>2</sub> from the lower parts of the footwall is offset by SiO<sub>2</sub> mass gain associated with quartz-pyrite alteration which is mainly confined to a stratabound zone immediately below the Favourable Horizon. The general mass gain in this zone could be readily accommodated by pore space filling in clastic lithofacies or upward volume extension.

Late hydrothermal fluids within the system might be expected to be supersaturated in silica which could be the cause for SiO<sub>2</sub> enrichment in rhyolite with late quartz±sphalerite alteration.

Calc-silicate alteration in the footwall rhyolite appears to be confined to the fringes of the alteration zone and extremely carbonate-rich rocks ('pseudo-exhalite') locally associated with mineralisation in west Thalanga were interpreted to represent the upper and outer parts of the hydrothermal system by Herrmann (1994).

Geochemical proximity indicators to the Thalanga mineralisation have been interpreted from the examination of the spatial distribution of geochemical data on six cross section through the Thalanga sequence (> 600 analyses). In general, Several compositional features can be regarded as reliable proximity indicators to Thalanga -style mineralisation on a district scale (Fig. 21):

- elevated sulphur which is directly correlated with the pyrite content of the rocks
- sodium depletion
- increase in Alteration Index and Carbonate-Chlorite-Pyrite Index
- elevated As, Bi and Mo
- increase in Rb/Sr ratio
- increase in X<sub>Mg</sub>-ratio of chlorite, biotite and whole rock
- elevated Zn (Cu and Pb generally less reliable)

Geochemical proximity indicators to the Thalanga mineralisation on a mine scale are:

# A model for the hydrothermal system of Thalanga

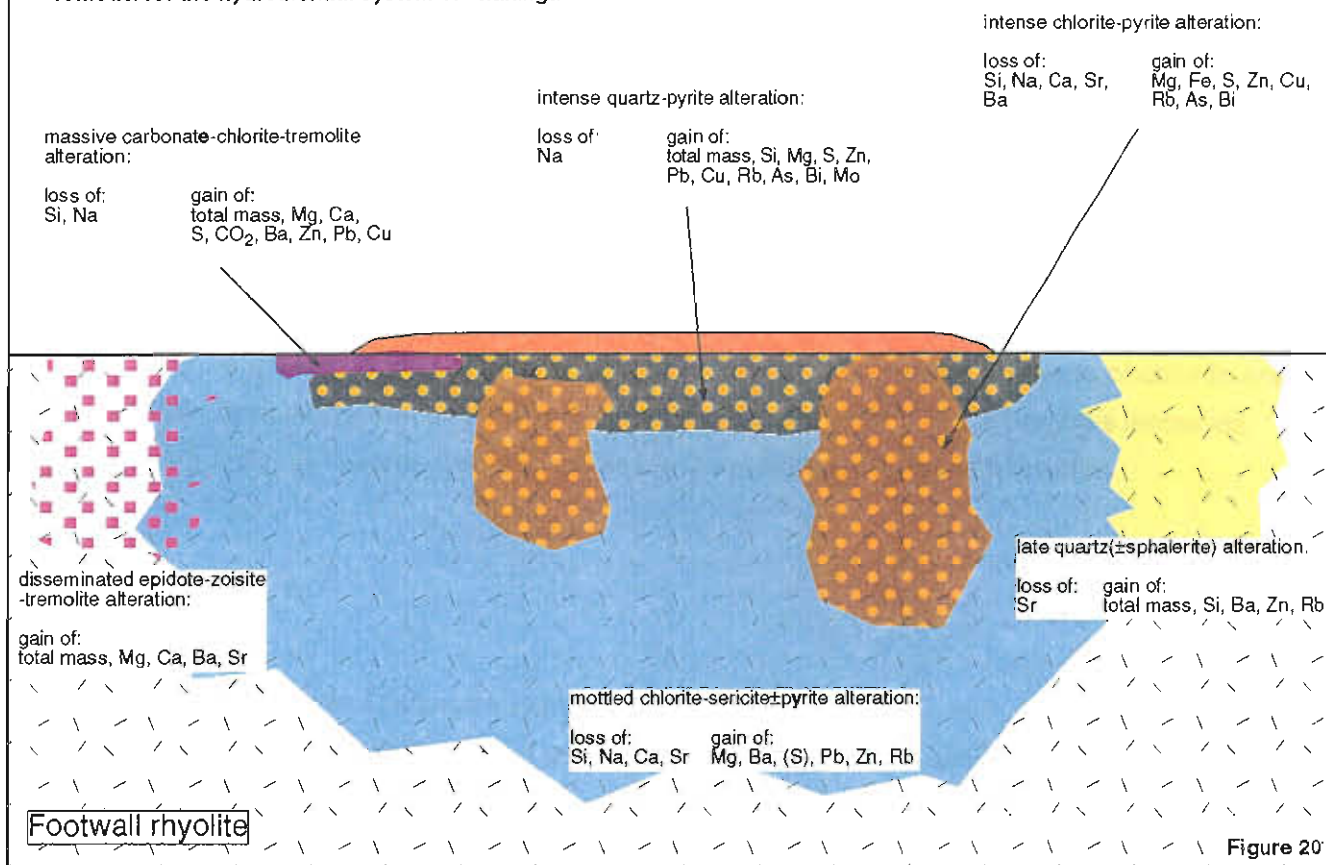


Figure 20

## Summary of geochemical proximity indicators to the Thalanga mineralisation on a district and mine scale

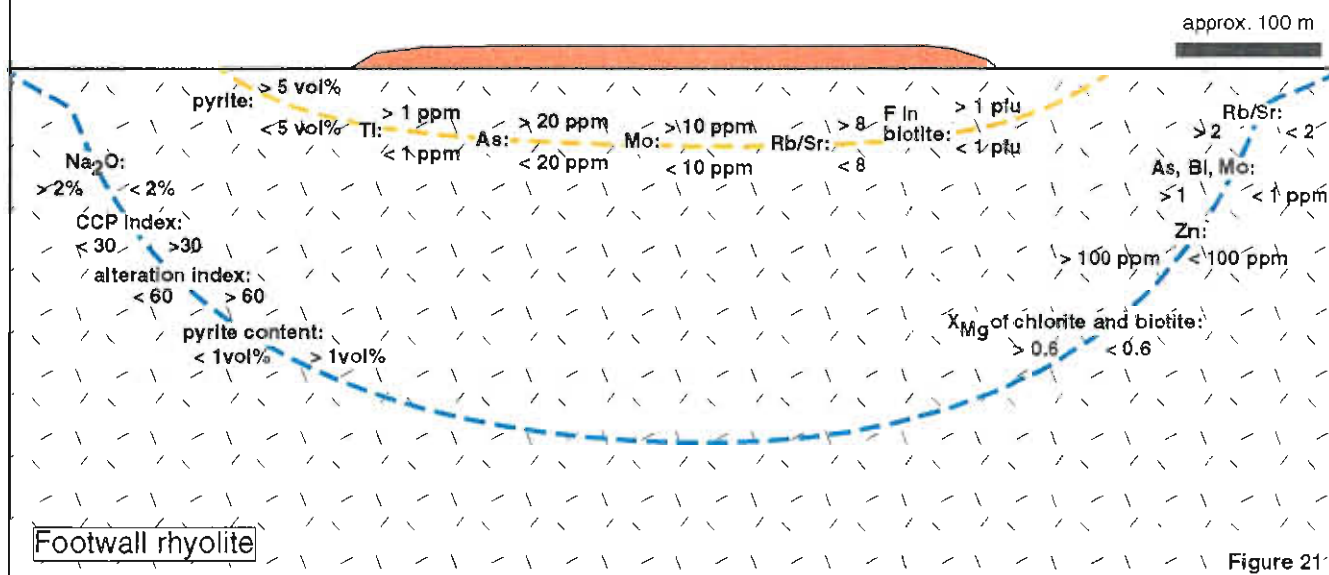


Figure 21

- strongly elevated As, Bi, and Mo
- elevated Ti
- locally strong Ba enrichment
- fluorine enrichment in biotite (? and whole rock)
- high Rb/Sr ratio

Whole rock analyses of rhyolite with mottled chlorite-sericite±pyrite alteration often show inconsistent trends with proximity to ore. By contrast, microprobe analyses of chlorite and biotite from this alteration zone reveal that the Mg : Fe ratio of these minerals increases systematically towards the Favourable Horizon with remarkable little scatter.

## STOP 2:

### *Ironstones in the Thalanga - West 45 area*

Poorly preserved thin lenses of quartz-magnetite-barite rocks are associated with several of the Thalanga ore lenses, and also exist in a cluster of small quartz-magnetite±hematite±barite bodies at two main stratigraphic positions extending 2.3 km west of Thalanga: one on the favourable horizon, and a second ~80m above this in the Trooper Creek Formation. Recent RGC drilling has determined that a small massive sulfide body (Thalanga West 45) exists at shallow depth in the midst of these western ironstones/Ba-quartzites ~1.8 km from the main Thalanga deposit, so that they are much closer to massive sulphides than previously thought.

The typical size range is 1–30 m long x 1–10 m thick in steeply dipping hostrocks; actual thickness and shape is difficult to determine in most instances because of the rubbly outcrop character.

As part of the AMIRA/ARC P439 study, (Davidson, 1998), twelve samples from two pods of iron-silica, TW1–7 and TW8–10, were analysed in detail to determine the uniformity of their major, trace and rare earth element characteristics. Samples were taken at 5m intervals across strike.

The TW1–7 ironstone is ~80 m stratigraphically above the Thalanga favourable horizon and 250m south east of the newly discovered West 45 sulphide lens. It consists of fine-grained red to grey chert, abundantly cross-cut by white to red sucrosic quartz veins with disseminated sulfide pitting, gossanous textures, and associated 1–3 cm wide irregular veins of barite. The textures are interpreted as a vein complex overprinting ferruginous chert, with sulphides and barite being emplaced during the vein stages.

The TW8–10 ironstone is hosted in the upper section of quartz phyric rhyolite, 5–10 m below its contact with feldspar phyric dacite, ~60m west of West 45 sulphide lens. It consists of massive reddish-purple jasper cut by numerous anastomosing medium-fine quartz±pyrite



veins up to 2 cm wide, with surrounding silicification haloes. Hematite exists as distinct patches with cusped edges up to 10 cm long. TW11 is from the jaspilitic portion of a small discontinuous barite-jasper zone ~3 m long, which is interpreted as the likely updip equivalent to massive sulphides in West 45 lens.

At the broad scale, Fe, Mn and Ba contents of ironstones peak at a distance of ~1500-200m west of the main Thalanga deposit, supporting the interpretation that the western ironstone pods are associated with a hydrothermal centre in the West 45 area, rather than the main Thalanga system. On the local scale, Ba contents are up to 3.5% in the TW1-7 lens and decrease from east to west, ~900 ppm in TW11 updip from mineralisation, and are below detection in TW8-10. Cu, Pb and Zn contents vary systematically with Ba, and are anomalously high compared to "barren" ironstone populations. TW11 contains the highest values, with 86 ppm Cu, 220 ppm Pb and 210 ppm Zn, and the other two ironstones also contain elevated values. Considering all base metal data together, and separating the data into its two main horizons, it is apparent that with the exception of the TW1-7 lens, most of the more anomalous response derives from the Thalanga-equivalent horizon; it favours this level for further exploration.

The TW1-7 and TW11 pods both have positive Eu anomalies but the adjacent TW8-10 ironstone has a flat to negative Eu pattern indicating that both ("near ore" and "barren") signatures can exist within 100m of sulphide lenses. Selenium exists in the range 1 to 4ppm, which is characteristic of "near ore" ironstones in the Mt Windsor Subprovince.

$\delta^{18}\text{O}_{\text{qtz}}$  values for three samples from TW1-7 and one from TW8-10 are all in the range 11.5 to 14‰, indicating moderate temperatures of quartz precipitation up to ~270°.

These geochemical features are characteristic of near ore ironstones in the Mount Windsor Volcanics. They have applications in VHMS exploration for identifying favourable horizons and higher temperature parts of hydrothermal systems, potentially in proximity to sulphide lenses.

## **DAY 2: IRONSTONES; MASSIVE SULFIDE MINERALISATION HOSTED BY LAVAS AND INTRUSIONS AT HIGHWAY- REWARD – Mark Doyle, Jason Grace**

The program today will focus on: (1) the significance of hematite alteration and ironstones in submarine volcanic successions hosting massive sulfide mineralisation; (2) evaluating the role of sub-seafloor replacement and seafloor precipitation during mineral deposition; (3) evaluating the depositional setting in submarine host successions to massive sulfide mineralisation; and (4) evaluating the role of volcanic facies and texture in influencing the form and distribution of mineralisation and alteration assemblages.

### **Stop 3: Trooper Creek prospect ironstone lenses**

Directions: Drive from Charters Towers along the Flinders Highway as for yesterday. Approximately 2 km south, turn left onto the Gregory Developmental Road, which runs south to Belyando Crossing and Clermont. Follow the Gregory Developmental Road for approximately 32 km to the Highway-Reward mine. Approximately 6 km past the Highway-Reward mine is a turn to the left signposted Elston Hills Station. Take this track (slow) to the homestead where there is a left hand turn and a short distance further on a track to the right. Take this track to Trooper Creek prospect (7742000mN, 426000mE).

Stop 3 is marked by a series of dark red ironstone outcrops up to 1.5 m high and 10 m wide. The ironstone lenses occur stratigraphically above stratified andesitic scoria breccia, forming a discontinuous conformable horizon (horizon 1) approximately 500 m in length. At stop 3 the ironstone varies from massive to tuffaceous. Samples of massive ironstone are composed primarily of quartz and hematite. In addition to quartz and hematite, various proportions of sericite, chlorite, albite, calcite and feldspar crystals are present in tuffaceous ironstone.

Petrographically, massive ironstone consists primarily of coalescing spherules, microcrystalline quartz, hematite patches and botryoidal structures. Recrystallisation of spherules to coarse quartz has destroyed many fibrous spherule textures. The result in hand specimen is a granular sandy texture in which apparent hematite “grains” are enclosed in an apparent quartz “matrix”.

In tuffaceous ironstone, quartz-hematite-rich patches and bands alternate with quartz-dominant pyroclast-rich bands. Quartz-rich bands comprise coalescing spherules, quartz+hematite-altered pumice clasts, subordinate hematite patches, botryoidal structures, filamentous structures and feldspar (sanidine and plagioclase) crystals and crystal fragments. Hematite-rich bands comprise single and coalescing hematite patches and feldspar crystals separated by finely crystalline (3-5  $\mu\text{m}$ ) quartz containing relic pumice and shards. Quartz-nodules are also present.

### **Stop 4: A shoaling volcano-sedimentary succession**

Directions: Traverse along strike to the ESE following the numerous rubbly ironstone outcrops. Stop 4 is marked by a small gully which drains to the south. At this locality the volcano-sedimentary succession hosting the ironstone lenses is better exposed.

#### **Stop 4.1 Lithofacies associations**

##### *Graded andesitic scoria breccia facies*

The base of the section comprises normally graded andesitic scoria breccia beds (Figs. 22-23). The breccia is framework supported and moderately well sorted. Scoriaceous clasts with 30-50% vesicles account for 90-99% of the fragment population. Large clasts (10-20 cm) are mostly elongate with irregular shapes but some fluidal spindle-shaped clasts (fragments of bombs) are present. Clasts have a trachytic texture or were formerly

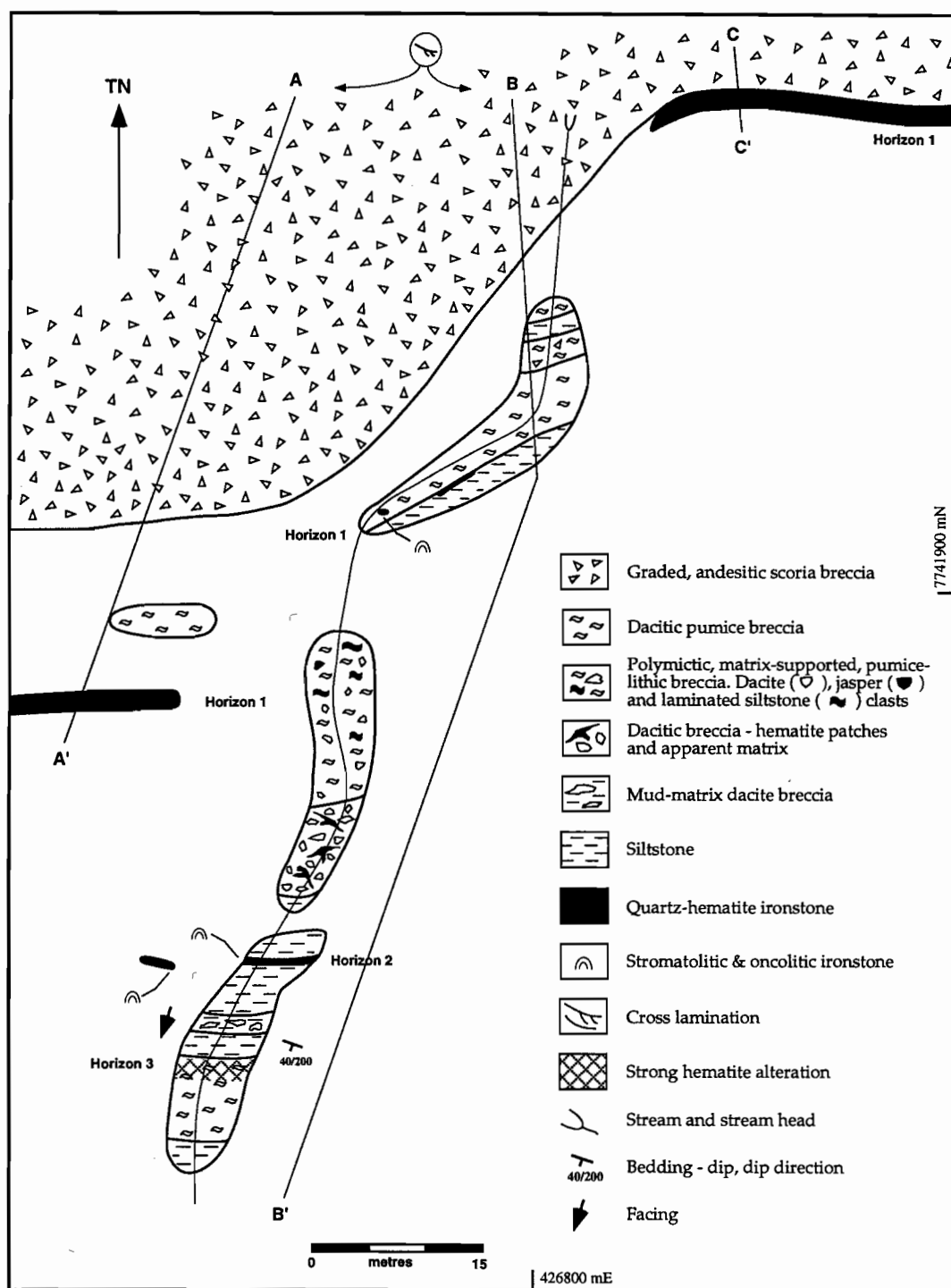


Figure 22: Detailed outcrop map showing the distribution of the principal lithofacies and iron oxide±silica horizons at Trooper Creek prospect (around 7741900 mN, 426800 mE).

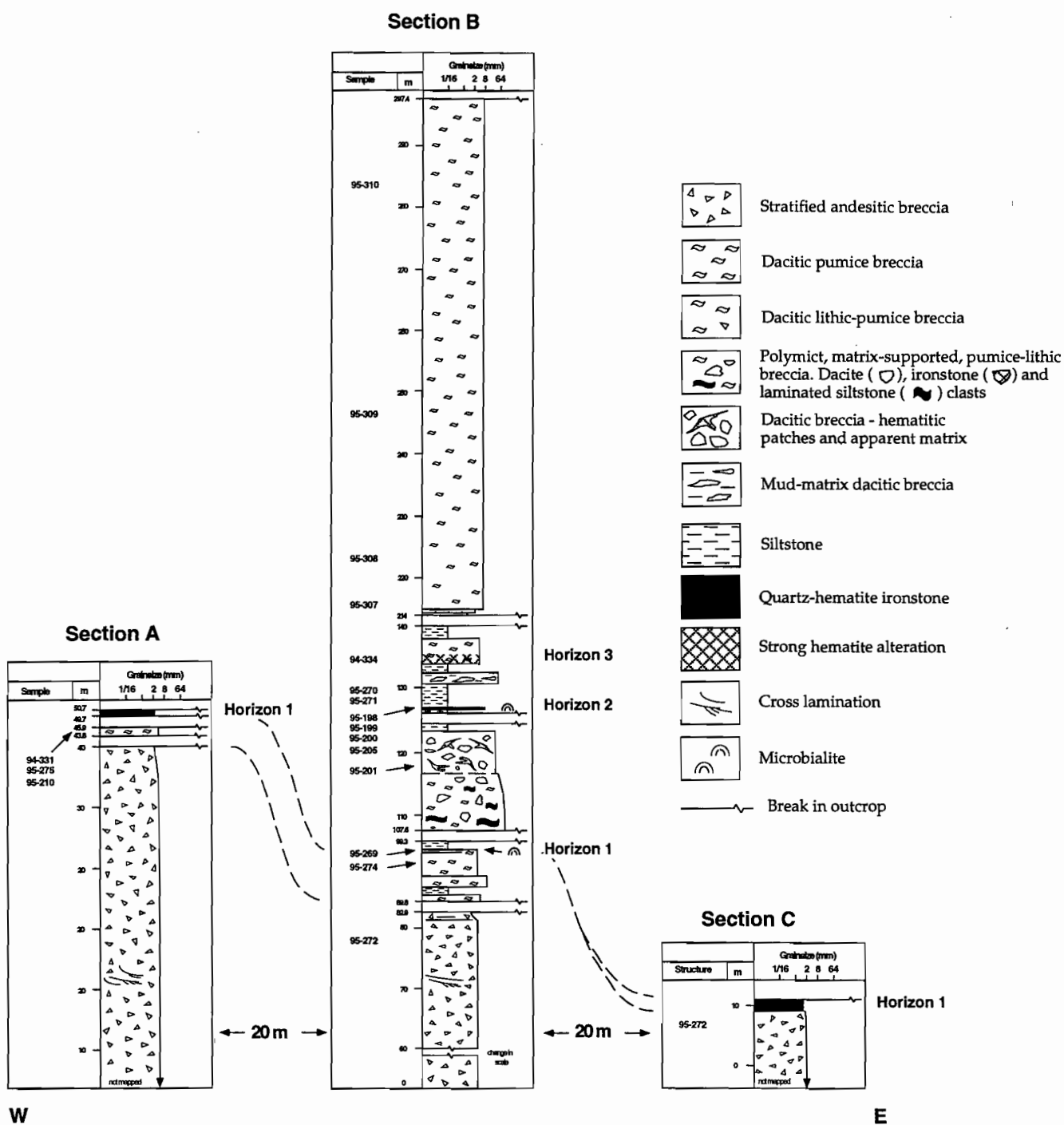


Figure 23: Measured sections presented as graphic logs for major lithologies in the Trooper Creek Formation in the area of the Trooper Creek Prospect. Locations of sections A-C are given in Figure XX

glassy with sparse feldspar microlites. In many clasts, the original groundmass textures and clast margins have been obscured by calcite, chlorite, epidote, quartz and/or sericite alteration. Vesicles are filled with calcite, chlorite, sericite, hematite or zones of quartz-chlorite or hematite-chlorite. Thin films of hematite define some clast margins and the vesicles within them.

The graded andesitic scoria breccia facies is composed of clasts were initially formed and deposited by pyroclastic processes, but were subsequently redeposited but not substantially reworked. Redeposition was more or less syn-eruptive; hence the deposits are essentially monomictic and primary clast shapes are largely unmodified. The bedforms and internal organisation are consistent with deposition from high-concentration gravelly turbidity currents (S3 and Td-e divisions; Lowe, 1982).

*Planar laminated dacitic pumice breccia (water-settled fall deposit)*

An irregular surface marks the boundary between lithofacies of the andesitic facies association with those of the overlying dacitic facies association (Fig. 22). The planar laminated dacitic pumice breccia facies is monomictic and comprises a clast-supported framework of ragged pumice fragments. The pumice breccia comprises upper and lower stratified divisions separated by a more massive, diffusely laminated interval (2.9 m thick). The breccia is pervasively sericite-hematite-altered. Clast margins and the vesicle walls are outlined by a thin hematite film. The phyllosilicate-altered pumice clasts are often deformed around quartz-hematite-altered pumice and feldspar crystals, and define a bedding-parallel compaction foliation.

The abundance of highly vesicular pumice within the laminated pumice breccia suggests this facies was sourced from explosive magmatic eruptions from a vent in a shallow subaqueous or subaerial environment. Although rich in juvenile pumice, there is no textural or lithofacies evidence for hot emplacement of the facies. Mantle bedding, good sorting and well-developed planar lamination within the pumice breccia bed suggest that the pumice settled through the water column.

*Microbialites*

"Microbialite" is a general term used for organosedimentary deposits composed of benthic microbial communities and sediments (Burne and Moore, 1987). Microbialites in ironstone at Trooper Creek prospect occur in two layers (upper and lower microbialites) separated by a thick interval of polymictic lithic-pumice breccia. The microlites are composed of oncolites, stromatolites, pyroclastic components (principally pumice, shards and crystal fragments) and fossil fragments. Laminae in oncolites and stromatolites are typically very thin (8-20  $\mu\text{m}$ ) and are quartz-rich or hematite-rich.

Branching networks of filamentous structures are preserved in the cores of oncolites or between grains in some samples. The filaments are similar to those interpreted by Duhig et al. (1992) as microaerophilic chemolithotrophic bacteria or fungi. Biogenic components include trilobite fragments, possible sponge spicules, gastropods and a brachiopod.

*Polymictic lithic-pumice breccia facies*

The next facies in the succession is a polymictic lithic-pumice breccia. The breccia is poorly sorted, matrix-supported and weakly normally graded. The clast population includes siltstone, ironstone and aphyric dacite clasts. Other clasts comprise dacite with indurated siltstone filled fractures and rinds.

The bedforms in this facies are consistent with deposition as a subaqueous mass flow. Some clasts suggest that the mass-flow may have been sourced by partial extrusion of a cryptodome through a succession of pumice breccia and ironstone beds.

### *Laminated siltstone and sandstone facies*

Siltstone and sandstone beds are more abundant towards the top of the succession. They are composed of devitrified ash and shards with subordinate crystal fragments (quartz and/or feldspar). Some beds display basal scours and flame structures. One siltstone bed contains sericitic pseudomorphs of gypsum crystals. Trace fossils of the *Cruziana* ichnofacies (Frey and Pemberton, 1984) are also present.

### **Assessing the depositional environment**

The succession is interpreted to record the progressive shoaling of the depositional environment to above storm wave base (Fig. 24). The graded andesitic scoria breccia facies accumulated in water depths below storm wave base as indicated by several lines of evidence: (1) the units are interpreted as turbidites which are, in general, diagnostic of subaqueous below storm-wave-base depositional settings; (2) hyaloclastite which is associated with a single intercalated lava suggests a subaqueous setting; (3) tractional structures which are abundant in subaerial environments and fluvial and shoreline settings are absent.

The high vesicularity of fragments in the graded andesitic scoria breccia facies (30-50%) suggests that eruptions took place in a relatively shallow water (<500 m) or subaerial setting (probably to the east) where confining pressure allowed vesiculation to proceed uninhibited (e.g. McBirney, 1963; Fisher and Schmincke, 1984). The graded andesitic scoria breccia facies are interpreted to record strombolian explosive eruptions which built ephemeral scoria cones subject to collapse and resedimentation into deeper water environments that existed in the western part of the area (Fig. 24A-D). The thickness (>70 m) of single mass flows in the graded andesitic scoria breccia facies suggests very rapid aggradation to an above-storm-wave-base environment recorded by the overlying facies.

The transition to shallow water conditions included erosion of some deposits from the andesitic facies association (Fig. 24E). Thick dacitic pumiceous mass-flow and water-settled fall deposits were emplaced onto the unconformity surface and microbialites colonised the platform (Fig. 24G-H). The morphologies of stromatolites at Trooper Creek prospect provide evidence for deposition in a quiet water environment, above fairweather wave base. Wave activity was of sufficient intensity to generate oncolites (Logan et al., 1964) and disrupt the growing mats. Intercalated siltstone and pumiceous water-settled fall deposits suggest that quiet water conditions prevailed during the deposition of these intervals. The appearance of microbialites was coeval with deposition of a thin horizon of ironstone. The ironstone partially replaced intervals of the pumice breccia substrate to the microbialites.

Volcanic siltstone and subordinate fine-grained vitric sandstone become increasingly abundant towards the top of the sequence, reflecting a return to relatively quiet water conditions following deposition of the upper microbialite horizon (Fig. 24I-J). Gypsum molds within siltstone immediately overlying the uppermost microbialite horizon are interpreted to have grown displacively within the sediment. Displacive gypsum is common in modern marginal marine sediments (Demicco and Hardie, 1994). Fossils of the *Cruziana* ichnofacies are suggestive of a subtidal environment (Frey and Pemberton, 1984).

### **Stop 4.2 Ironstone lenses and associated alteration**

Horizon 1 ironstone occurs at the contact between the graded andesitic scoria breccia facies and overlying dacitic pumice breccia. The ironstone lenses are discontinuous and mostly 10-20 m in exposed length (max. 116 m). The tops of the ironstone lenses are sharp and sometimes overlain by hematitic siltstone. Bases and margins of the lenses are

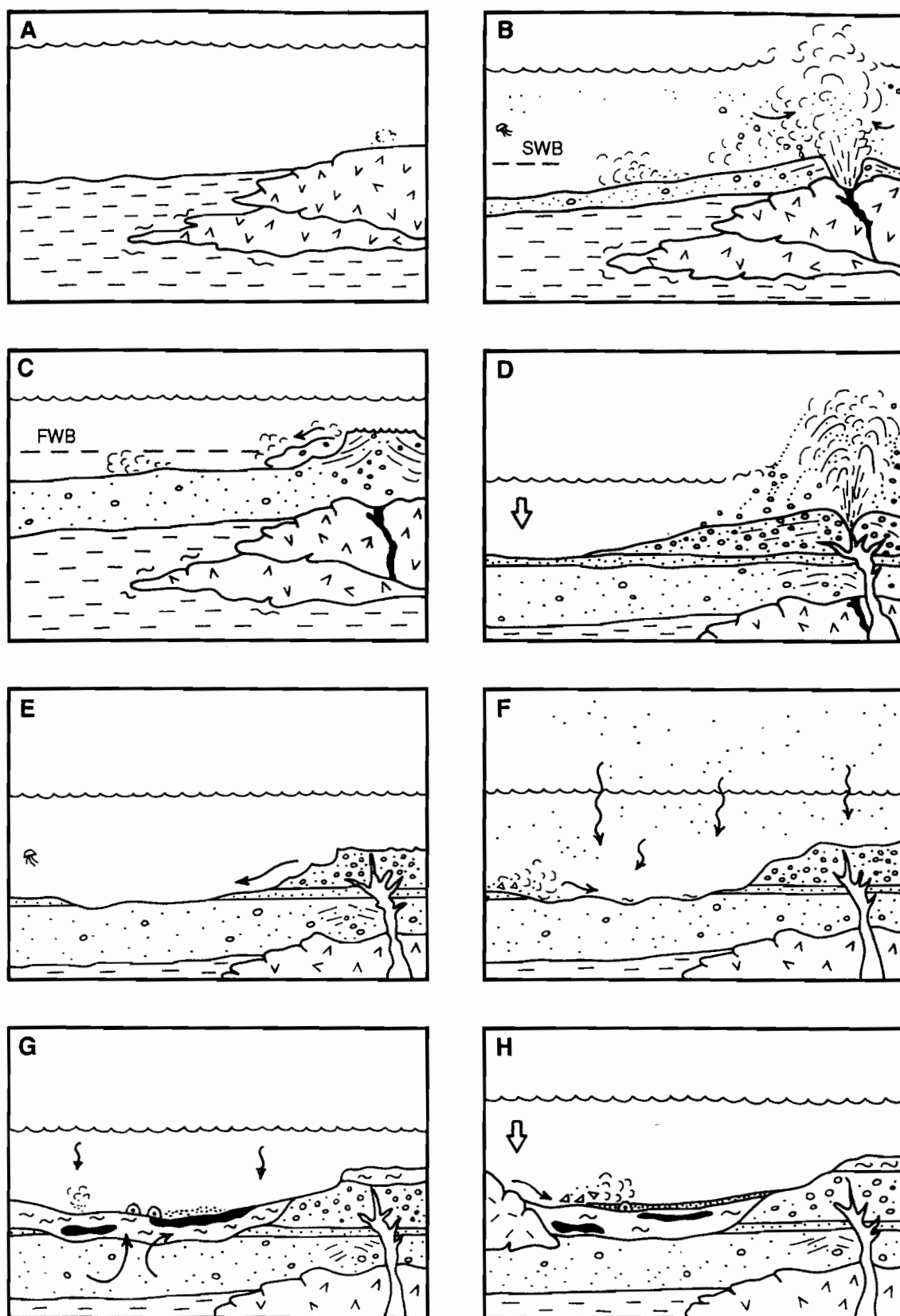
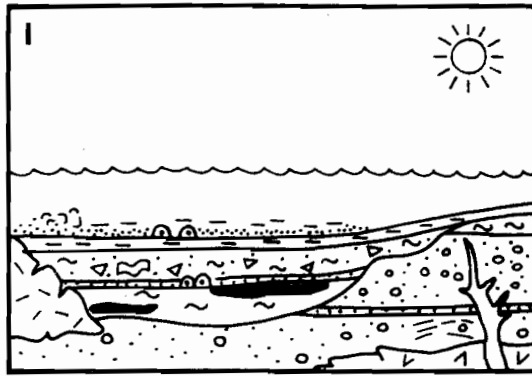
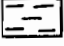
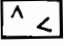
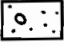
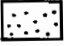
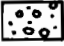
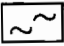
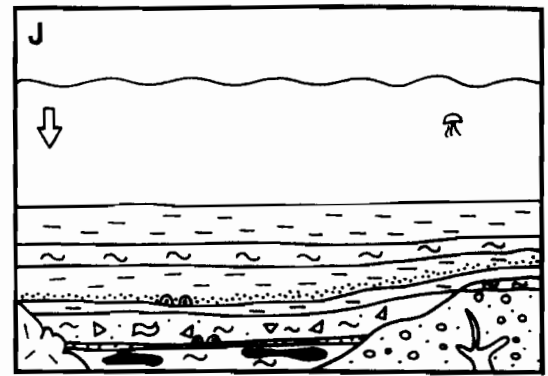



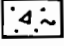
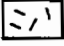
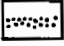
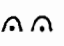

Figure 24. Cartoon of the principal stages in the deposition of lithofacies at Trooper Creek prospect. At this locality, only stages E-J are represented. (B-D) Strombolian style volcanism and resedimentation of pyroclasts. Depositional setting shallows to above storm wave base; (E) Slumping and post-eruptive degradation of volcanic edifice; (F) Mass-flows and water-settled fall of pyroclasts sourced from distal dacitic eruptions; (G) Colonisation of platform by microbialites. Ironstone deposition from circulating, low-temperature hydrothermal fluids (arrows); (H) Partial extrusion of a cryptodome generating a polymictic debris flow;





-  Siltstone
-  Andesite
-  Scoria breccia from strombolian eruption
-  Traction-current deposits & mass-flow deposits
-  Bomb-rich breccia
-  Dacitic pumice breccia (water-settled fall)



-  Ironstone
-  Polymictic lithic-pumice breccia (debris flow deposit)
-  Dacite
-  Vitric sandstone
-  Microbialite
-  Settling of fines through water column

(I) Deposition of volcanogenic sediments and recolonisation of platform by microbialites. Minor evaporite minerals. Ironstone emplacement; (J) Subsidence and transition to siltstone-dominated sedimentation.

often marked by gradations from massive ironstone, through tuffaceous ironstone into sericite-hematite-altered pumice breccia.

Horizon 2 ironstone comprises domed bioherms up to 8 cm across and 6-7 cm high. The intercolumn matrix comprises crystal fragments, lithic clast, pumice clasts and oncolites.

Relic pyroclasts suggest that some ironstone lenses formed by sub-seafloor replacement of pumice breccia units, or sedimentation was synchronous with hydrothermal activity and precipitation of iron and silica occurred at, above, and below the seafloor during ironstone deposition. The distance below the seafloor at which infiltration and replacement occurred is difficult to interpret, but was not excessively deep because clasts of ironstone were incorporated into overlying subaqueous mass-flow deposits. The ironstone lenses may mark the seawater-mixing zone, whereas the hematite-sericite alteration may mark feeder zones within the sub-seafloor strata.

### Stop 5: Regional hematite alteration, Highway East prospect

Directions: Return to the Gregory Developmental Road and drive (north) towards the Highway-Reward mine. Approximately 500 m south of the entrance to the Highway-Reward mine is a track to the right which runs along the mining lease boundary fence. Take this track to a small ephemeral creek that cuts the path. Walk upstream for about 50 m and examine the exposures in the creek bed.

In the Trooper Creek Formation, hematite alteration is regionally distributed but forms discrete alteration domains ranging from a few metres wide to around 500 m across. The most widespread domains of hematite alteration are associated with quartz-hematite±sericite±chlorite lenses ("ironstone") such as those exposed at stop 4. At stop 5, hematite alteration is spatially (and possibly genetically) associated with a dacitic intrusion.

Rock exposures in the creek bed comprise silicified (vitriclastic?) siltstone, tuffaceous sandstone and non-welded, normally graded pumice-lithic breccia. Crystals and crystal fragments or pumice clasts dominate the breccia and sandstone beds. The crystal and phenocryst populations suggest rhyodacitic and dacitic compositions. Some thick units have polymictic lithic-rich bases. The outcrop at the margin of the creek comprises evenly porphyritic dacite.

### Stop 6: The Highway-Reward mine

Directions: Now return to the Gregory Developmental Road and reassemble at the Highway-Reward mine office. BEWARE of heavy vehicles on haul road.

	Highway	Reward
Primary	1.2 m.t. @ 5.5% Cu, 6.5 g/t Ag, 1.2 g/t Au	0.2 m.t. @ 3.5 Cu, 13 g/t Ag, 1 g/t Au
Supergene		0.3 m.t @ 11.6% Cu, 21 g/t Ag, 1.8 g/t Au
Oxide	0.07 m.t. @ 6.04 g/t Au	0.1 m.t @ 33 g/t Ag, 6.49 g/t Au

Table 7. Grade and tonnage data for the primary, oxide and supergene ore zones at Highway-Reward. The Highway oxide resource is a pre-mining resource estimate. Data from Beams and Dronseika (1995).

## **Stop 7: A syn-sedimentary intrusion dominated host succession to the Cu-Au Highway-Reward VHMS deposit**

Directions: Return to Charters Towers. The RGC Highway-Reward core store is located on Moores St.

### **Stop 7.1 DDH REM 560 and REW 805: Lavas, syn-sedimentary intrusions and associated autoclastic facies**

Lavas and intrusions in the host succession to the Highway-Reward deposit comprise coherent lithofacies and associated autoclastic facies. Diamond drill holes REM 560 and REW 805 provide examples of some of these facies (Fig. 25).

#### *Massive and flow-banded rhyolite, rhyodacite and dacite*

Intervals of this facies are characterised by even distributed quartz and/or feldspar phenocrysts. Feldspar phenocrysts are euhedral and are unaltered or variably altered to sericite, chlorite, carbonate, albite or quartz. Quartz phenocrysts are embayed and rounded as a result of magmatic resorption.

The groundmass has devitrified to a quartzofeldspathic mosaic or else altered to various assemblages of chlorite, sericite, carbonate, epidote, quartz and albite. In some samples, the groundmass includes relic spherical spherulites, microspherulites, lithophysae, and/or micropoikilitic quartz that enclose sericitised feldspar microlites. Relic classical- and banded-perlite suggest that parts of the groundmass in many units were formerly glassy.

Flow banding occurs in some units, particularly along flow or intrusion margins. Flow foliations are defined by alternating siliceous (spherulitic) and phyllosilicate-rich (formerly glassy) bands.

#### *Monomictic rhyolitic to dacitic breccia facies*

In drill hole REM 560, coherent rhyolite to dacite passes gradationally into zone of in situ and clast-rotated breccia interpreted as hyaloclastite (Fig. 25). Intervals of this facies are massive, non-stratified, clast-supported frameworks of dacite or rhyodacite clasts. Clasts are evenly porphyritic (quartz and/or feldspar), non-vesicular and have blocky to elongate shapes bound by planar to curvilinear or irregular finely jagged margins. The groundmass within the fragments can be perlitic, spherulitic, devitrified to an interlocking mosaic of quartz and feldspar, or altered to various assemblages of chlorite, sericite, albite, and quartz. Perlite suggests that many of the clasts were originally glassy. Clasts are separated by small amounts of millimetre- to sub-millimetre-sized matrix composed of juvenile fragments, crystals and crystal fragments. In some cases, preferential quartz, sericite and/or chlorite alteration of the matrix and margins of clasts has generated an apparent matrix-supported fabric.

Flow banded clasts are common in some intervals and highlight two styles of breccia. In the first, continuity of flow banding between fragments suggests that the clasts are in situ and moved little following fragmentation. In the second style of breccia (clast-rotated breccia facies), significant rotation and translation of clasts is implied by flow banding at different orientations. Clasts have undergone rotation following fragmentation, implying that autobrecciation accompanied quenching. Clast rotation and additional fragmentation occurred in response to stresses imposed on the chilled parts of the lavas and intrusions by continued movement of the more ductile interior.

#### *Non-stratified sediment-matrix breccia facies*

This facies is a texturally complex mixture of rhyolite to andesite and either grey cherty siltstone, sandstone, non-welded pumice breccia-sandstone or crystal-rich sandstone. The relative proportions of each component varies considerably. In sediment matrix-poor breccia, the rhyolite to andesite is coherent, mildly fractured, or comprises tightly packed jigsaw-fit clusters of clasts separated by up to 1 cm of siltstone or pumice breccia and

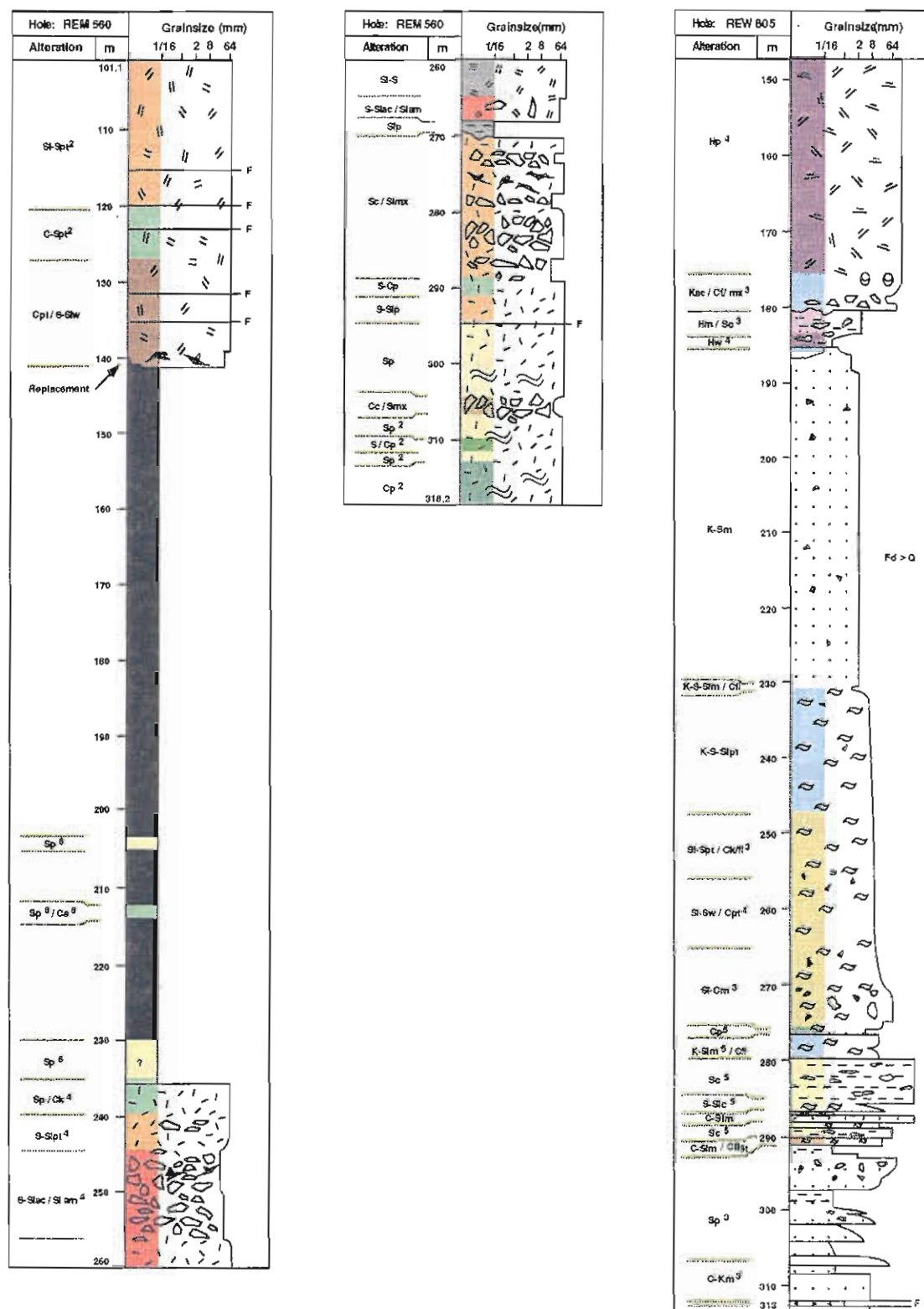


Fig. 25: Simplified graphic lithological logs for drill holes REM 560 and REW 805

sandstone. Clasts form jigsaw-fit aggregates or else are dispersed widely in the sediment matrix. Matrix-rich breccia often grades into matrix-poor breccia which in turn grades into coherent facies or in situ hyaloclastite of the same composition (Fig. 26).

Clasts vary from blocky, cuneiform, ragged to globular in shape. The non-stratified sediment-matrix breccia facies may be dominated by one clast shape, or consist of a mixture of clasts with different shapes, or comprise distinct zones of clasts with different shapes.

Lamination or bedding in the surrounding siltstone or sandstone rarely extends into the non-stratified sediment-matrix breccia facies. Where lamination or bedding in the host is preserved, it is generally contorted. Along many contacts, the sediment is silicified and has a different colour to the surrounding host, suggesting that it is indurated.

The components and organisation favour interpretation of the non-stratified sediment-matrix breccia facies as peperite (e.g. Jones, 1969; Williams and McBirney, 1979). Peperite provides evidence for the mixing of magma or lava and wet unconsolidated sediment and has been described in many subaqueous, particularly submarine, volcanic successions.

### **Discussion: Interpreting the lithofacies associations**

Syn-sedimentary sills, cryptodomes, and partly extrusive cryptodomes have been identified in the host succession to the Highway-Reward massive sulfide deposit. Upper contact relationships and the distribution and arrangement of coherent facies, hyaloclastite, peperite and resedimented autoclastic breccia are the basis for determining the mode of emplacement.

#### *Syn-sedimentary sills and cryptodomes*

Contacts of the syn-sedimentary intrusions show varying effects of quenching and of interaction with the poorly consolidated, water-saturated host sequence. Along parts or all of some contacts, matrix-rich peperite passes through a zone of matrix-poor peperite with jigsaw-fit clasts into a coherent core. In situ hyaloclastite locally occurs between the coherent facies and peperite.

#### *Partly extrusive cryptodomes*

Partly extrusive cryptodomes are high-level domes that intrude the sediment pile and locally breach the sediment surface. They combine facies common to shallow syn-volcanic intrusions and extrusive domes. Intrusive contacts comprise complex associations of peperite, hyaloclastite and coherent facies. Within the contact zone, bedding in the sediment has been destroyed or disrupted. Along extrusive margins a coherent core passes gradationally out through in situ hyaloclastite into resedimented hyaloclastite sourced from the oversteepened dome margins.

### **Stop 7.2 DDH REW 805: The enclosing facies: evaluating depositional environments in which volcanism occurred**

The lavas and intrusions and associated autoclastic facies are intercalated with and overlain by volcanoclastic and sedimentary facies association comprising siltstone, sandstone turbidites, and rhyolitic to dacitic pumice breccia and sandstone. Combined the lithofacies associations and regional context indicate that the volcanism was submarine, below storm wave base, and possibly not in extremely deep water, but rather, around 500 m.

#### *Siltstone facies*

The siltstones are massive, thickly bedded or finely planar laminated. Pale to dark grey siltstone units sometimes contain quartz and/or feldspar crystal fragments and devitrified shards indicating a rhyolitic to dacitic composition. Devitrification and alteration have destroyed primary volcanic particles, hampering their interpretation.





**Lithology**

	Unaltered andesite		Crystal-pumice breccia-sandstone
	Dacite		Crystal-lithic breccia-sandstone
	Rhyolite		Pumice breccia
	Rhyodacite		Siltstone
	Flow banding		Massive pyrite-chalcopryite±sphalerite
	Perlite		Semi-massive pyrite-chalcopryite±sphalerite
	Non-stratified monomictic breccia (hyaloclastite)		Massive/banded pyrite-sphalerite±barite
	Siltstone seams in coherent facies		Stringer veins
	Siltstone-matrix-poor breccia (peperite)		Intensely altered volcanic
	Siltstone-matrix-rich breccia (peperite)	F	Feldspar-bearing
	Stratified monomictic breccia-sandstone (resedimented hyaloclastite)	F>Q	Feldspar > quartz volcaniclastic unit
	Stratified polymictic breccia-sandstone	Q&F	Quartz & feldspar
	Crystal-vitric sandstone	— F	Fault

**Alteration**

	Clay		Chlorite-sericite
	Sericite		Chlorite-sericite-quartz
	Sericite-quartz		Albite/K-feldspar-sericite-quartz-chlorite
	Quartz-sericite		Hematite±quartz
	Quartz ± pyrite		Hematite±sericite±chlorite
	Sericite-quartz-chlorite		Chlorite (± sericite)-carbonate
	Sericite-chlorite		Sericite-carbonate
	Chlorite		

## Facies codes for alteration in volcanic rocks

### (a) Phase(s)

- mineralogical and textural changes accompany hydrothermal alteration. Each alteration mineral can be referred to as a phase.
- each alteration domain comprises an area of rock that is characterised by a particular alteration mineral assemblage or by different proportions of similar minerals (phases) in similar mineral assemblages.

C	- chlorite	S	- sericite
SI	- quartz	K	- albite/K-feldspar
H	- hematite	CB	- carbonate
PY	- pyrite		

e.g. SI-S quartz-sericite (alteration domain comprising quartz and sericite)

### (b) Relative abundance (phases - domains)

- the least abundant mineral within an alteration domain is presented on the right hand side (RHS) and the most abundant mineral on the left hand side (LHS).

e.g. S-SI (sericite-quartz) dominant phase - subordinate phase

- in a rock comprising two or more alteration domains, the phase(s) comprising the dominant domain are presented on the LHS and those of the remaining domains on the RHS in order of relative abundance

e.g. C / S-SI (chlorite & sericite-quartz domains) dominant - subordinate

### (c) Intensity

- allocation of a number to describe the intensity of alteration within each domain

Weak (1-2)      Moderate (3-4)      Strong to intense (5-6)

- e.g. C<sup>5</sup> (strong chlorite alteration)  
S-SI<sup>3</sup> (moderate sericite-quartz alteration)

### (d) Controls/textures

The distribution of alteration minerals and domains can be controlled by the pre-alteration texture or superimposed structures. Alternatively, the alteration phases/ domains can generate a range of new textures and patterns in the rock.

x	- crystal	am	- apparent matrix
mx	- matrix	ac	- apparent clast
c	- clasts	mo	- mottled
fr	- fracture (perlite, quench)	w	- wash
hf	- hydraulic fracture	fi	- fiamme
fb	- flow banding	k	- fleck
sh	- shear	s	- spotty
v	- vein	pt	- patchy
d	- disseminated		

- e.g. Cp<sup>5</sup> (strong pervasive chlorite alteration)

- e.g. Cp<sup>5</sup> / SI<sup>3</sup> (strong pervasive chlorite alteration and moderate, fracture-controlled quartz alteration)

Siltstone beds overlying normally graded pumiceous mass-flow units locally contain outsized (3-10 cm) chloritic, evenly quartz- and feldspar-phyric clasts with wispy shapes. The clasts have similar phenocryst assemblages to the associated pumiceous units and either truncate, or are mantled by, laminae in the enclosing siltstone. Some laminae are highly contorted. Although vesicular microstructures are rarely preserved, clast shapes and lithofacies characteristics are consistent with interpretation of the lenses as compacted pumice clasts.

The siltstones are generally host to the other main facies and so define the ambient depositional conditions. The lithofacies character suggests an origin through the settling of fines in dilute currents trailing sediment gravity flows, pelagic or hemi-pelagic sedimentation and water-settled fallout.

#### *Graded lithic-crystal-pumice breccia facies*

Lithic-crystal-pumice breccia and sandstone units are an important component of diamond drill hole REW 805. The breccia and sandstone beds are dominated by quartz- and feldspar-phyric pumice and crystal fragments, suggesting a rhyodacitic composition. Units are non-welded and are normally graded with massive or diffusely bedded tuffaceous sandstone tops, and in some instances, polymictic lithic-rich bases. The thickest bed has a thin (<2m) reverse-graded sandstone base overlain by normally graded breccia and sandstone. Phyllosilicate-altered pumice is often deformed around quartz-feldspar-altered pumice and nodules, defining a diagenetic compaction foliation.

This facies association is the submarine record of a distal volcanic terrain that is not exposed, not preserved, or located outside the study area. Pumice, shards, and crystals within the facies are interpreted to be pyroclasts and reflect the importance of explosive magmatic and/or phreatomagmatic eruptions and suggest that the source vents were in shallow water, or else in basin margin or subaerial settings. The mass-flow deposits are widespread and not restricted to the areas dominated by lavas and intrusions. The pumiceous mass flows may have infilled seafloor topography generated by lavas, syn-sedimentary intrusions and syn-volcanic faults, but there is no positive evidence that they were not sourced locally.

The lithofacies characteristics of the graded lithic-crystal-pumice breccia and sandstone units are consistent with deposition from syn-eruptive, cold (or cool), water-supported, high-concentration sediment gravity flows.

### **Stop 7.3 Cross-sections through a syn-sedimentary intrusion-dominated volcanic centre**

Detailed mapping of phenocryst populations and contact relationships indicates the presence of more than thirteen distinct porphyritic units in a volume of 1x1x0.5 km (Fig. 27, Doyle, 1994; Doyle, 1997a,b). Peperitic upper margins suggest that at least 75% of the rhyolites to dacites were emplaced as small (< 350 m diameter) syn-sedimentary sills and cryptodomes (Table 8). Another 15% remain as undifferentiated lavas and intrusions, as critical upper contact relationships are not preserved. The intrusions have steep margins and are separated from neighbouring intrusions by thin (0.2 to 30 m) disrupted intervals of siltstone, sandstone turbidites, polymictic lithic breccia, and non-welded pumice- and crystal-rich breccia. Evidence for extrusion of magma onto the seafloor is limited to a single, partly extrusive cryptodome (rhyolite 4).

The Highway and Reward pyrite-chalcopyrite pipes occur within, but close to, the steep margins of cryptodomes within the host succession (Fig. 27; Doyle, 1997a,b). The Highway Pipe is bound by four porphyries: Dacite 1 (western margin), rhyodacite 2 (footwall), and rhyolite 3 and 4 (hanging wall, northern margin). The upper contact of the Highway orebody partly replaces the peperitic base of the partly extrusive cryptodome (rhyolite 4). The massive sulfides and peperite are not mixed and sulfides have more often

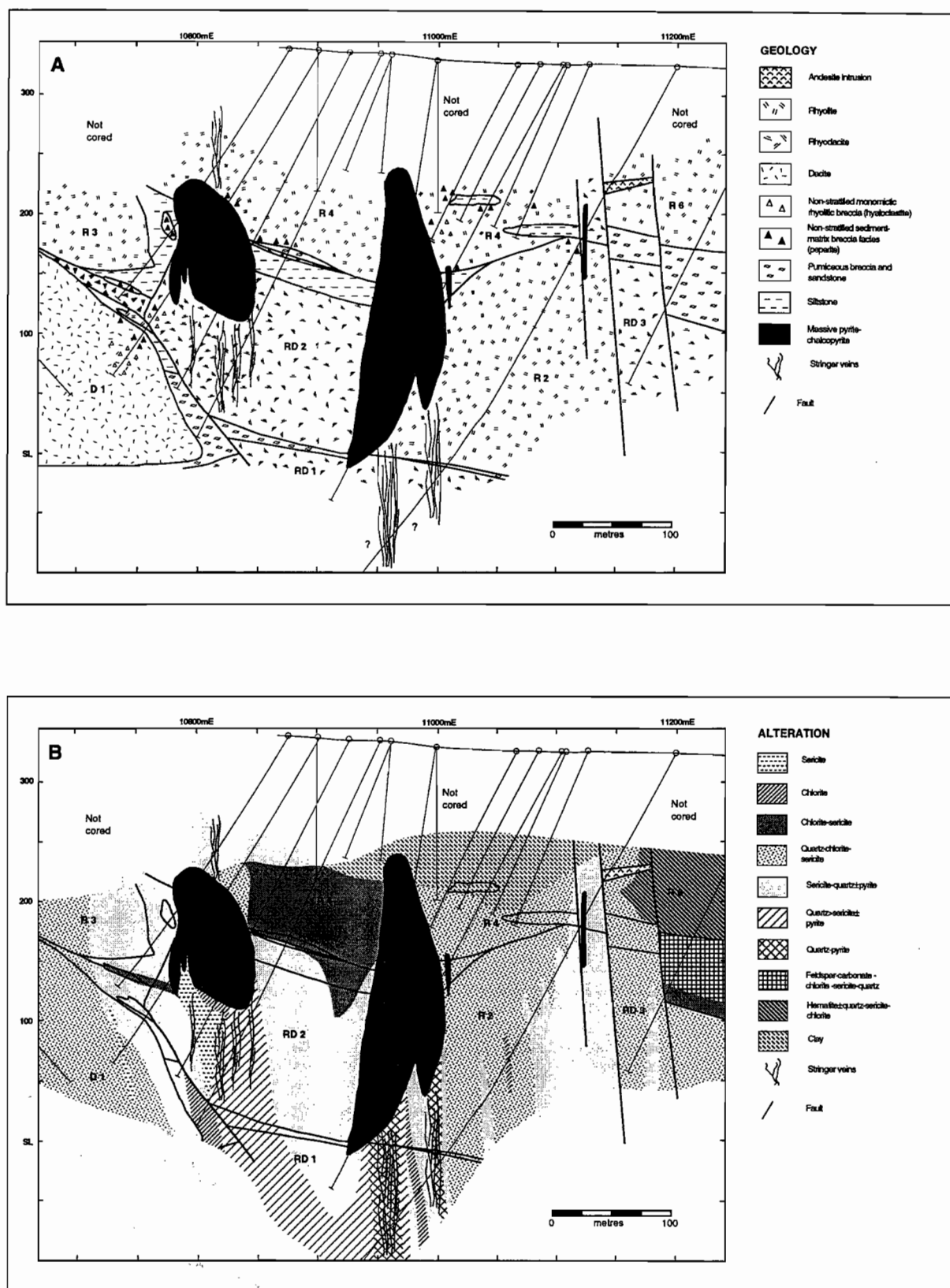


Fig. 27. Simplified geological cross section showing the distribution of (A) lithofacies and (B) alteration at 10150N. The position of the massive sulfide bodies is also shown. Dacite D1, rhyodacites RD1-RD3 and rhyolites R2-4 and R6 are exposed on section 10150mN (after Doyle, 1997b).

replaced rhyolite clasts than siltstone in the matrix or filling fractures. The main Reward pipe is elongate sub-parallel to the boundary of two cryptodomes: rhyodacite 2 (western margin) and rhyolite 2 (eastern margin). The northern extent of the Reward orebody is marked by a northerly thickening cryptodome (rhyolite 9). The southern margin is poorly constrained. The upper margin of the pipe often corresponds to the top of Rhyolite 4. However, several smaller pyrite pipes cut across the overlying resedimented hyaloclastite deposits, pumice breccia beds and hanging wall intrusions (rhyolites 5-6). Pumiceous mass-flow deposits that overlie rhyolite 4 host strata-bound pyrite-sphalerite-galena-barite mineralisation.

Table 8. Form, dimensions and phenocryst populations for sills, cryptodomes and partly extrusive cryptodomes at Highway-Reward.

Unit	Form	Dimensions (m)			Quartz		Feldspar	
		Length	Width	Thickness	%	size (mm)	%	size (mm)
Dacite 1	cryptodome	250	300	>300	—	—	5	0.5-1.5
Rhyodacite 1	sill	150	>250	>100	2-3	0.5-2	6-7	1-2
Rhyodacite 2	cryptodome	175	≥275	50-150	sparse	< 1	2-3	0.5-1.5
Rhyodacite 3	?	>50	>75	>80	2	0.5-3	8-10	1-3
Rhyolite 1	sill	?	?	?	9-10	0.5-4	?	?
Rhyolite 2	cryptodome	>100	>125	120-170	10-12	1-3	6	1-2
Rhyolite 3	cryptodome	175	5 - >150	20-100	6-7	1-3	7	1-3
Rhyolite 4	partly ext.	312	>300	40-120	6-7	1-4	7	1-2
Rhyolite 5	sill	38	25-140	5-10	6-7	1-6	7-8	1-3
Rhyolite 6	sill	150	>300	25 to >60	7	0.5-2	5	1-2
Rhyolite 7	?	>37	>60	>30	4-5	1-3	5	1-3
Rhyolite 8	sill	75	>300	35 to >85	6-7	0.5-7	7	1-2
Rhyolite 9	cryptodome	?	>350	>225	6	1-3	10-12	1-2

#### Stop 7.4 DDH REM 560: The massive pyrite-chalcopyrite pipes and associated stringer veins

##### *Highway pyrite-chalcopyrite pipe*

The massive pyrite-chalcopyrite pipes comprise pyrite and chalcopyrite, with minor tennantite, sphalerite, quartz and sericite. In thin section, trace minerals including chlorite, aikinite, galena, barite, hematite, rutile and a carbonate can be identified. Pyrite is typically subhedral to euhedral and fine to medium grained (20-500 µm). Patches of coarse-grained (2-5 mm) pyrite are often associated with shear zones. Chalcopyrite flecks, veinlets (< 1 mm wide) and patches cut across massive pyrite. Chalcopyrite and quartz fills the interstices between pyrite crystals. Quartz is intergrown with pyrite, forms patches up to 2 cm across, or occurs in bands of pyrite-quartz±barite (e.g. 205.4 m)

Semi-massive and massive pyrite with relic patches and segments of sericite±quartz±pyrite-altered coherent rhyodacite and peperite occur at the top and base of the drill hole (e.g. 200-230 m). Relic quartz and/or feldspar phenocrysts are identifiable in

some of the altered volcanic intervals (e.g. 200.5 m). Contacts between the volcanic facies and mineralisation vary from sharp to finely bulbous and many are sheared. A halo of disseminated and patchy pyrite extends out into the surrounding altered rhyolite and dacite or peperite.

#### *Stringer pyrite-quartz veins*

Pyrite±quartz±sericite stringer veins occur below the Highway pyrite-chalcopryrite pipe and in this hole also at the top of the pipe. Veins are dismembered in the cleavage or fractured internally. Fibre quartz fills the fractures or forms a selvage surrounding a pyrite±sericite±quartz core. Disseminated fine to coarse-grained, euhedral to subhedral pyrite occurs within the altered wall rock.

### **Stop 7.5 DDH REM 116: Replacement of peperite at the top of the Reward pipe**

Diamond drill hole REM 116 (182-190 m) passes through the hanging wall rhyolite (rhyolite 4) into the margin of the Reward pyrite pipe (Fig. 26). A distinctive style of mineralisation occurs within a thin zone (<1 m) at the margin of the pipe. It consists of massive to finely banded pyrite-chalcopryrite-barite replacing peperite. The bands are 1-2 mm wide and strongly contorted. Rhyolite clasts are pervasively chloritised and pyritic, whereas the siltstone is pale grey and silicified. The peperite occurs at the base of a partly extrusive cryptodome (rhyolite 4) and records the mixing of the rhyolite and wet unconsolidated sediment during emplacement. There is no evidence for mixing of sulfides and the rhyolite clasts, implying that the mineralisation deposited sub-seafloor.

Disseminated and spotty sphalerite occurs within sericite-quartz-chlorite-altered rhyolite and peperite at the margin of the pipes.

### **Stop 7.6 DDH HMO 60: Assessing a sub-seafloor vs. seafloor origin**

Drill hole DDH HMO 60 intersects the northern part of a stratabound pyrite-sphalerite-chalcopryrite-barite lens. The lens is around 60 m long and occurs around 20 m above the southern margin of the main Reward pipe. The northern part of the lens comprises a discordant massive pyrite-chalcopryrite pod. In DDH HMO 60, the massive sulfide mineralisation has been fractured (tectonic) and comprises jigsaw-fit clasts. Minerals in the supergene zone include clay, bornite and covellite.

The southern part of the lens has a progressively thinning pyrite-rich base and passes into massive and finely banded sphalerite-rich massive sulfide (e.g. DDH HMO 89).

### **Stop 7.7 DDH HMO 89: Stratabound pyrite-sphalerite-galena-barite lens**

In DDH HMO 89, the mid-section of the stratabound pyrite-sphalerite-chalcopryrite-barite lens is intersected. The mineralisation consists of varying proportions of pyrite, sphalerite, chalcopryrite and galena, with a gangue dominated by quartz, sericite and barite. Petrography indicated the presence of minor tennantite, carbonate, chlorite, bismuth minerals, marcasite, hematite and electrum (Huston, 1992). Supergene minerals include clay, bornite and covellite. Pyrite is euhedral or exhibits snowflake, colloform, or spongy textures (Huston, 1992). Sphalerite occurs as anhedral intergrowths with pyrite and chalcopryrite, and often exhibits chalcopryrite disease. Barite laths are commonly pseudomorphed by quartz.

Fine lamination in the strata-bound pyrite-sphalerite-chalcopryrite-barite mineralisation closely resembles bedded sulfide sediments. Laminae consist of 1-2 mm microcrystalline bands of anhedral quartz intergrown with pyrite, alternating with 1-20 mm bands of pyrite-sphalerite-chalcopryrite with interstitial coarser grained (0.05-0.2 mm) anhedral quartz and minor sericite.



The base of the hole comprises siltstone matrix rhyolitic breccia interpreted as peperite.

### **Stop 7.8 DDH HMO 47: Sphalerite-pyrite mineralisation at the margins of the pyrite-chalcopyrite pipes**

The halo of Pb-Zn mineralisation surrounding the Highway and Reward orebodies extends up to 20 m into the hanging wall and 80 m laterally. Veins, veinlets and segments of pyrite-sphalerite±galena-barite within altered volcanic rocks along the margins and tops of the pyrite pipes. In DDH HMO 47 (240-275 m), intervals (0.2-3 m) of massive to semi-massive sphalerite-pyrite-chalcopyrite-galena occur in strongly sericite-quartz-pyrite-chlorite-altered rhyolite. Relic quartz phenocrysts are locally identifiable. The core is strongly foliated and cut by numerous faults and shears.

### **Stop 7.9 DDH REM 154: Footwall quartz-sericite-pyrite zone**

DDH REM 154 (237-328 m) passes through the footwall quartz-sericite±pyrite alteration zone of the Highway orebody (Fig. 26). The quartz-sericite±pyrite alteration is pervasive or patchy and obscures or destroys original volcanic textures creating apparent clastic textures. Relic quartz phenocrysts are locally recognisable in the rhyodacite, particularly in sericitic apparent clasts enclosed by more intensely silicified wall rock. In some areas, disseminated pyrite preferentially replaced the sericitic component. The quartz-sericite±pyrite alteration includes zones of intense pervasive quartz alteration, which are associated with strong, quartz-pyrite stringer vein development.

### **Stop 7.10 DDH REM 154 and REM 116 Chlorite-sericite±quartz zone**

Outward from the quartz-sericite zone is a widespread quartz-chlorite-sericite zone. The zone comprises a complex alteration assemblage in which the dominant phase can be chlorite, sericite-quartz, or chlorite-sericite. The alteration intersected in drill hole REM 116 (140-180 m) is representative of this zone. The distribution of the various assemblages is strongly controlled by primary volcanic textures, particularly fracture and matrix permeability and flow banding. Pale to dark phyllosilicate-rich alteration is typically patchy or alternates with quartz-feldspathic bands in flow banded rhyolite. Domains of chlorite-sericite and chlorite alteration are often overprinted by quartz-sericite alteration.

Further examples of the quartz-chlorite-sericite zones are exposed in drill hole REM 154 (167-180 m). In this hole, quartz-sericite±pyrite alteration is strongly controlled by fractures and the matrix in autoclastic breccia, and has overprinted earlier phyllosilicate-rich alteration assemblages.

### **Stop 7.11 DDH HMO 41 (258-306 m): Chlorite±anhydrite zone**

Drill hole HMO 41 intersects the margin of the Reward pipe. The drill hole includes zones of very fine-grained (30-50 µm), weakly foliated chlorite contain abundant euhedral anhydrite crystals up to 1.5 cm. The foliation wraps around the anhydrite, which indicates a pre- or syn-kinematic timing for anhydrite crystallisation (cf. Huston, 1992). This observation contradicts the late-kinematic timing for anhydrite proposed by some earlier workers.

### **Stop 7.12 DDH REM 140: Hanging wall quartz-sericite alteration and veins**

Drill hole REM 140 (80-243 m) passes through a discordant zone of strong quartz-sericite±pyrite alteration which extending up to more than 60 m above the Highway pipe into the overlying rhyolite and volcanoclastic deposits. This style of alteration obscures primary textures, but only in the most silicified domains are the lithofacies unrecognisable. The rhyolite has peperitic upper margins which indicate that at this position it is intrusive.

### Stop 7.13 DDH REW 805: Regional diagenetic alteration assemblage

Low intensity feldspar-chlorite-sericite-quartz-carbonate alteration of pumice-crystal breccia and sandstone is evident in drill hole REW 805 (188 m+). The alteration is very heterogeneous, forming pale feldspar and/or quartz-rich domains and green chlorite-sericite-rich areas. The alteration is nodular or coalescing nodules form pervasive and patchy feldspar±quartz±sericite±chlorite-alteration (276 m). The feldspar±quartz alteration often encloses phyllosilicate-altered domains which are typically strongly elongate and define a bedding-parallel diagenetic compaction (or early tectonic) foliation (Allen and Cas, 1990). Other pumice beds have entirely altered to sericite-chlorite. In these domains, most pumice fragments are compacted generating an evenly porphyritic texture more typical of coherent lavas and intrusions.

### Stop 7.14 Core display: modification of primary volcanic textures during alteration

Drill core at Highway-Reward provides examples of the role volcanic textures and facies play in influencing the distribution of hydrothermal and diagenetic alteration assemblages. In the lavas and syn-sedimentary intrusions, vesiculation, crystallisation, devitrification and hydration have combined to generate a complex textural zonation, which strongly influenced subsequent mineralogical and textural changes during diagenetic and hydrothermal alteration and metamorphism. Like their modern counterparts, the lavas and intrusions at Highway-Reward comprised glassy margins which pass inward to cores characterised by zones of glass, glass with coalescing spherulites and/or crystalline domains characterised by spherulitic and micropoikilitic textures. The textural progression of the lavas and intrusions is well preserved in all but the most intense hydrothermally altered zones. The textural progression is briefly summarised below and illustrated in Figures 28 to 30 and representative drill core from Highway-Reward.

#### *Glassy margins and domains*

The glassy domains originally comprised coherent volcanic glass (Fig. 28.1A), in situ quench fractured glass (Fig. 28.1B) and variably matrix-rich autoclastic (hyaloclastite, autobreccia) breccia facies (Fig. 28.1C). After emplacement and late in the cooling history of glass, or following cooling to surface temperatures, perlitic cracks sometimes developed in response to hydration of the glass. Circulating fluids moved out from fractures (perlitic, quench) and the matrix progressively altering the glass in several stages. The initial alteration was either pervasive (Fig. 28.3.2) or ceased before completely affecting the whole rock, leaving domains of glass that were altered during a second alteration step or stage (Fig. 28.4.1).

Outside the Highway-Reward hydrothermal alteration envelope, perlite kernels and clasts in autoclastic breccia have often completely altered to feldspar (albite) during initial diagenetic alteration. Later sericite, chlorite or quartz alteration often commenced along fractures and moved out from these into the albite-altered domains. Elsewhere, initial chlorite alteration extended out from fractures into all the glassy parts. Subsequent generations of sericite and/or quartz alteration overprinted earlier phyllosilicate alteration and were also fracture controlled. In some samples, feldspar alteration has been partially replaced by quartz±feldspar. The result in hand specimen and thin section, is abundant cusped-shaped domains which resemble shards in pyroclast-rich rocks (cf. Allen, 1988; McPhie et al., 1993).

A similar style of alteration characterises glassy facies within the Highway-Reward hydrothermal alteration envelope. Hyaloclastite clasts often pervasively sericite-chlorite-altered and feldspar phenocryst are variably sericite, chlorite and/or carbonate-altered. Subsequent quartz-sericite alteration commenced along fractures and the matrix of autoclastic breccia (Fig. 28.4.2). In other cases, perlitic fractures and the matrix between

clasts have altered to sericite, whereas perlite kernels have altered to fine quartzo-feldspathic mosaics (HMO 40, 158.5m). More advanced alteration rarely extends far from the fractures or matrix, possibly due to the reduction in porosity accompanying initial alteration stages.

#### *Mixed glassy and devitrified domains*

Prior to alteration, mixed glassy and devitrified domains comprised devitrification structures (spherulites, lithophysae) scattered in glass (Fig. 29.1A), coalescing spherulites enclosing cusped patches of residual glass (Fig. 29.2B), and flow bands of glass alternating with devitrified bands (Fig. 29.1C). Hydrothermal and diagenetic alteration of the glassy domains has progressed along a similar path to the glassy margins. Most often the glass has altered to assemblages of sericite, chlorite, feldspar and sometimes carbonate or micropoikilitic quartz, whereas phenocrysts are now sericite, albite or chlorite. In contrast, crystalline and devitrified domains are silicified or have recrystallised to quartzo-feldspathic mosaics (Fig. 29.4). Relic radial fibrous textures are preserved in some spherulites. The original bulbous outline of the bands is generally preserved, even when radial fibrous textures are completely recrystallised. The exception is in zones of intense hydrothermal alteration, where patchy and mottled textures are common.

In autobreccia facies, clasts are often flow banded and show a similar alteration history. Apparent polymictic breccia textures sometimes develop as alteration mineralogy varies between clasts in response to different degrees of devitrification and overprinting alteration. Phenocrysts are often obscured in quartzo-feldspathic bands and accentuated in formerly glassy phyllosilicate domains. This sometimes results in apparent variation in phenocryst abundance between domains or clasts, and so apparent polymictic textures.

#### *Crystalline domains*

Large parts of some lavas and intrusions have a groundmass comprising spherulites, micropoikilitic texture or granophyric texture. In many samples, hydrothermal alteration and metamorphism have recrystallised original fibrous devitrification textures to pale quartzo-feldspathic mosaics with interstitial sericite±hematite±pyrite (Fig. 30.3-30.5). Other spherulites are now monocrystalline quartz or comprise a few subgrains (e.g. REW 600, 245.5m). Outside the hydrothermal alteration envelope, devitrification textures are better preserved and comprise feldspar and quartz with interstitial sericite and chlorite. The result in hand specimen is a granular texture (e.g. HMO 86, 169.3m).

Moderate to strong hydrothermal alteration generates mottled and patchy domains of different mineral assemblages. Feldspar phenocrysts are variably altered to sericite, chlorite, pyrite, quartz and carbonate. This alteration style often generates apparent clastic and polymictic textures.

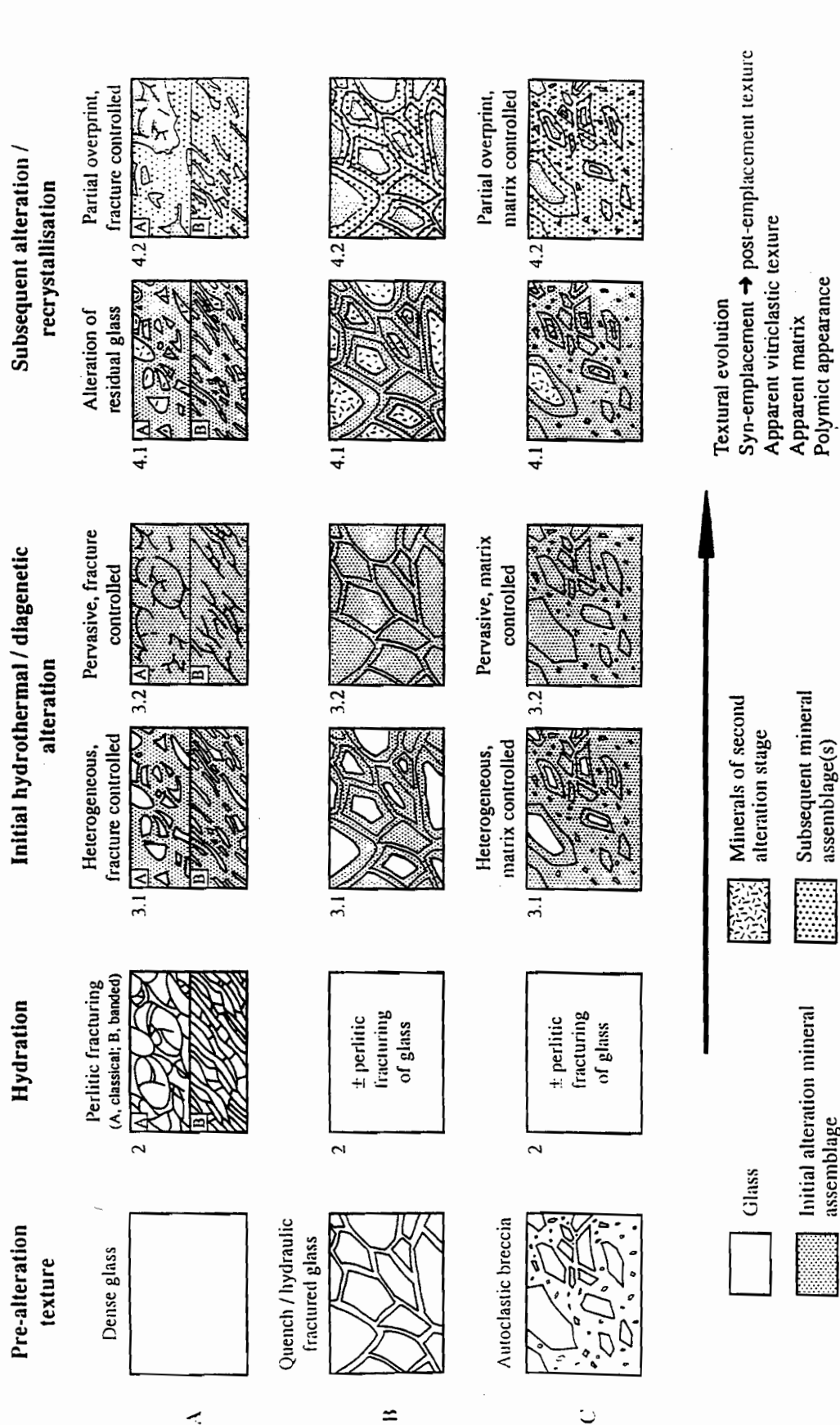


Figure 28. Stages in the textural evolution of the glassy margins of lavas and syn-sedimentary intrusions. 1—Prior to the onset of alteration the glassy margins comprised: (1A) dense glass; (1B) quench fragmented glass; and/or (1C) autoclastic breccia. 2—After emplacement and late in the cooling history of glass, or following cooling to surface temperatures, perlitic cracks sometimes developed in response to hydration of the glass. The cracks can be arcuate and concentrically arranged (classical perlitic) or form rectilinear networks (banded perlitic). 3—Initial hydrothermal or diagenetic alteration can proceed by a combination of fracture and/or matrix-controlled alteration or pervasive alteration. Two cases arose: (3.1) Alteration minerals progressively replaced glass out from perlitic fractures (3.1A), quench fractures (3.1B) or the matrix in autoclastic breccia (3.1C). However, the alteration was incomplete, leaving isolated kernels or domains of glass. (3.2) Alteration commenced along fractures and progressed right through the glass generating a pervasive alteration style. 4—Subsequent alteration and recrystallisation. In cases where the first alteration stage was incomplete, residual glassy cores were replaced during the second alteration stage (4.1). Subsequent alteration was also mainly localised along fractures or the matrix of autoclastic breccia or overprinted alteration domains of similar mineralogy (4.2).

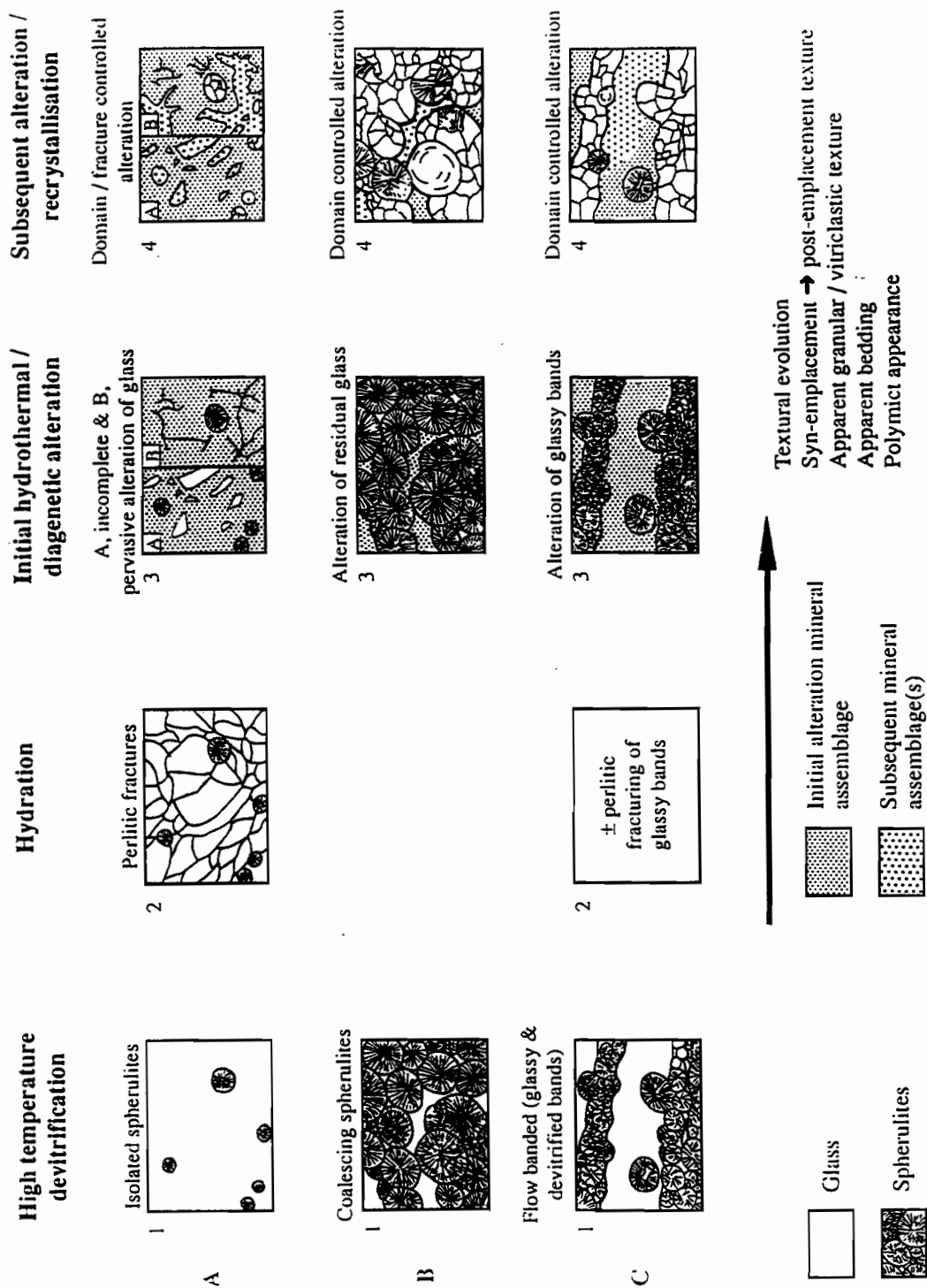


Figure 23 Stages in the textural evolution of the mixed glassy and devitrified domains in lavas and syn-sedimentary intrusions. 1— Prior to the onset of alteration the mixed glassy and spherulitic zones comprised: (1A) glass with scattered spherulites; (1B) coalescing spherulites with cusped areas of glass; and/or (1C) devitrified bands alternating with glassy bands. 2— After emplacement perlitic cracks sometimes developed in glassy bands. 3— Initial hydrothermal or diagenetic alteration of the glassy domains was similar to alteration in the glassy margins. Alteration was fracture controlled or pervasive and trended towards sericite- or chlorite-rich assemblages. 4— Subsequent alteration of the glassy domains was also mainly localised along fractures or overprinted alteration domains of similar mineralogy. In contrast, single spherulites and bands or nodules of devitrification structures were recrystallised, silicified or replaced by feldspar during alteration.

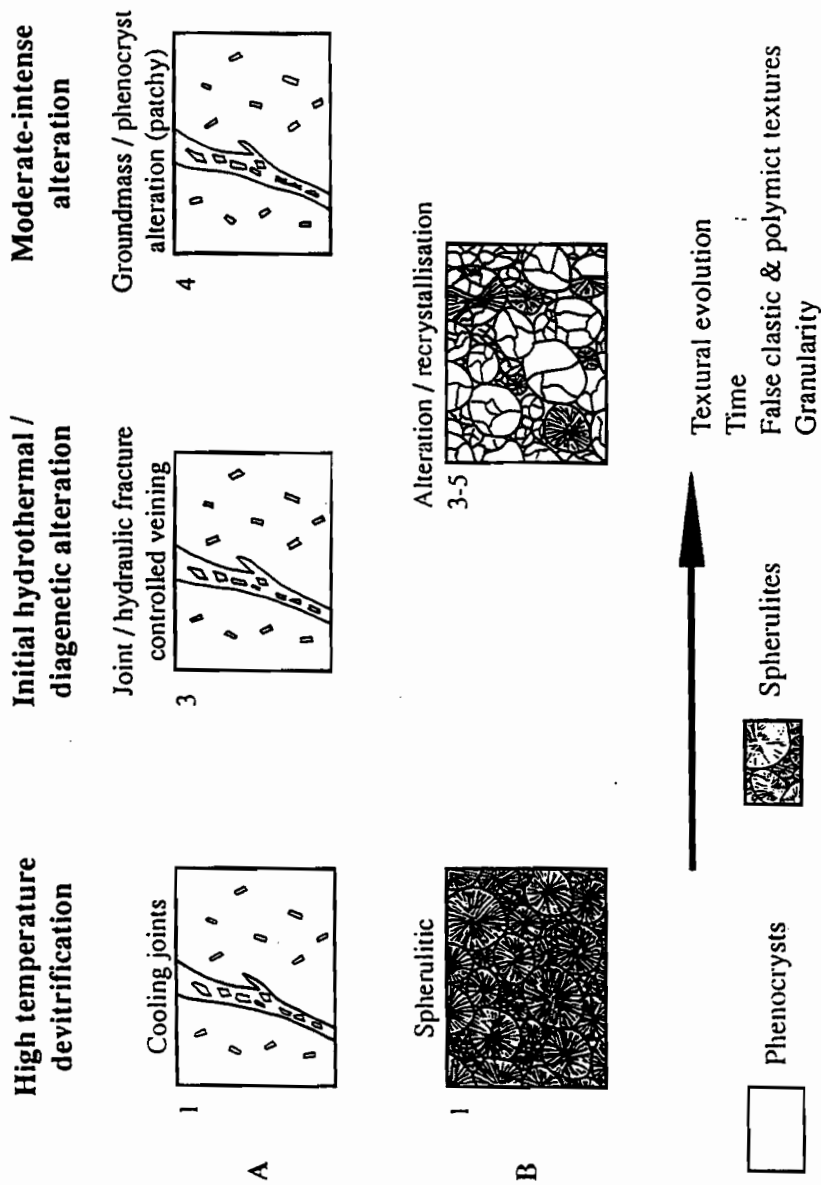


Figure 30 Stages in the alteration of the crystalline and devitrified domains in lavas and syn-sedimentary intrusions. 1— These domains have a groundmass of closely packed spherulites, microlites or micropoikilitic quartz. Joints are sometimes present. 3— Diagenetic and hydrothermal alteration often commence along joints or hydraulic fractures. 4— Subsequent alteration attacked phenocrysts (e.g. feldspar) and generated patchy and mottled textures. 5— Recrystallisation and silicification of spherulites during hydrothermal alteration and metamorphism destroys fibrous devitrification structures generating a quartzo-feldspathic mosaic.



## DAY 3 MASSIVE SULFIDE MINERALISATION HOSTED BY PUMICE BRECCIA UNITS

### Stop 8: Liontown mine site — Mark Doyle, Craig Miller

Directions: Drive south from Charters Towers along the Gregory Developmental Road, as for yesterday. Approximately 25 km south of Charters Towers, there is a hard right turnoff onto an unsealed road signposted Liontown/Windsor/Trafalga. Follow this road and proceed past a turnoff to the Liontown Station. The Liontown core yard and historic workings are located to the left of the road 1.2-1.6 km past the turn off.

#### *Exploration and Mining History*

The Liontown deposit was discovered in 1905 and originally referred to as the Carrington Goldfield. The early workings concentrated on mining Au-Cu ores hosted in the Liontown footwall stringer zone. The oxide, carbonate and supergene resources were worked underground to a depth of 676 feet and over a strike length of 920 feet. In the period 1905-1911 the workings yielded 28,126 ounces of gold bullion (Livingston, 1972). Production ceased in 1911 when the hypogene ore was reached and dewatering became prohibitive.

In the period 1951-1961, an additional Au-Ag-Zn resource (Carrington lode; Miller, 1996) was identified and developed. Over 9,285 tons of ore were treated yielding 2990 ounces of gold, 53957 ounces of silver, and 520 tonnes of lead (Livingston, 1972).

The potential for discovery of new massive sulfide deposits and extensions of the Liontown resource has driven the modern phase of exploration. In 1993, Pancontinental Mining Limited/RGC Exploration Pty Ltd acquired the Liontown deposit and adjoining leases. Re-evaluation of the Liontown drill core indicated the presence of 1.8 M.t @ 6.16% Zn, 2.2% Pb, 0.48% Cu, 29 g/t Ag and 0.9 g/t Au (Miller, 1996).

### Stop 9: Liontown core store — Mark Doyle, Craig Miller

#### **Stop 9.1 DDH LDD 128: Lithofacies associations hosting the seafloor and sub-seafloor replacement style Liontown VHMS deposit**

The Liontown deposit is located at the top of the Trooper Creek Formation. Strata in the area dip at angles of around 70° south (Miller, 1996). The sequence is cut by several faults. Diamond drill hole LLD 128 provides a continuous section through the volcano-sedimentary succession hosting the deposit (Fig. 31). In descending order, the principal lithofacies are siltstone, feldspar-phyric dacite, carbonaceous and pyritic black shale, arenite, interbedded (vitriclastic ?) sandstone-siltstone and footwall dacitic pumice breccia. Massive sulfide mineralisation is hosted by the footwall pumice breccia (Carrington Lode) and occurs within the overlying siltstone and sandstone beds (locally termed the "Liontown Horizon").

#### *Rhyodacite intrusion and associated peperite*

Coherent rhyodacite at Liontown is feldspar-, quartz- and hornblende-phyric and poorly vesicular. Feldspar phenocrysts are evenly distributed through out a variably sericite, chlorite±quartz-altered groundmass which is locally perlitic (formerly glassy). Aligned chloritic wisps (< 5 mm) define a foliation (flow foliation) which wrap around phenocrysts and defines an eutaxitic-like texture in the core.

The upper and lower contact zones are marked by intricate interpenetration of the rhyodacite and pale grey siltstone and crystal-lithic breccia and sandstone beds. In some cases (e.g. DDH LLD 128), a thin (25 cm) zone at the upper contact the rhyodacite is light grey and sericite-altered. Relatively coherent rhyodacite passes out into a breccia in which blocky clasts and liberated crystals are separated by siltstone. Downward from the contact seams of sediment penetrate the rhyodacite and locally enclose blocky to ragged

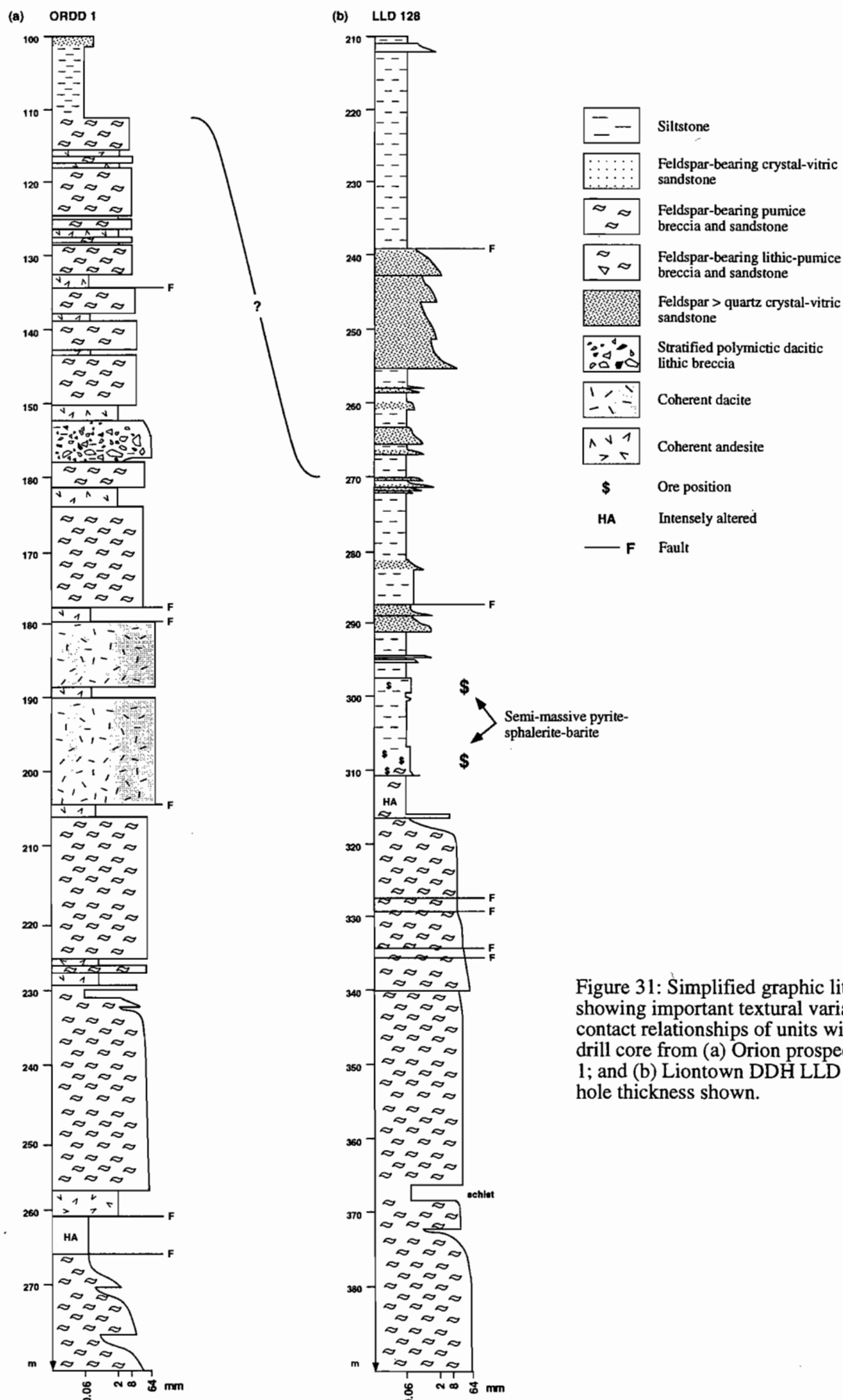


Figure 31: Simplified graphic lithological logs showing important textural variations and contact relationships of units within diamond drill core from (a) Orion prospect, DDH ORDD 1; and (b) Lontown DDH LLD 128. Down hole thickness shown.

rhyodacite clasts. In drill hole DDH LLD 125, siltstone inclusions occur in coherent rhyodacite up to 15 m away from the contacts with the siltstone facies. Along the lower contact of DDH LLD 128, feldspar and quartz crystals and crystal fragments and former glassy fragments (now chlorite) are mixed with the siltstone and occur as pods in the rhyodacite. These features are consistent with fluidisation of the wet unconsolidated sediment by the rhyodacite during emplacement (cf. Kokelaar, 1982). Heating of the pore waters is interpreted to have mobilised the sediment, rhyodacite fragments and crystals into fractures and away from the contact. These features are common in other examples of peperite. The peperitic upper margin of the rhyodacite is consistent with emplacement as syn-sedimentary sills.

The rhyodacitic sills intruded interbedded siltstone and crystal-lithic breccia and sandstone beds. The crystal-lithic breccia beds are typically normally graded with diffusely laminated sandstone tops and in some cases polymictic lithic-rich bases. One bed has a reversely graded sandstone base. The clast population includes carbonaceous siltstone, feldspar-phyric dacite and quartz- and feldspar-phyric rhyodacite clasts with angular to sub-rounded shapes.

#### *Carbonaceous and pyritic black shale*

The distinctive black shales are massive to finely laminated, often carbonaceous and generally contain 1-2% disseminated pyrite. Normally graded, sericitised, crystal-vitric sandstone beds are interbedded with the shales and occur in intervals up to 16 m thick (e.g. LLD 125). Thinner intervals comprise a single graded unit whereas thicker intervals are made up of a small number of beds each up to 5 m thick. The beds are typically feldspar-quartz-bearing but rare units contain only feldspar crystals (e.g. LLD 128, 211 m). The crystal populations suggest rhyodacitic to dacitic provenance.

Intervals of the facies range from 20 to 80 m thick. Small (10-20 cm amplitude) folds deform beds. In some sections of drill core, quartz and carbonate veins cut units.

The black shales represents the ambient conditions in the depositional environment and suggest a relatively deep, quiet, anoxic environment. Crystal-vitric sandstone beds represent small turbidites which interrupted the ambient sedimentation.

#### *Quartz-sericite-altered sandstone-siltstone*

The carbonaceous black shales pass down into a succession of interbedded grey siltstone and graded sericitic sandstone beds. The boundary with the overlying facies is often gradational and characterised by intervals of black shale alternating with grey to green siltstone/mudstone. Patchy domains (5 cm across) of silicified mudstone/siltstone sometimes characterises contacts with the black shale (e.g. LLD 125, 258 m). Siltstone intervals are strongly silicified and vary from massive to finely laminated. Occasional beds contain outsized, chloritic, evenly feldspar-phyric clasts with wispy shapes (e.g. LLD 125, 262 m). These may represent compacted pumice clasts that settled through the water column and deposited with the siltstone.

Massive to normally graded vitric-crystal sandstone beds occur in intervals of 1 to more than 7 m thick. Beds vary in thickness from a few centimetres to 5 m and are separated by varying (1 cm to 4 m) intervals of siltstone. Bases are sharp to diffuse and amalgamated units are evident. Petrographically the beds comprise feldspar-quartz crystal fragments and devitrified (quartz, sericite) shards and tube pumice clasts. Sandstone beds are more strongly foliated than the interbedded siltstone units which are silicified, occasionally hematite-altered and cut by numerous carbonate veins.

#### *Liontown Horizon – interbedded sandstone, siltstone and massive sulfide*

The Liontown Horizon comprises similar lithofacies to the overlying succession but is dominated by dacitic volcanic detritus. In drill core, the upper boundary of the Liontown Horizon is often indistinct (e.g. LLD 128, 291.6 m). Siltstone units are light grey and variably sericite-quartz-altered. Sandstone units are normally graded and often contain sphalerite-barite-pyrite mineralisation (e.g. LLD 128, 310 m). The beds locally contain

relic pumice clasts (e.g. LLD 125, 304 m) and presumably originally comprised former glassy fragments (now sericite-chlorite).

The sandstone units are interpreted as turbidites, indicating deposition below storm wave base. Intercalated siltstone beds are consistent with deposition in a relatively quiet and/or deep-water environment. Geochemically the units are dacites (Miller, 1996). This suggests that the Liontown Horizon may comprise detritus that deposited in the post-eruptive phase of sedimentation that followed emplacement of the underlying dacitic pumice breccia and sandstone facies ("Footwall pumice breccia").

*Pumice breccia and sandstone ("Footwall pumice breccia")*

The pumiceous sandstone and breccia facies is characterised by variably quartz-sericite-chlorite-altered feldspar-phyric pumice clasts and subordinate feldspar crystal fragments. Volcanic lithic clasts are a minor component in the bases of some units. Beds are 1 to 110 m thick (apparent) and normally graded with thin (<4 m) tuffaceous sandstone tops. Bedding varies from sharp to poorly defined and amalgamated units are present. Some units are separated by thin intervals (< 1 m) of light grey (formerly ashy?) siltstone. Siltstone intervals are more common at the top of the section and intercalated with thin (1-5 m) pumice breccia beds which separate some very thick (10's m) pumiceous units (e.g. LLD 114, 252-270 m).

The lithofacies character of the pumice breccia and sandstone beds is consistent with deposition from cold (or cool) water-supported, high-concentration sediment gravity flows. Deposition of the facies was rapid as indicated by the lack of thick interbedded siltstone units. Pumice and shards within the facies are interpreted as pyroclasts sourced from sustained explosive silicic magmatic eruptions of the type that are generally considered to be limited to shallow subaqueous or subaerial settings. The thickness of the pumice breccia and sandstone facies and regional extent (>6 km; Miller, 1996) suggests that the facies was rapidly emplaced and is syn-eruptive.

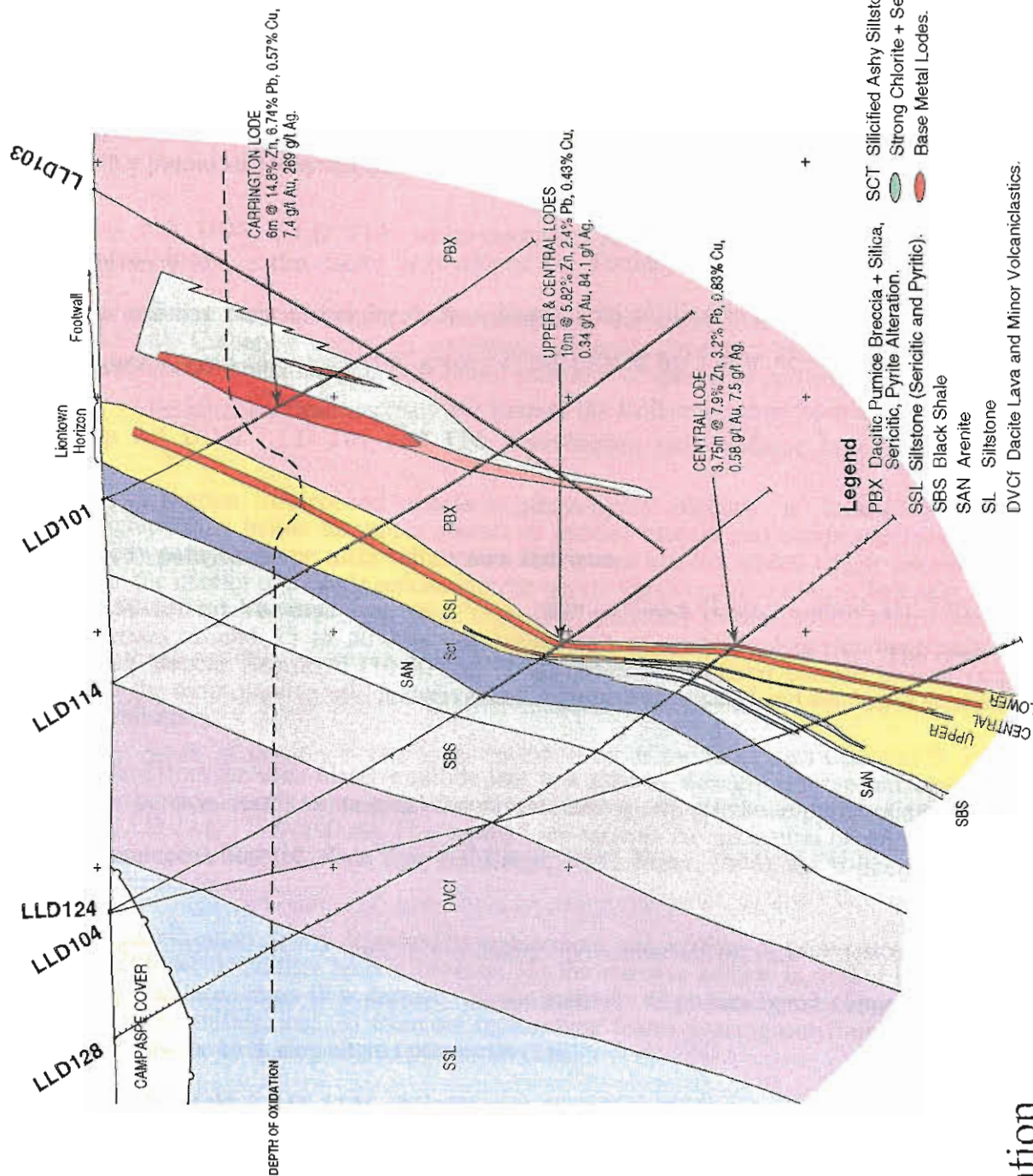
**Stop 9.2 DDH LLD 128: Stratiform lodes deposited by seafloor exhalation and sub-seafloor replacement and infilling of pore space**

Siltstone and sandstone units of the Liontown Horizon host three stratiform Zn-Pb lenses that are locally termed the upper, central and lower lodes (Miller, 1996; Fig. 32). The *upper lode* occurs near the top of the Liontown Horizon and comprises thin (1-2 m), discontinuous sphalerite-pyrite-barite-quartz-bearing lenses (e.g. LLD 128, 296.8 m). Sphalerite is pale grey to cream in colour suggesting a low iron content. Sericite-carbonate-altered volcanic rock (former tuffaceous detritus?) accounts for 50 to 95% of the lenses. Relic quartz crystals (< 1 mm) suggest that the mineralisation contains rhyolitic to rhyodacitic volcanic detritus (e.g. LLD 104, 214.5 m). In some cores (e.g. LLD 114, 213.6 m; LLD 128, 296.8 m), fine (0.5-5 mm) bands of sphalerite-barite are dismembered by a moderate to strong foliation. Quartz-carbonate porphyroblasts are rotated in the foliation. In other cores (e.g. LLD 128, 297.8 m), sulfide bands and sericite-quartz-altered bands are deformed by small folds and displaced by fractures. These observations imply that both tectonic banding and primary depositional banding characterise the ores.

The central *lode* is located 3 to 12 m below the upper lode and ranges from 3 to 12 m in thickness (Miller, 1996). Siltstone and sandstone units separating the upper and central lodes are variably sericite-chlorite-carbonate-altered and contain disseminated, spotty and banded sphalerite and pyrite (e.g. LLD 104, 217.7-220.2 m). The boundaries of the upper and central lodes are sharp where the intervening units are siltstone (e.g. LLD 128, 299-307 m), and less well defined when sandstone units dominate the interval (e.g. LLD 104, 217.7-221 m). The central lode comprises semi-massive barite-sphalerite-pyrite bands alternating with sericite-rich bands and siltstone. Banding is deformed around small (0.5-3 cm), ellipsoidal carbonate-sphalerite nodules. The mineralisation is strongly sheared and asymmetrical pressure shadows are common. Disseminated sphalerite-pyrite mineralisation is also present (e.g. LLD 101, 52-54 m). There are replacement fronts



# Mount Windsor Project Liontown Section 10200 E



85

within the central lode and possible relic pumice fragments (e.g. LLD 128, 307-310.7 m). Petrographically the ores comprise low-iron sphalerite, minor galena and chalcopryrite and trace tennantite-tetrahedrite (Miller, 1996). Sphalerite in the central lode is darker grey in colour than the upper lode, and lighter than the lower lode, which suggests an increasing iron content passing from the upper to lower lodes (cf. Miller, 1996).

The *lower lode* forms a discontinuous horizon (typically < 0.5 m thick) at the contact between the "Liontown Horizon" and underlying dacitic pumice breccia and sandstone (Miller, 1996). Part of the mineralisation is hosted by the pumice breccia (e.g. LLD 128, 319.2-324 m). Distinction between the central and lower lodes is often difficult as the intervening lithofacies are strongly sericite-altered and contain disseminated and patchy sphalerite (e.g. LLD 128, 310.2-310.7 m). The lower lode locally comprises patchy (up to 2 cm across) and semi-massive sphalerite with a sericite±quartz-altered gangue. Other mineralisation types are sphalerite-galena, quartz±carbonate and barite veins. Relic pumice fragments suggests the alteration and mineralisation have selectively replaced former pumice breccia and sandstone units.

### **Stop 9.3 DDH LLD 114: semi-massive carbonate at the margins of the central lode**

Semi-massive carbonate occurs at the margins of the upper lodes (e.g. LLD 114, 121-124.5 m). Carbonate occurs as coalescing spheroids separated by sericite wisps. This alteration style contains spots (< 0.2 mm) and veins of sphalerite and minor pyrite.

### **Stop 9.4 DDH LLD 101 and 114: Carrington sub-seafloor lode**

The Carrington stratabound sphalerite-galena-pyrite orebody is located 30-50 m stratigraphically below the upper contact of pumice breccia and sandstone facies. The orebody comprises one main sulfide lens and several smaller lenses which are enclosed within the interior of a single sericite-chlorite-quartz-altered pumice breccia bed (e.g. LLD 101, 80-130 m). The main lens has a "cigar-like" geometry (Miller, 1996). Matrix gangue comprises around 15 to 50% of the lenses and is sericite-chlorite±carbonate-altered pumice breccia. Segments (10-30 cm) of sericite-chlorite-altered pumice breccia occur within the semi-massive sulfide interval and contain disseminated and vein-style sphalerite mineralisation.

Outward from the semi-massive sulfide lens is a zone of strongly chlorite-sericite-quartz-altered pumice breccia containing disseminated and spotty sphalerite-pyrite mineralisation (e.g. LLD 114, 177.9-190 m). The "spotty" ore records the nucleation of sulfides within the pumiceous host (cf. Khin Zaw and Large, 1992; Miler, 1996) and is interpreted as a replacement front.

The mineralisation clearly deposited by replacement and infilling of pore space within the enclosing dacitic pumice breccia because: (1) the massive sulfide is hosted by a single rapidly emplaced mass-flow deposit; (2) relic intervals of pumice breccia are preserved in the massive sulfide; and (3) there are replacement fronts passing out from the massive sulfide into the enclosing altered pumice breccia.

### **Stop 9.5 DDH LLD 114: chlorite-sericite alteration**

Zones of strong chlorite-sericite-altered pumice breccia occur at the margin of the Carrington Lode. In the most intensely altered domains, relic sericite, chlorite or carbonate-altered feldspar crystals are the only indication of a former pumiceous character. In other domains, pumice fragments and shards are identifiable with a hand lens.

### **Stop 9.6 DDH LLD 114: nodular quartz>sericite-chlorite alteration**



In much of the core (e.g. LLD 114, 205-232 m), intervals of dacitic pumice breccia have an augen schist texture. Quartz alteration forms small (0.6-1 cm) nodular domains (augen) which coalesce to form larger patches. The augen are separated aligned chlorite±sericite wisps (0.2-4 cm) which define a well-developed foliation. Relic uncompact vesicles are preserved in some quartz nodules suggesting the pumice breccia is non-welded. Only in the most intensely quartz-altered domains are pumice textures completely destroyed. Although vesicular textures are rarely preserved, the chlorite-sericite wisps are also interpreted as compacted pumice fragments. Augen schist texture often better developed at the base of units. This observation suggests that quartz augen were able to grow to a larger size within the coarser pumiceous base. Nodules are alteration of single pumice and larger domains. It is uncertain if quartz was the first alteration mineral or if earlier alteration minerals (e.g. albite, clay, zeolite) were present. Fine (< 0.2 mm, 1-2%) disseminated and patchy (2-7 cm) pyrite occurs within some quartz-sericite-chlorite-altered domains (e.g. LLD 128, 382.4-399.3 m). Pyrite is locally concentrated in some chlorite-altered pumice fragments. In some cores, pyrite±chalcopyrite-quartz, carbonate and sphalerite veins are locally abundant.

### **Stop 9.7 DDH LLD 128: patchy sericite-chlorite>quartz alteration**

Other intervals of the dacitic pumice breccia and sandstone facies are characterised by mottled and patchy sericite-chlorite>quartz alteration. Pumice clasts are strongly compacted and define a well-developed foliation which is parallel to the cleavage. Occasional small quartz nodules are present and contacts with the more quartz-rich domains are gradational. Quartz veins are common within some segments of the core (e.g. LLD 128, 349.2-355.7 m). Feldspar crystals and phenocrysts are altered to sericite, chlorite and/or carbonate. An even distribution of feldspar crystals generates an evenly porphyritic texture that is more characteristic of a coherent lava or intrusion (e.g. LLD 113, 181.5-188.9 m). Chlorite veinlets cut the core and locally coalesce to form patches (e.g. LLD 117, 111-172 m).

### **Stop 9.8 DDH LLD 128: Muscovite geochemistry**

Plots of the geochemical characteristics for muscovite in the Liontown alteration zones are presented in figure 33.

### **Stop 9.9 DDH CGD 001: Cougar town prospect ("distal" alteration types)**

Cougar Town prospect is located approximately 1.5 km to the west of Liontown. A Pb-Zn-enriched gossan is developed at surface within altered dacitic pumice breccia beds. The pumiceous units are correlated with those hosting the Carrington Lode (cf. Miller, 1996). A quartz>sericite-chlorite zone is centered beneath the ore position and closely resembles that in the footwall of the Liontown deposit (e.g. CGD 001, 90-140 m). Quartz occurs as coalescing nodules and irregular patches (2-4 cm) separated by compacted chlorite-sericite-altered pumice fragments. Chlorite veinlets cut the core and merge to form irregular and wispy patches. Feldspar crystal fragments and phenocrysts within the pumice clasts have altered to chlorite, sericite, quartz and/or carbonate. Downward (and outward?) from the quartz>sericite-chlorite zone is a sericite-quartz-chlorite zone (CGD 001, 140-154 m). The quartz-sericite alteration is relatively pervasive and encloses chlorite wisps up to 2.5 cm long. Lithic clasts (1-3 cm) and feldspar crystals are albite-altered in contrast to the former glassy pumice walls, implying that the albite is earlier. This alteration style gives way to increasing feldspar-rich alteration. There is a gradation from sericite-quartz-feldspar (albite)-chlorite alteration (CGD 001, 154-185 m) into a feldspar-sericite-chlorite alteration (CGD 001, 185-215 m). Quartz-albite-sericite nodules and patches (0.5-4 cm) are separated by compacted chlorite wisps (former pumice fragments) (1-3 cm long). In the feldspar-sericite-chlorite-altered pumice breccia, albite forms small (1-10 cm) patches between chlorite-epidote-sericite wisps with abundant feldspar crystals.

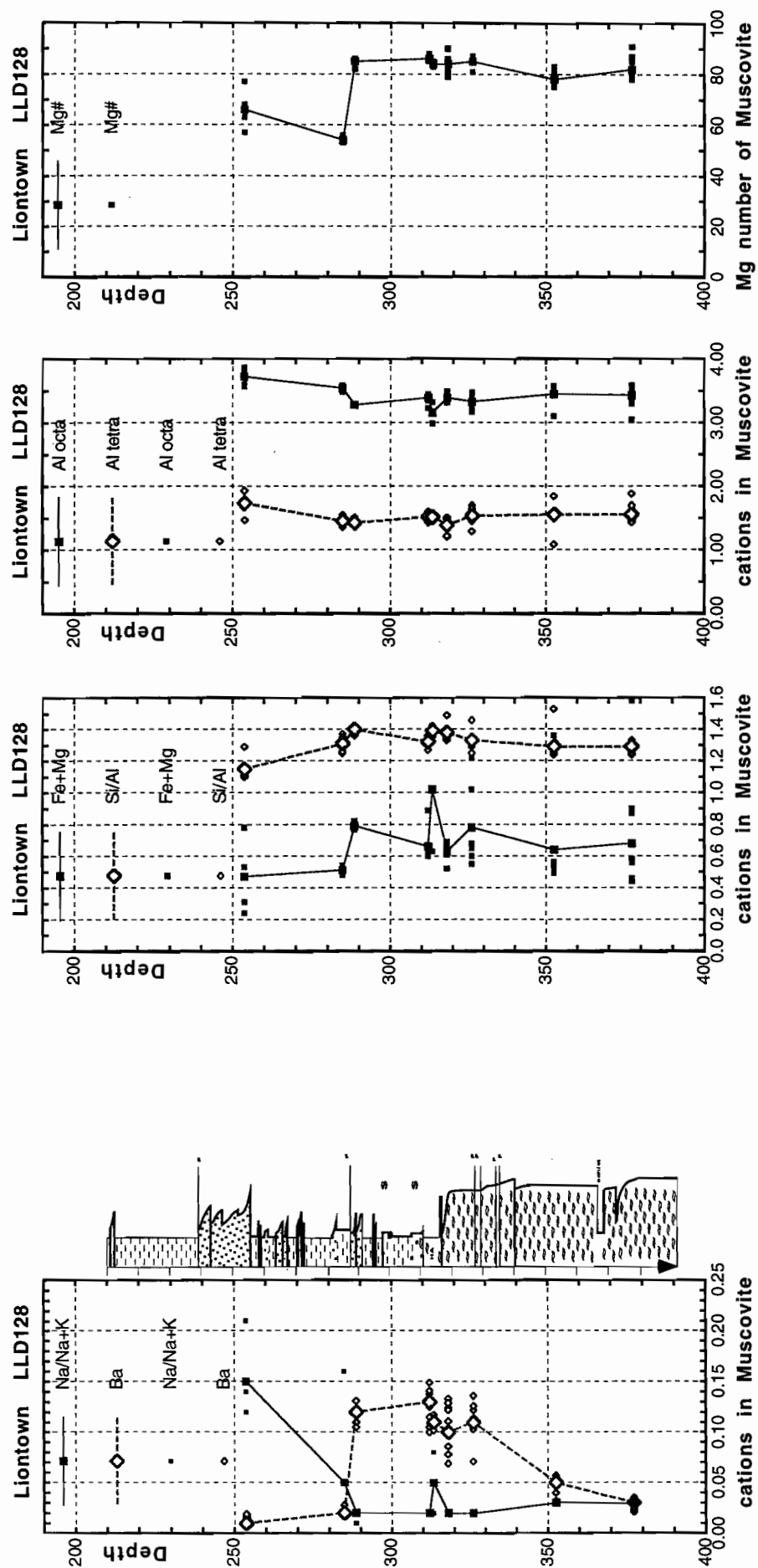


Figure 33. Liontown Muscovites

The alteration assemblages intersected at Cougartown are similar to those intersected in pumice breccia units at the margins of the Liontown alteration halo (e.g. DDH LLD 117).

### **Stop 10: RGC Exploration core yard, Charters Towers**

Directions: Return to Charters Towers and assemble at the RGC exploration core store (Brisk St). To get to Brisk St follow the Flinders Highway (becomes Thompson St) and turn right onto Armstrong St. Follow Armstrong St. to the intersection with Brisk St. The RGC core yard is located at the intersection of Brisk St and Phillipson Road.

#### **Stop 10.1 Orion prospect, DDH ORDD 1 — Regional diagenetic alteration**

Orion prospect is located approximately 5.5 km's to the north east of the Liontown deposit. At Orion prospect, the succession is dominated by feldspar-only (dacitic) pumice breccia which is intruded by a feldspar-phyric dacite syn-sedimentary sill (Fig. 31). The section is dissected by numerous andesite/dacite intrusions. The thickness of dacitic pumice breccia in ORDD 001 and scarcity of intercalated siltstone units, suggest that it may be correlate with similar pumice breccias intersected at the same stratigraphic position around Liontown. Panthertown prospect is located 2.5 km NE of Liontown and approximately 3 km SW of Orion. At Panthertown, feldspar-only crystal-lithic sandstone beds intersected in the top of diamond drill hole LLD 138 (102-119.4 m) are interpreted as the base of the regionally extensive key facies association. Doyle (1997b) and Doyle (1998a) propose that the distinctive feldspar-only pumice breccia unit is regionally extensive and may be traceable to Snake Oil prospect and Trooper Creek prospect tens of km's to the east.

In Orion drill hole ORDD 1, the pumice breccia beds are normally graded and have fine tuffaceous sandstone tops (e.g. 230-257 m). A few beds have polymictic lithic rich bases (e.g. 152-157 m). Patchy and pervasive sericite-albite-carbonate-chlorite alteration has preserved or obscured vesicular textures in the pumice breccia. Sericite-chlorite-altered pumice clasts and domains are strongly compacted. Feldspar phenocrysts and crystal fragments have altered to albite, carbonate, sericite and/or chlorite. Numerous carbonate veins and veinlets cut the core.

The sericite-albite-carbonate-chlorite assemblage is a common alteration style in the Trooper Creek Formation. The albite-rich alteration often replaces glassy pumice breccia beds distal to mineralisation and is interpreted as background diagenetic alteration.

#### **Stop 10.2 Snake Oil Pb-Zn prospect (DDH SODD 001, 002)**

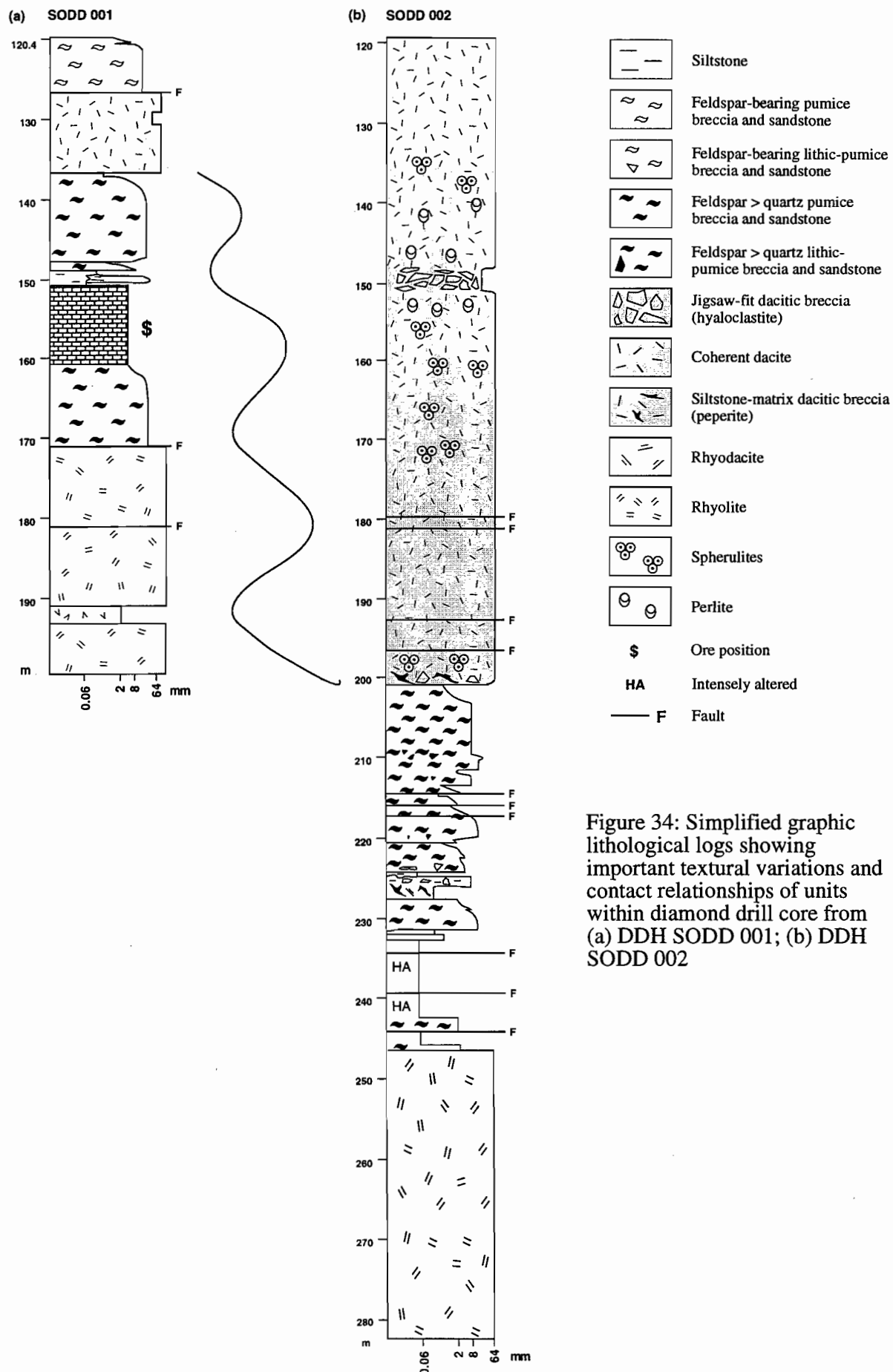
— Mark Doyle

Snake Oil is a small Pb-Zn prospect located to the south east of the Highway-Reward mine. The prospect occurs at the top of the Trooper Creek Formation near the contact with the overlying Rollston Range Formation. Four drill holes from Snake Oil (SODD 001, SODD 002) and surrounding prospects (Rustler, REW 812; Stocksquad, REW 813) were logged at 1:200 scale as part of the AMIRA P439 project. The snake Oil diamond drill holes provide examples of carbonate alteration textures, evidence for sub-seafloor carbonate deposition and the influence of volcanic facies on alteration.

In the Snake Oil area, the Trooper Creek Formation comprises coherent facies which are intercalated with rhyodacitic to dacitic volcanoclastic units and volcanic to non-volcanic sedimentary facies (Fig. 34).

Massive and flow banded rhyolite and dacite

This facies is characterised by an even distribution of quartz and/or feldspar phenocrysts in a finely crystalline groundmass. The phenocryst assemblages and percentages suggest



that the coherent facies are rhyolitic to dacitic in composition. Dacites contain 5-7% feldspar phenocrysts, 1 to 3 cm across, whereas rhyolites have 5% quartz phenocrysts, ranging from 0.4 to 4 mm, and 6% feldspar phenocrysts (0.5-1.5 mm). Quartz phenocrysts are euhedral or embayed. Feldspar phenocrysts are euhedral and are unaltered or variably altered to sericite, chlorite or carbonate. Intervals of dacite contain 3-5% ellipsoidal vesicles up to 4 cm long. Vesicles are aligned and filled with chlorite, quartz, carbonate or zones of quartz and chlorite.

The groundmass has altered to various assemblages of sericite, chlorite, carbonate, hematite and quartz. In dacite units, the groundmass has devitrified to coalescing spherical spherulites separated by cusped chlorite patches a few millimetres across (presumably after glass; SODD 002, 171-173 m). Relic classical perlitic fractures suggest that parts of the groundmass were formerly glassy. Fractures are delineated by quartz-sericite alteration, and outline sub-spherical kernels of feldspar (albite ?), sericite and/or chlorite-altered dacite.

#### Monomictic breccia facies

Intervals of this facies comprise non-stratified, clast-supported aggregates of dacite clasts (e.g. SODD 002, 148-151 m). Clasts are evenly porphyritic (feldspar), weakly vesicular and have blocky shapes bound by planar to curvilinear margins. The groundmass of clasts can be perlitic, flow banded or altered to sericite and/or chlorite (e.g. SODD 001, 130 m). Fractures and the matrix between clasts have altered to quartz and sericite.

Clasts form jigsaw-fit aggregates with fragments and crystals at clast margins showing progressive stages of disintegration and contributing to the matrix. In some intervals, minor rotation and translation of clasts following brecciation is implied by flow banding at different orientations.

Thicknesses of the monomictic breccia facies range from 1 to 3 m thick. Contacts between the monomictic breccia facies, sediment-matrix breccia facies and coherent dacite are sharp but gradational.

#### *Origin and significance of the massive facies and monomictic breccia facies*

Textural characteristics and contact relationships are consistent with interpretation of the rhyolite and dacite intervals as coherent igneous rocks. Gradational contacts between coherent dacite and the monomictic dacitic breccia facies suggest that the facies are genetically related. Clast shapes and widespread preservation of jigsaw-fit is consistent with interpretation of the monomictic breccia facies as hyaloclastite. Clast rotation and translation occurred in response to stresses imposed on the quenched parts of the dacite during continued movement of the more ductile interior (cf. Pichler, 1965).

#### Non-stratified sediment-matrix breccia facies

This facies comprises jigsaw-fit rhyodacite (SODD 002, 224-225 m) or dacite clasts (e.g. SODD 002, 200.2-200.6 m) separated by grey siltstone. Along some clast margins, fragments and crystals display arrested stages of fragmentation and dispersion in the siltstone matrix. Dacite clasts are blocky and bound by planar to curvilinear margins. Rhyodacite clasts are evenly porphyritic with 7% feldspar phenocrysts and 3% quartz phenocrysts ranging from 0.5 to 1 mm across. Clasts vary from blocky to ragged in shape.

In siltstone matrix-poor breccia, clasts form jigsaw-fit aggregates or siltstone seams cut relatively coherent rhyodacite or dacite. In sediment matrix-rich breccia, clasts are more widely dispersed in the siltstone matrix. Matrix-rich breccia sometimes grades through matrix-poor breccia into hyaloclastite or coherent facies. Other intervals of the non-stratified sediment-matrix breccia facies consist solely of matrix-poor breccia (e.g. SODD

002, 200.2-200.6 m). Intervals of the non-stratified sediment-matrix breccia facies are less than 1 to 2m thick.

#### *Origin and significance of facies*

These breccias display characteristics consistent with peperite. Peperite forms by the mixing of lava or magma and wet unconsolidated sediment and is widespread within the Trooper Creek Formation (e.g. Doyle, 1994, 1997b). Peperite often occurs at the base of lavas and along the margins of syn-sedimentary intrusions and burrowing parts of lava flows. The shape of clasts in peperite is an indication of the style of magma-sediment interaction. Clasts with blocky and ragged shapes imply that quench fragmentation and dynamic stressing were important in generating peperite at Snake Oil prospect. Dewatering and induration of the siltstone may have accompanied mixing of the magma and sediment during peperite formation (cf. Doyle, 1997b).

#### Graded lithic-crystal-pumice breccia and sandstone facies

Diamond drill holes from Snake Oil, Rustler and Stocksquad prospects include thick intervals of lithic-crystal-pumice breccia and sandstone. The breccia beds are dominated by quartz- and/or feldspar-phyric pumice fragments (up to 6 cm) and subordinate crystal fragments (quartz and/or feldspar). The phenocryst and crystal populations suggest a dacitic to rhyodacitic composition. Units are non-welded, normally graded with tuffaceous sandstone tops and, in a few cases (e.g. SODD 002, 209-213 m), polymictic lithic-rich bases. Rare beds have reversely graded, lithic-rich bases (e.g. SODD 001, 147.5 m). Pumice clasts which have altered to feldspar (albite ?), carbonate and quartz-sericite contain relic uncompact tube vesicles identifiable with a hand lens. Lenticular pumice clasts which have altered to sericite and chlorite often define a bedding-parallel, diagenetic compaction foliation (S1) in the core (cf. Allen and Cas, 1990; Doyle, 1997b).

Single beds range from 0.3 to 10 m thick. Contacts between beds are sharp or marked by subtle variations in grain size, suggesting that they are amalgamated. Intervals of the facies range up to 110 m thick and comprise multiple units of widely varying thickness.

#### *Origin and significance of facies*

The abundance of pumice fragments and crystals within this facies, and the substantial thickness of some units, suggest that the facies was sourced from explosive magmatic and/or phreatomagmatic eruptions at a subaerial or shallow subaqueous volcanic centre. Pyroclasts are unmodified implying that resedimentation was syn-eruptive and bedforms are consistent with deposition from subaqueous sediment gravity flows, most likely cold (or cool) high-concentration turbidity currents. There is no evidence for hot emplacement (e.g. welding textures, columnar joints, vapour phase alteration, gas-segregation pipes) and the S1 foliation is interpreted as a diagenetic compaction foliation.

The turbidite deposits and associated siltstone units imply that the depositional setting was below storm wave base, and regional context further constrains the environment as submarine. The depth to storm wave base varies, but is typically around 150 m.

#### 1.4 Local and regional correlations

Correlations based on tracing pyroclast-rich units with similar phenocryst assemblages suggest that some units within the host succession to the Snake Oil mineralisation may be traceable over large distances (cf. Doyle, 1997b). In Snake Oil diamond drill holes SODD 001 and SODD 002, pumice breccia beds underlying the hanging wall dacite are feldspar > quartz-bearing and similar to pumiceous units intersected in the lower portions of diamond drill holes at Rustler (REW 812, 200-297 m) and Stocksquad (REW 813, 239.15-261m; Fig. 35). The mineralogy of these units contrasts with the overlying mass-flow units, which in drill holes (SODD 001, 120.4-126.9 m; REW 812, 132.6-150.2m; and REW 813, 115-220.2 m) comprises feldspar-only (dacitic) crystal-pumice breccia and sandstone. The thickness (106m) of dacitic pumice breccia in REW 813 suggests it



may be a potential marker horizon (Doyle, 1997b). At Snake Oil prospect, an undifferentiated lava or intrusion occurs at the contact between the feldspar-only (dacitic) pumice breccia units and feldspar > quartz (rhyodacitic) interval. Feldspar-only pumice breccia was not intersected in Snake Oil diamond drill hole SODD 002, due to a substantial thickening of the hanging wall dacite at this position.

Doyle (1997b) suggested that the key association of facies intersected in drill holes at Rustler and Stocksquad may allow correlation of the drill hole sections to Trooper Creek prospect (~15 km to the east) and Liontown (~15 km to the west). Detailed logging of drill core at Liontown confirms the presence of a thick (>170 m) interval of feldspar-only pumice breccia in the footwall to mineralisation (cf. Berry et al., 1992; Miller, 1996; Fig. 35). Sub-seafloor replacement style sphalerite-galena-pyrite mineralisation occurs within the footwall dacitic pumice breccia beds (Carrington lode; cf. Miller, 1996).

The new data for Snake Oil prospect and Liontown support the correlations proposed by Doyle (1997a). In particular, the dacitic pumice breccia at Liontown may be continuous to the east for over 30 km and represent clear targets for further exploration.

#### Nature of mineralisation/alteration

Massive sulfides were not intersected in diamond drill holes SODD 001 and SODD 002. However, a thick (10 m, apparent thickness) stratabound horizon of massive to semi-massive carbonate with minor pyrite marks the ore position in SODD 001 (150.55-160.4m). Carbonate mineralisation is interpreted to occur at the margins of sphalerite-rich mineralisation intersected in adjacent RC drill holes. Relic quartz crystals, carbonate pseudomorphs of euhedral feldspar, and well preserved pumice clasts suggest that the carbonate-sphalerite-pyrite is replacing rhyodacitic pumice breccia. In the hanging wall, a pale grey halo comprising carbonate rhombs (<1mm across) extends around 3 cm into siltstone and rhyodacitic peperite overlying the rhyodacitic pumice breccia. In drill hole SODD 002, carbonate-sericite-chlorite-hematite-barite-altered rhyodacitic pumice breccia, carbonate-hematite ("jasper") and banded quartz-pyrite-sericite (SODD 002, 227.3-231.5 m) marks an equivalent stratigraphic position. In both drill holes, discordant sphalerite, carbonate and quartz-pyrite veins/veinlets cut across quartz-sericite-altered volcanic rocks beneath the ore position. Spotty (0.5-1 cm) and disseminated sphalerite  $\pm$  chalcopyrite  $\pm$  carbonate within sericite > quartz ( $\pm$  albite/hematite)-altered rhyodacitic pumice breccia occurs beneath the semi-massive carbonate zone in SODD 001. A thin (11 cm) zone of diffusely carbonate-altered pumice breccia occurs at a sharp contact between the two zones. Intense quartz > sericite alteration is restricted to the underlying footwall rhyolite. In drill hole SODD 002, intense patchy and pervasive quartz > sericite and sericite > quartz alteration extends up through the footwall rhyolite into the overlying rhyodacitic pumice breccia. The alteration has destroyed most primary textures. However, rare relic pumice and quartz crystals and are locally preserved (e.g. 242-244 m).

#### Hanging wall alteration

In diamond drill hole SODD 001, low intensity chlorite-sericite  $\pm$  carbonate alteration characterises hanging wall lithofacies above the carbonate-pyrite mineralisation. In drill hole SODD 002, moderate sericite-chlorite-carbonate-hematite alteration extends into the hanging wall lithofacies up to around 15 m above the ore equivalent position. Further away from the hanging wall contact, volcanic facies have altered to various assemblages of sericite, chlorite, hematite, quartz and albite. The alteration is weak, and like that in SODD 001, is strongly controlled by primary volcanic textures. Coherent facies, perlite kernels and clasts in autoclastic breccia have typically altered to assemblages of sericite, chlorite and sometimes feldspar (?albite). Quartz and/or sericite alteration often moved outward from fractures or the matrix partially overprinting earlier sericite-chlorite  $\pm$  albite alteration. Spherulitic domains are pale pink in colour and presumably comprise recrystallised mosaics of quartz and feldspar. In pumiceous units, sericite-chlorite  $\pm$  carbonate alteration has replaced former glassy vesicle walls and filled vesicles. Pumice which have altered to phyllosilicate minerals (particularly chlorite) are more compacted

and define a bedding parallel, diagenetic compaction foliation (cf. Allen and Cas, 1992; Doyle, 1997a). In SODD 002, segments of the hanging wall dacite are pale purple and hematite-sericite-chlorite-altered. The hematite alteration is accompanied by minor quartz-hematite veins and is probably related to the circulation of low temperature fluids around the dacite during intrusion (cf. Doyle, 1997a).

#### Massive carbonate alteration

This mineralisation style is dominated by carbonate with subordinate sericite, chlorite, pyrite, barite and hematite. Carbonate occurs as coalescing spherical spherules (0.2-4 mm) and semi-massive zones containing well preserved, variably oriented, uncompacted pumice clasts (to 6 cm across). Pumice clasts and the vesicles within them are delineated by thin films of hematite. The areas between spherules were presumably originally glassy pumice or shards, but have altered to chlorite and/or sericite±disseminated (0.2 mm) pyrite. Patches (7 cm) of the core are dominated by coalescing microspherules (<0.2 mm) without interstitial phyllosilicate minerals. Semi-massive carbonate locally encloses chlorite patches (15-20 cm) containing carbonate laths presumably after feldspar crystals. Relic quartz crystals (2%, 1-4 mm) are also locally identifiable in the carbonate-pyrite mineralisation. Hematite can occur as a dissemination, wash, or vuggy intergrowth with carbonate. Carbonate-hematite patches ("jasper") are also present. In drill hole SODD 002, barite laths (1-6 mm long) and cross-cutting carbonate-chlorite veins are identifiable.

#### Stringer veins

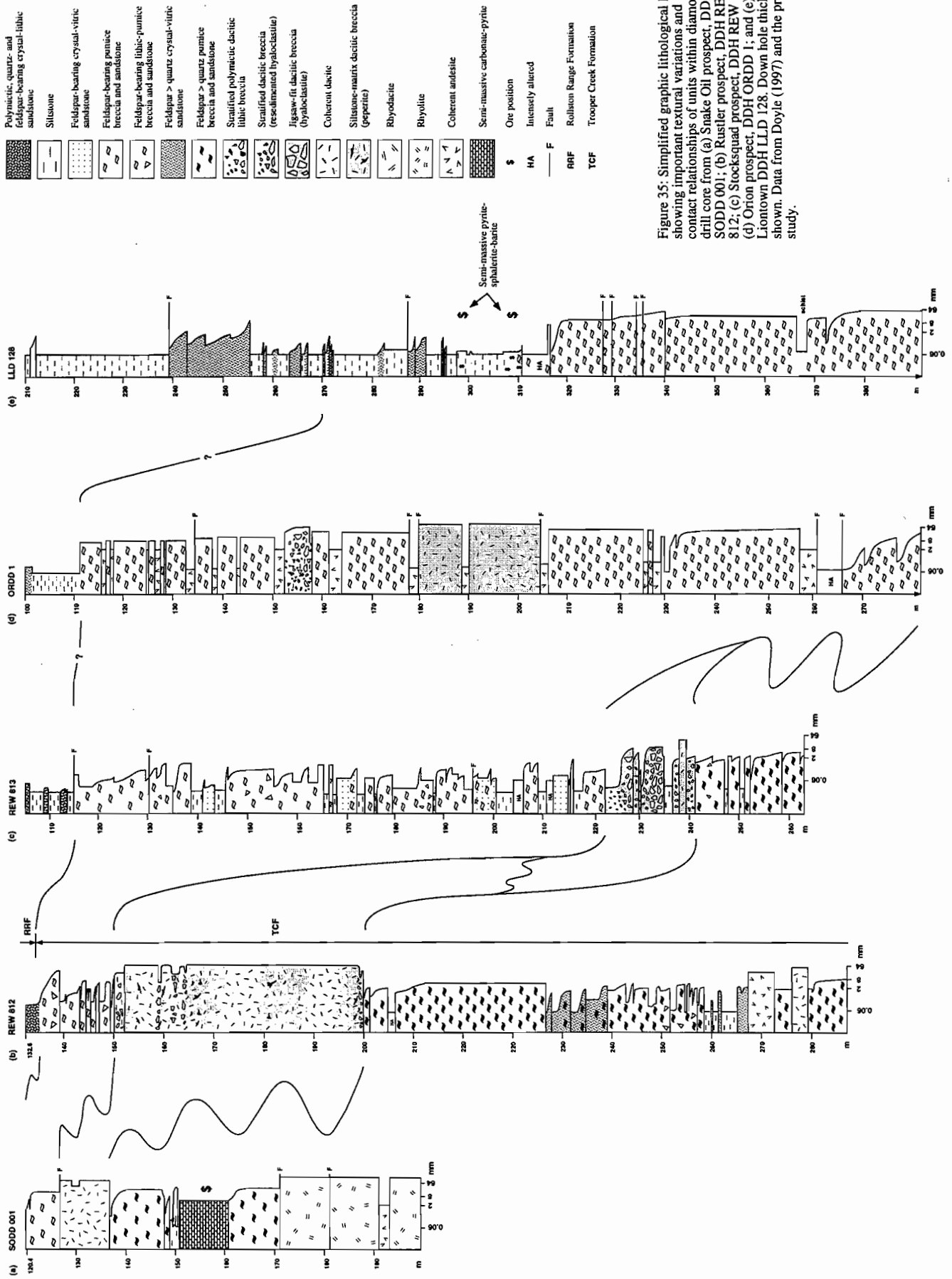
Stringer veins comprising assemblages of quartz-pyrite, carbonate±quartz, sphalerite-chalcopyrite and carbonate-sphalerite-galenite±barite occur within quartz-sericite-altered coherent rhyolite and rhyodacitic pumice breccia beneath the ore position. In general, disseminated and spotty sphalerite and pyrite account for less than 3% of wall rock, and veins are generally less than 1 cm wide, but can be up to 10 cm wide. Within the quartz-sericite alteration zone the relative proportions of sericite and quartz vary significantly, but quartz is generally the dominant phase. Intense pale to dark grey quartz alteration encloses patches (8-15 cm) of early sericite±quartz alteration. Sericite-rich domains have a weak pinkish colouration, suggesting the presence of minor hematite or feldspar (?albite). Phenocrysts are obscured within the quartz-altered domains, locally generating an apparent matrix between phyllosilicate-rich apparent clasts. Feldspar phenocrysts have altered to carbonate, sericite or chlorite. Segments (e.g. SODD 002, 243.9-245.4m) of the footwall rhyolite have pervasively altered to chlorite.

#### Discussion

##### *Evidence for sub-seafloor replacement*

Doyle (1997b) critically assessed the criteria for evaluating the role of syn-genetic sub-seafloor replacement and seafloor accumulation during massive sulfide deposition. At Snake Oil prospect, the stratabound carbonate precipitated by sub-seafloor replacement and infilling of pore space within rhyodacitic pumice breccia because: (1) the mineralisation is hosted by a thick, mass-flow emplaced unit (cf. Allen, 1994); (2) relic pumice clasts and crystals (feldspar > quartz) are preserved in the mineralisation; and (3) there are replacement fronts passing down through the carbonate-altered pumice breccia into quartz-sericite-altered pumice breccia with sphalerite blebs.

The semi-massive carbonate is interpreted as the distal and/or low temperature equivalent of the massive sulfides intersected in adjacent RC holes. Mixing of acidic, CO<sub>2</sub>-bearing fluids and seawater in the permeable and porous, glassy pumice breccia probably initiated carbonate deposition (cf. Khin Zaw and Large, 1992). Carbon-dioxide in the fluid may have been sourced from seawater and/or the magmatic fluid.



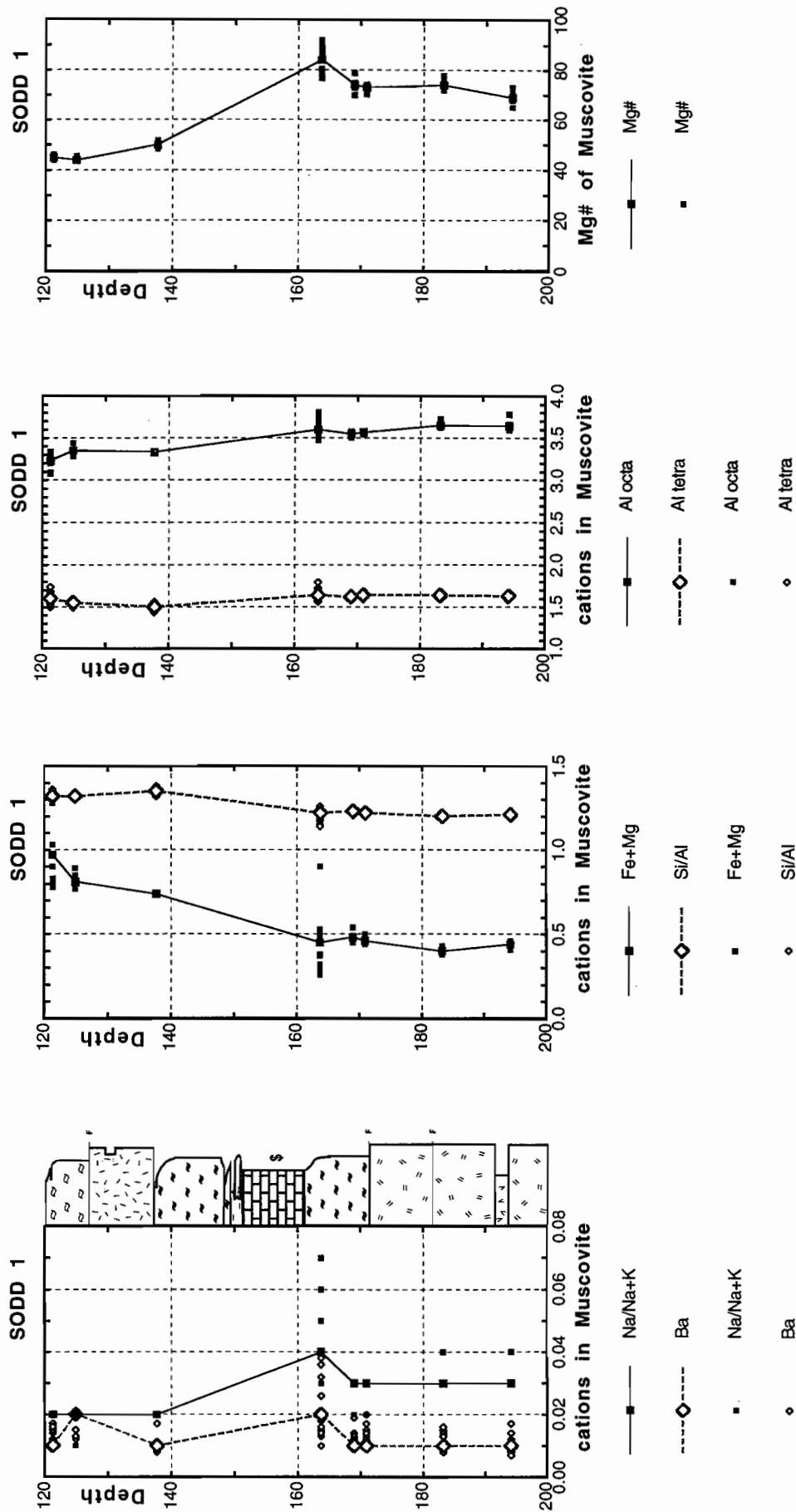


Fig. 36: Snake Oil Muscovites:

Are not significantly sodic  
 Have background Ba contents (cf: Liontown) with little variation downhole  
 Are moderately phengitic (Fe+Mg 0.4 to 1.0); the least phengitic compositions are in the footwall - contrasts with Liontown  
 Muscovites in the footwall have high Mg # ((70-85) compared to hangingwall (40-50) and appear to increase upward  
 toward the favourable horizon (cf: Chlorite at West Thalanga?); similar HW-FW contrast exists at Liontown.

## Alteration Associated with the Waterloo VHMS prospect, North Queensland

Thomas Monecke<sup>1</sup> and J. Bruce Gemmell<sup>2</sup>

<sup>1</sup>Freiberg University of Mining and Technology (Germany)

<sup>2</sup>Centre for Ore Deposit Research, University of Tasmania

### Summary

A brief overview on the geology of the Waterloo prospect, the lithologies and the types of alteration is given. Waterloo mineralisation consists of two high-grade zinc-copper-rich VHMS lenses that occur near the contact of a subvertical sequence of andesite lavas and breccias and an overlying sequence of volcanoclastics, including andesite to dacite lavas. Footwall andesites exhibit epidote and weak to strong sericite  $\pm$  chlorite  $\pm$  carbonate  $\pm$  pyrite alteration. The sericite $\pm$ chlorite alteration has been divided into seven types, based on distinct mineral assemblages. Mineralogical zonation within the "sericite-chlorite" alteration halo has caused prominent changes in the whole rock chemistry for the major and trace elements, leading to number of chemical vectors; Alteration Index, S/Na<sub>2</sub>O and Rb/Sr. Styles of alteration in the hangingwall include sericite $\pm$ chlorite, carbonate, hematite-quartz, epidote and albite.

### Introduction

This study forms part of the ongoing CODES SRC research activities on VHMS-related alteration and part of a PhD project being undertaken by TM at the Freiberg University of Mining and Technology (Germany). The study is focused on the Waterloo prospect, Mt. Windsor subprovince, North Queensland (Fig. 37), which contains a geological reserve of 0.372 Mt at 3.8 % Cu, 19.7% Zn, 2.8% Pb, 94 g/t Ag, and 2 g/t Au (Berry et al. 1992).

Field work was conducted between December 1996 and February 1997 and included the re-logging of selected drill core from the Waterloo (WT1A, WT2, WT6, WT5, WT7, WT9A, WT16, WT17, WT18, WT21, WT22, WT23, WT24, WT25, WT26, WT27) and Agincourt (AGDD1, AGDD5, AGDD7B) prospects. Agincourt is located only 1 km west of Waterloo and occurs at approximately the same stratigraphic level. Approximately 400 core samples were taken at 15 m intervals through the foot- and hangingwall packages and at 5 m intervals in the hangingwall adjacent to the hangingwall-footwall contact. Whole rock major and trace element analyses (200 samples – included in the P439 database), thin section work (100 thin sections) and a statistical examination of the company assay data are in progress.

*Note:* Thomas returned to Germany in mid 1997 to begin a 13 month national service obligation. He will be resuming full time studies in the second half of 1998.

### Prospect Geology

The Waterloo prospect is located in the central portion of the Trooper Creek Formation within the volcano-sedimentary succession of the Mount Windsor subprovince (Fig. 38). The regional and prospect geology have been previously described by Henderson (1986), Berry (1989), Huston (1991), Berry et al. (1992), Stolz (1995) and Huston et al. (1995). As the prospect is covered by 30-60 m of Tertiary sediments, the geology is inferred from the detailed drill logs. The drill hole location plan of the Waterloo prospect is given in Figure 39.

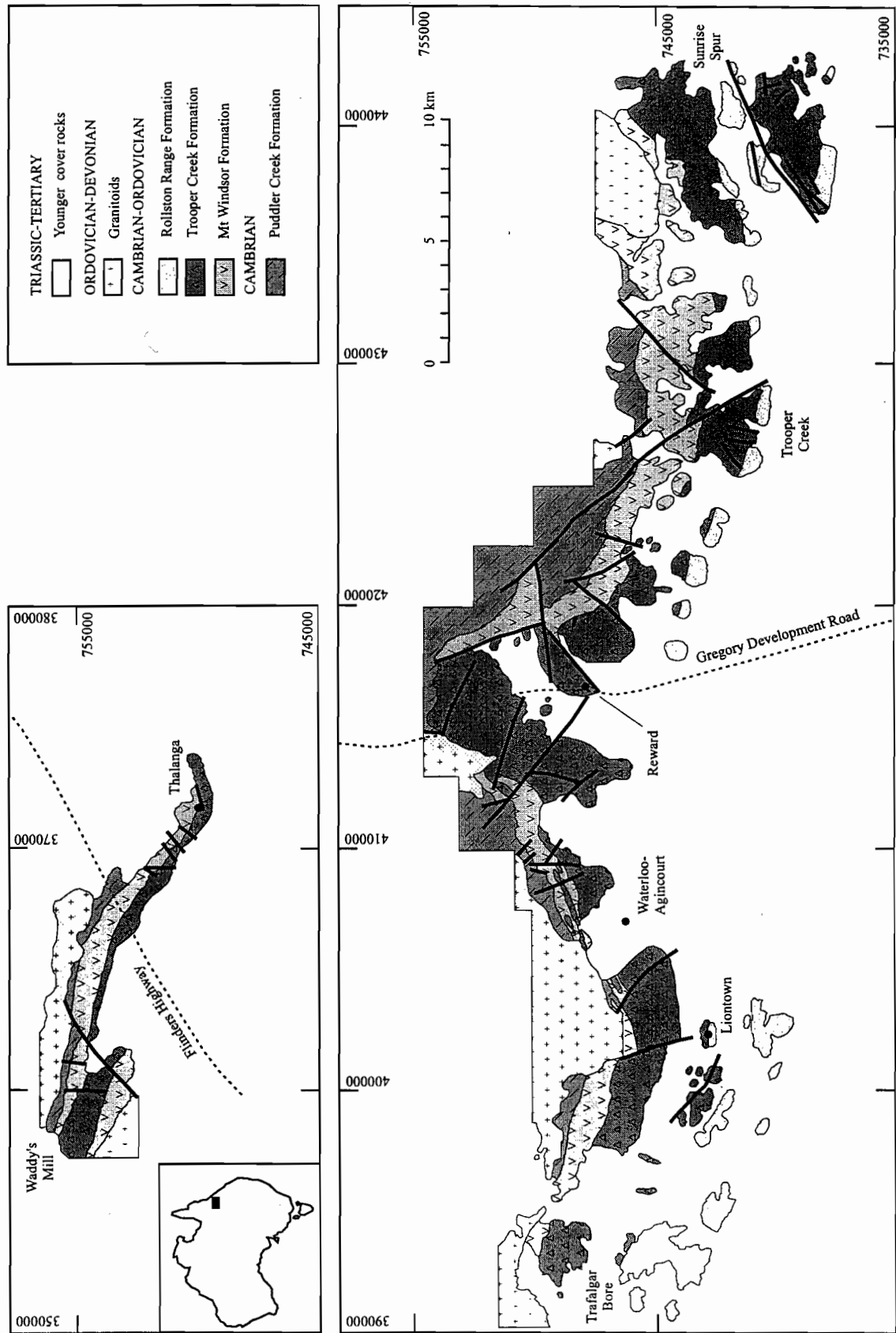


Fig. 37: Geological map of the Mount Windsor subprovince between Waddy's Mill and Sunrise Spur showing the distribution of the principal units and younger granitoid intrusions (Stolz, 1995).



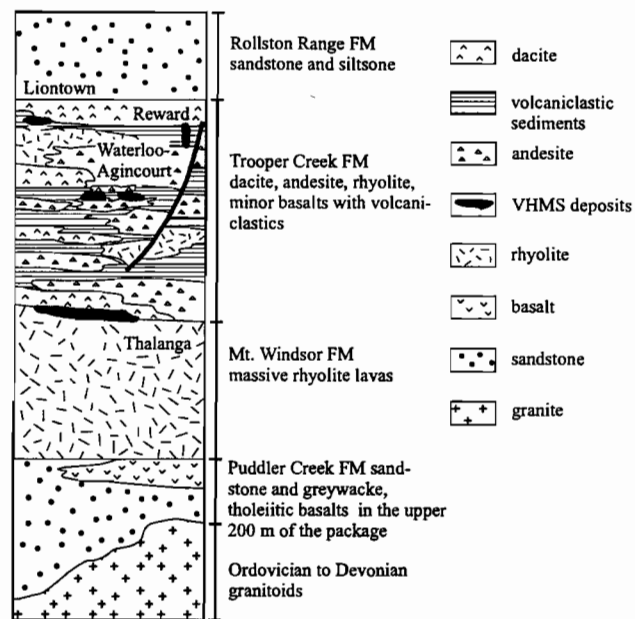


Fig.38 : Schematic volcano-stratigraphic section of the Mount Windsor subprovince (after Large, 1992).

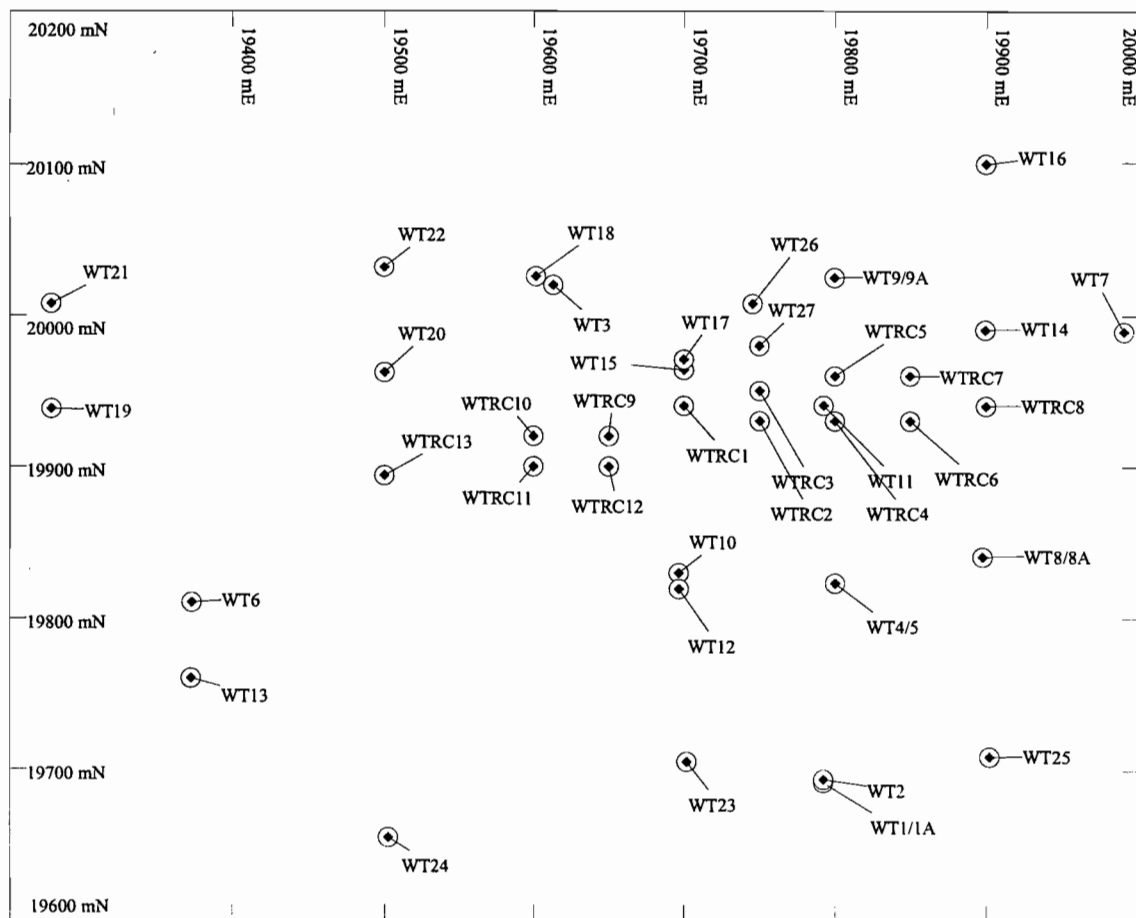


Fig. 39: Drill hole location plan of the Waterloo prospect (scale= 1:5 000).

Base metal mineralisation occurs near the contact of a subvertical sequence of pyritic sericite±chlorite and pyritic quartz-sericite±chlorite schists (footwall alteration zone) and an overlying sequence of volcanoclastic rocks (rhyolitic sandstone, siltstone, greywacke, and shale) and andesitic to dacitic lavas (hangingwall sequence) (Fig. 40). Massive andesitic lavas occur stratigraphically below the zone of pyritic sericite ± chlorite and pyritic quartz-sericite ± chlorite schists. The footwall and hangingwall sequences are commonly cut by andesite dykes (Fig. 41). Figure 42 shows the distribution of lithologies and alteration throughout the Waterloo prospect.

The footwall alteration zone below the massive sulphide mineralisation at 19800mE is 20 to 30 m (drill holes WT5 and WT9A) thick, and thickens towards the west to over 100 m (section 19300mE). The true thickness of the footwall alteration zone also seems to increase with depth, although no reliable data can be obtained from the drill holes WT23, WT24, and WT25 because they did not penetrate through the alteration zone. In some places, the less altered footwall andesites contain zones (0.5 to 2 m) of pyritic sericite±chlorite schists (e.g. WT16).

#### *Footwall andesites*

The footwall is dominated by coherent aphyric to moderately plagioclase-phyric andesitic lavas, subordinate andesitic autobreccias, and andesitic volcanoclastic rocks. The lavas are sparsely to moderately vesicular with quartz- and/or carbonate ± chlorite-filled vesicles. Phenocrysts of plagioclase and chlorite-epidote pseudomorphs of original pyroxene phenocrysts are evenly distributed through a fine groundmass by flow-aligned plagioclase laths, with interstitial chlorite and patchy epidote. Commonly, there are traces of sericite, disseminated pyrite cubes and patchy carbonate alteration in the groundmass.

#### *Hangingwall sediments*

The footwall alteration zone and mineralisation are overlain by a mixture of volcanoclastic and sedimentary lithologies. The most abundant sediments are volcanoclastic sandstones and siltstones. The former are typically composed of abundant angular plagioclase and quartz grains (0.5 to 2 mm in size) with subordinate lithic fragments, while the latter are composed of tiny angular quartz and feldspar grains in a very fine grained matrix of quartz and feldspar. Blue quartz has been recognised in the volcanoclastic sandstones, usually in the immediate hangingwall of massive sulphides (e.g. WT9A).

#### *Hangingwall dacites and andesites*

The hangingwall dacitic to andesitic lavas are aphyric to moderately plagioclase-phyric. Peperites occur at several locations and indicate the mixing of coherent lava with unconsolidated wet sediment.

### **Alteration**

There are several styles of alteration in both footwall and hangingwall at Waterloo:

Styles of footwall alteration:

- (1) sericite±chlorite
- (2) disseminated and vein pyrite

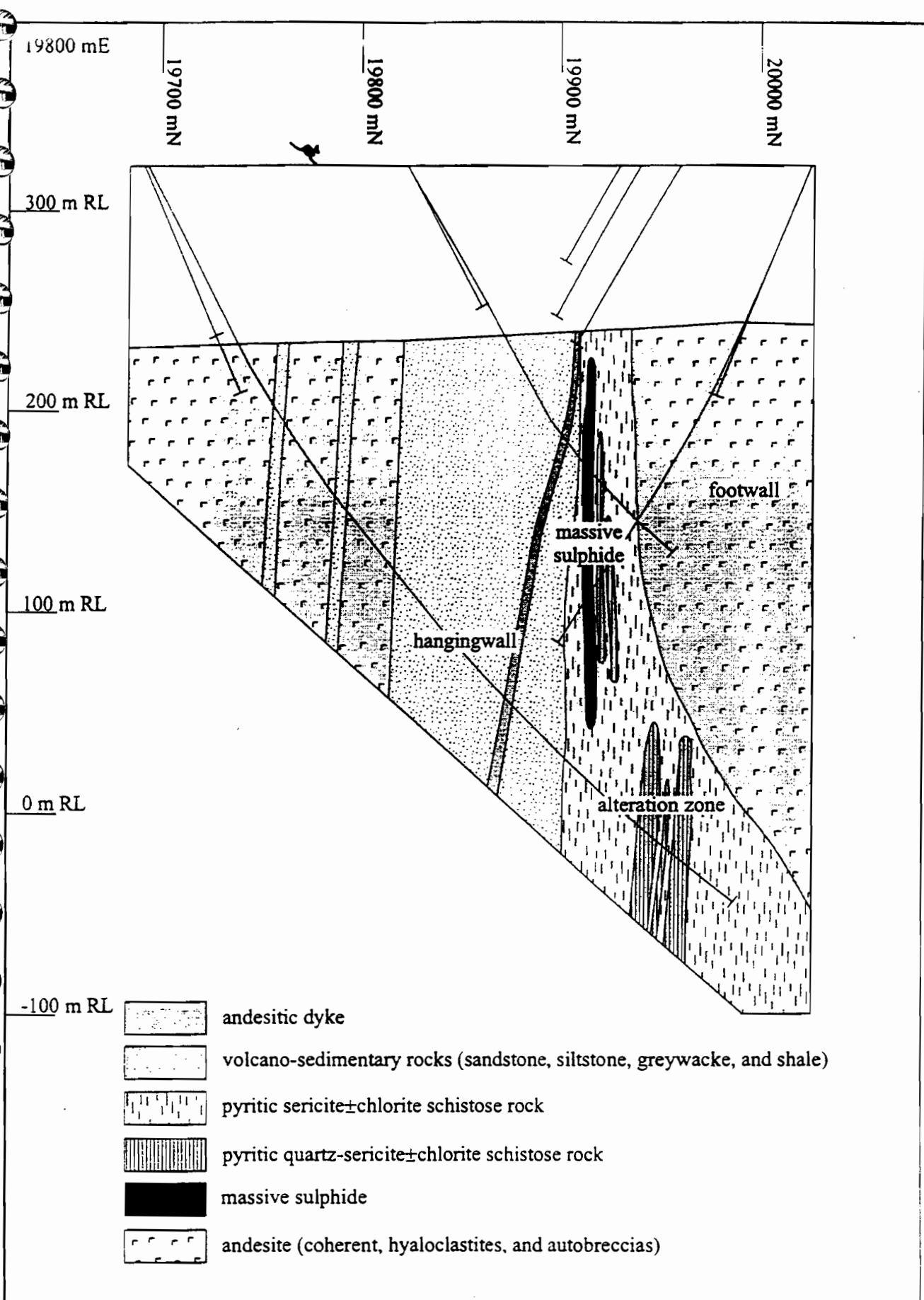


Figure 4c Cross-section showing the interpreted geology at 19800 mE.

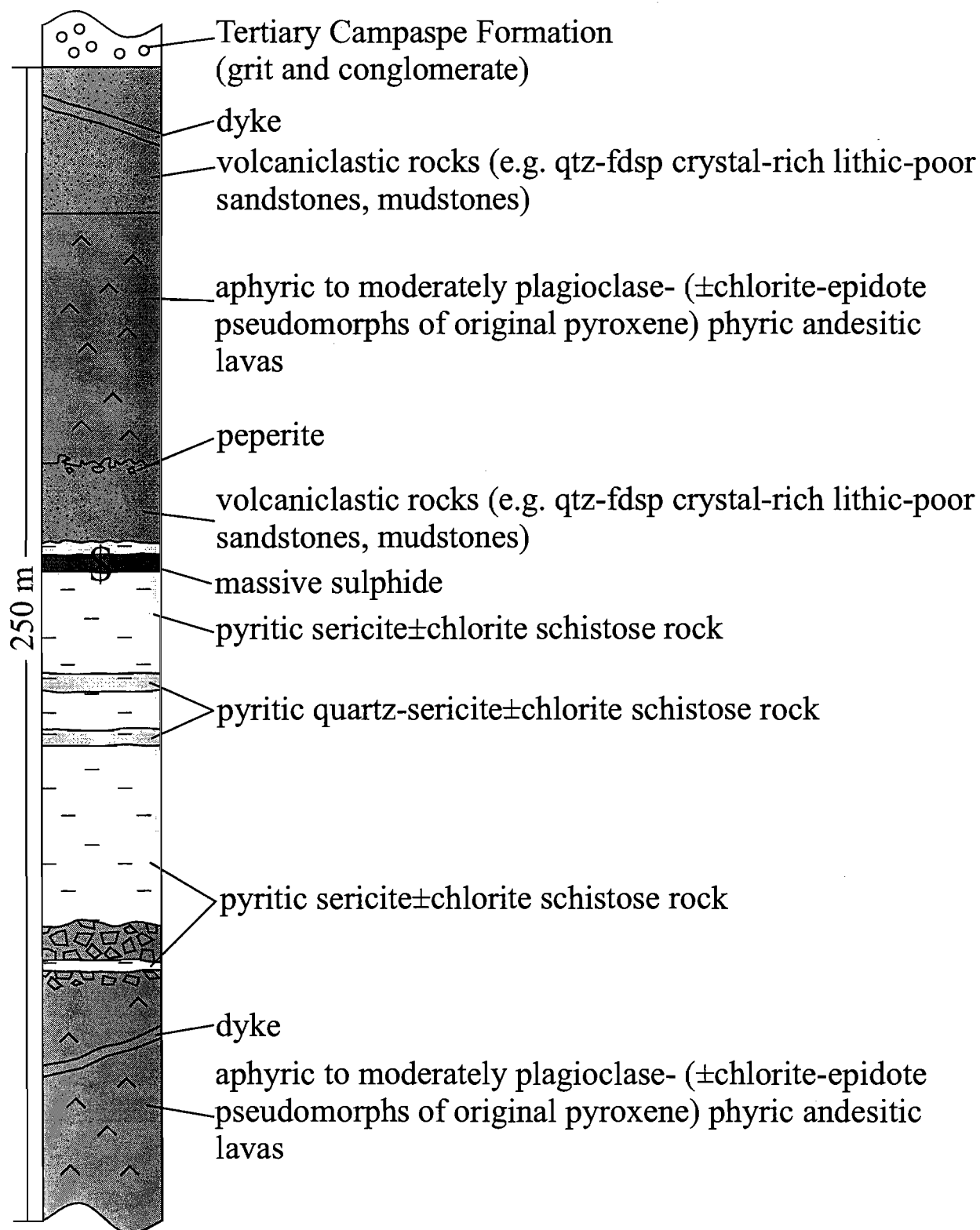


Figure 41: Schematic stratigraphic section of the Waterloo prospect

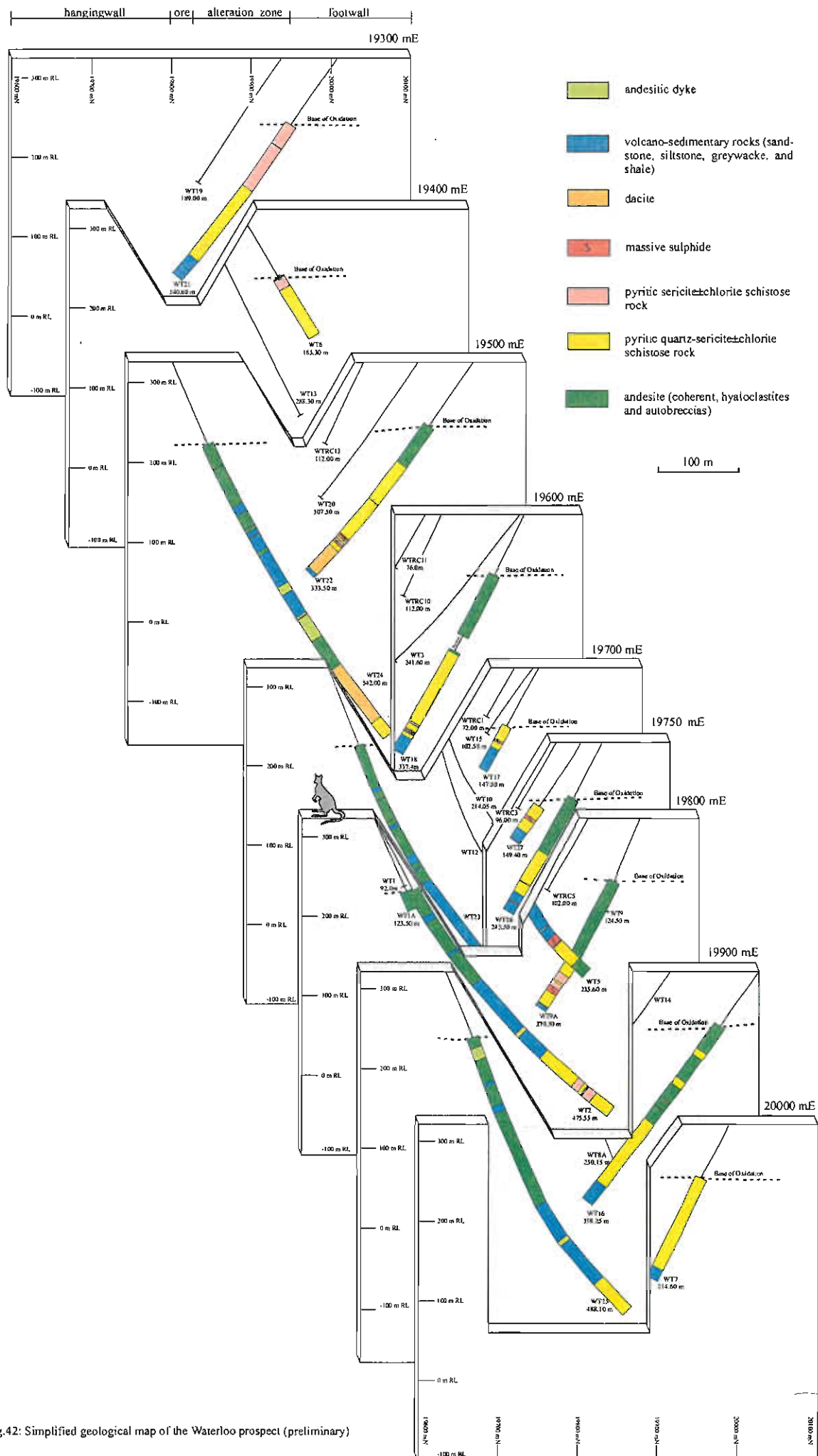


Fig.42: Simplified geological map of the Waterloo prospect (preliminary)

- (3) carbonate
- (4) epidote
- (5) silicification

Styles of hangingwall alteration:

- (1) sericite±chlorite
- (2) carbonate
- (3) epidote
- (4) albite
- (5) hematite-quartz
- (6) silicification

#### Sericite±chlorite alteration

The most widespread and obvious alteration is an assemblage of sericite±chlorite which makes up most of the footwall alteration zone at Waterloo. A weak pervasive sericite±chlorite alteration is widespread in the groundmass of most of the footwall andesites and feldspar phenocrysts show partial replacement by sericite±chlorite. Contacts between the less altered lavas and the strongly altered pyritic sericite±chlorite schists in the footwall are sharp to gradational. Within the more strongly altered zones primary volcanic textures are largely destroyed. The pyritic sericite ± chlorite and pyritic quartz-sericite ± chlorite schists are strongly cleaved. Pyrite grains exhibit significant flattening parallel to the cleavage. Large grains have pressure shadows which are filled with quartz and chlorite, hence the alteration predates the development of the cleavage (which is D2, as D1 is not recognised in the Waterloo area - Berry, 1989). Due to pyrite breakdown and acid attack much of the core from the footwall alteration zone is in an advanced state of oxidation and deterioration. The sericite ± chlorite alteration commonly penetrates a few metres (5-10 m) into sediments in the hangingwall above the ore position.

Based on XRD, thin section work, and field data, seven mineralogical assemblages can be distinguished in the "sericite±chlorite" footwall/hangingwall alteration. These are listed from from deep in the footwall towards the ore position (Fig. 43):

- (1) pyritic quartz-muscovite-paragonite-clinocllore-albite+/- calcite assemblage
- (2) pyritic quartz-muscovite-paragonite-albite+/-calcite assemblage

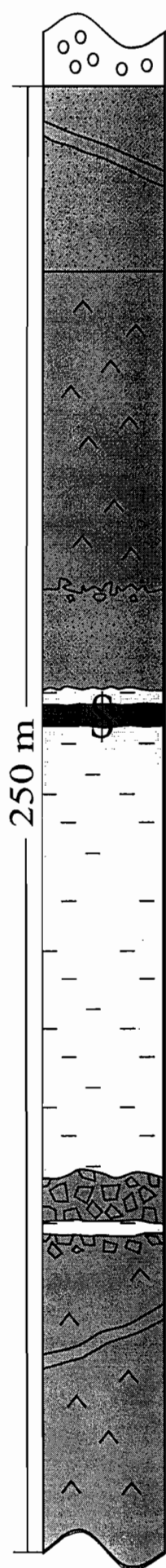
These two assemblages represent the "weakly" altered parts of the "sericite" alteration halo and form the outermost mineralogical zones. The pyritic quartz-muscovite-paragonite-clinocllore-albite+/- calcite assemblage is more abundant in the footwall and possibly represents mainly altered coherent lithological units (mainly andesites). The pyritic quartz-muscovite-paragonite-albite+/-calcite assemblage is less abundant and more common in the hangingwall, but has also been recognised in the footwall. It occurs mainly in volcanoclastic units.

- (3) pyritic quartz-muscovite-paragonite-clinocllore+/-calcite assemblage
- (4) pyritic quartz-muscovite-paragonite+/-calcite assemblage

The pyritic quartz-muscovite-paragonite-clinocllore+/- calcite assemblage is the most widespread mineralogical zone in the alteration halo and is situated closer to the ore than the



# ALTERATION



epidote, hematite, quartz

qtz-muscovite-paragonite-albite-calcite-hematite

qtz-muscovite

qtz-muscovite-chlinoclore-calcite

qtz-muscovite-paragonite-calcite

qtz-muscovite-paragonite-chlinoclore-calcite

qtz-muscovite-paragonite-albite-calcite

qtz-muscovite-paragonite-chlinoclore-albite  
-calcite

sericite-chlorite, epidote

Figure 43: Schematic representation of the alteration associated with the Waterloo prospect.

zones that contain albite. The lack of Mg in the pyritic quartz-muscovite-paragonite+/- calcite assemblage is probably caused by the Mg-poor precursor lithological units.

(5) pyritic quartz-muscovite-pyrophyllite-dickite+/-clinochlore+/-calcite

This zone is very unusual and is recognised in only 3 of 74 samples investigated. The assemblage pyrophyllite-dickite characterises advanced argillic alteration (high sulphidation) and is generally formed from highly acidic solutions of magmatic derivation.

(6) pyritic quartz-muscovite-clinochlore+/- calcite assemblage

This is the next mineralogical zone approaching the mineralisation. Paragonite is absent from this assemblage. Galena, barite and sphalerite are present as disseminations.

(7) pyritic quartz-muscovite assemblage

This zone is in the immediate footwall of the mineralisation. It is intensely silicified and contains up to 80 wt.% SiO<sub>2</sub>. Galena, barite, and sphalerite are present as disseminations. Na<sub>2</sub>O is very low (<0.5% Na<sub>2</sub>O) due to the absence of Na bearing minerals.

Nearly all samples from the above alteration assemblages contain apatite, which is a hydroxylapatite with some minor chlorine and low MnO. Rutile is present in all samples replacing former Fe-Ti-minerals. In some samples outlines of a former Fe-Ti minerals are composed of pyrite and a network of rutile needles and leucoxene. Epidote grains are present in some samples that also contain albite. Calcite replaces albite and occurs as patches in the groundmass. The calcite is relatively pure (i.e. low MnO and MgO). Pyrophyllite is of the 2M polytype. According to the most recent classification of chlorites, the chlorites from the above alteration assemblages are clinochlore. The Fe/(Fe+Mg) in the octahedral sites is generally below 0.3. Chlorite is of the IIb polytype.

With regards to the "sericite", muscovite-paragonite is of the 2M1 polytype. However, the split of the basal 00l reflections suggests the presence of micaceous minerals of intermediate composition between muscovite and paragonite. These phases are present in the samples that also contain paragonite. The correct identification of hydrothermal micas is extremely difficult and can only be viewed by TEM images. Microprobe work is not suitable for identification as more than one mineral phase will be analysed. However, in some samples the irregular d(00l) suggest that muscovite/paragonite mixed-layer minerals are present. In other samples the d(00l) is more regular indicating the presence of a true mica of intermediate composition that should not exist in theory due to the gap in the solid solution muscovite-paragonite. However, according to the literature a mica of intermediate composition has been documented in only three cases. One is of particular interest as the mica has been observed as a metastable alteration product of plagioclase. To the best of our knowledge such intermediate micaceous minerals have never been observed in VHMS alteration halos.

The above mineralogical zonation within the "sericite" alteration halo obviously causes prominent changes in the whole rock chemistry for the major and trace elements, leading to number of chemical vectors, e.g.:

- Alteration Index: increases with intensity of alteration.

- S/Na<sub>2</sub>O: The pyrite content is usually higher in the zones that lack paragonite => good vector within the alteration halo
- Rb/Sr: Rb shows a perfect correlation with K<sub>2</sub>O, and is incorporated into muscovite. Sr is most likely in feldspars => good vector for altered (low Rb/Sr) vs. less altered rocks (high Rb/Sr)

#### Disseminated and vein pyrite alteration

This style of alteration is widespread and the pyrite content varies from traces to about 20%. The pyrite typically forms euhedral grains (0.1 mm to 1 mm), but there is some remobilisation of pyrite into narrow (2 mm) veins.

#### Carbonate alteration

This alteration is widespread and pervasive. Carbonate replaces plagioclase grains, and occurs in patches or aggregates in the volcano-sedimentary units and coherent lavas in both footwall and hangingwall. Mobilisation of carbonates into narrow veins (1 mm) is very common.

#### Epidote alteration

Epidote is common in most of the weakly altered footwall andesites and the hangingwall extrusives. Epidote occurs in the groundmass of the andesites, partially replacing plagioclase phenocrysts, and forms up to 4 cm patches. Epidote alteration in the least altered footwall andesites appears to be more intense than in the hangingwall andesites.

#### Albite, hematite-quartz alteration and silicification

Due to its pink color, albite has been recognised in hand-specimens at several locations in the hangingwall sediments. Hematite-quartz alteration is observed in some of the hangingwall dacites and hangingwall sediments. Silicification is weak to moderate in intensity, widespread and pervasive in distribution, and occurs in the footwall andesites as well as hangingwall andesites and dacites.

### **Conclusions**

The following preliminary conclusions can be drawn from this study:

- Waterloo mineralisation contains two high-grade zinc-copper-rich VHMS lenses which occur near the contact of a subvertical sequence of andesite lavas and breccias and an overlying sequence of volcanoclastics, including andesite to dacite lavas
- footwall andesites exhibit epidote and weak to strong sericite ± chlorite ± carbonate ± pyrite alteration. The sericite ± chlorite alteration surrounding the ore zone has been subdivided into seven types, based on distinct mineral assemblages.
- mineralogical zonation within the "sericite±chlorite" alteration halo obviously causes prominent changes in the whole rock chemistry for the major and trace elements, leading to number of chemical vectors; i. Alteration Index: increases with increasing intensity of alteration, ii. S/Na<sub>2</sub>O: The pyrite content is usually higher in the zones that lack paragonite

=> good vector within the alteration halo and ii. Rb/Sr: Rb shows a perfect correlation with K<sub>2</sub>O while Sr is most likely in unaltered feldspars => good vector for altered (high Rb/Sr) vs. less altered rocks (low Rb/Sr).

- styles of alteration in the hangingwall include the assemblages sericite±chlorite, carbonate, hematite-quartz, epidote and albite
- silicification is common both footwall and hangingwall.

### **Stop 10.3 – Waterloo Drill Core**

**WTDD22:** (see Figure 42 for drill hole location and Appendix 1 for geochemical data)

98 m (base of oxidation) to 112 m: footwall coherent andesite ( $Ti/Zr = 46$ ) with autobreccia on top

112 to 156 m: footwall coherent andesite ( $Ti/Zr = 70$  to  $71$ )

156 to 281 m: footwall "sericite" alteration zone

163 m: pyritic quartz-muscovite-paragonite-clinocllore-albite-calcite assemblage  
( $Na_2O = 2.74\%$ ;  $AI = 59$ ;  $CCPI = 84$ ;  $S/Na_2O = 2.87$ ;  $Ti/Zr = 70$ )

176 m: pyritic quartz-muscovite-paragonite-clinocllore-albite-calcite assemblage  
( $Na_2O = 2.93\%$ ;  $AI = 58$ ;  $CCPI = 80$ ;  $S/Na_2O = 2.60$ ;  $Ti/Zr = 74$ )

190 m: pyritic quartz-muscovite-paragonite-clinocllore-albite-calcite assemblage  
( $Na_2O = 3.85\%$ ;  $AI = 33.10$ ;  $CCPI = 58$ ;  $S/Na_2O = 1.47$ ;  $Ti/Zr = 76$ )

208 m: pyritic quartz-muscovite-paragonite-clinocllore assemblage  
( $Na_2O = 1.23\%$ ;  $AI = 78$ ;  $CCPI = 83$ ;  $S/Na_2O = 4.89$ ;  $Ti/Zr = 55$ )

222 m: pyritic quartz-muscovite-paragonite-clinocllore assemblage  
( $Na_2O = 1.40\%$ ;  $AI = 71$ ;  $CCPI = 75$ ;  $S/Na_2O = 3.32$ ;  $Ti/Zr = 27$ )

237 m: pyritic quartz-muscovite-clinocllore assemblage  
( $Na_2O = 0.51\%$ ;  $AI = 91$ ;  $CCPI = 78$ ;  $S/Na_2O = 10.86$ ;  $Ti/Zr = 35$ )

256 m: pyritic quartz-muscovite-clinocllore assemblage  
( $Na_2O = 0.39\%$ ;  $AI = 88$ ;  $CCPI = 70$ ;  $S/Na_2O = 16.23$ ;  $Ti/Zr = 35$ )

277 m: pyritic quartz-muscovite assemblage  
( $Na_2O = 0.50\%$ ;  $AI = 85$ ;  $CCPI = 64$ ;  $S/Na_2O = 10.28$ ;  $Ti/Zr = 41$ )

281 to 284 m: "ore position" with disseminated sulphides

284 m to 299 m: hangingwall "sericite" alteration zone

286 m: pyritic quartz-muscovite-paragonite-clinocllore assemblage  
( $Na_2O = 1.04\%$ ;  $AI = 83$ ;  $CCPI = 70$ ;  $S/Na_2O = 11.23$ ;  $Ti/Zr = 27$ )

295 m: pyritic quartz-muscovite-paragonite-clinocllore-calcite assemblage  
( $Na_2O = 1.13\%$ ;  $AI = 56$ ;  $CCPI = 63$ ;  $S/Na_2O = 4.18$ ;  $Ti/Zr = 28$ )

299 m to 328 m: hangingwall coherent dacite ( $Ti/Zr = 27$  to  $29$ ) with a quartz-haematite-chlorite-sericite-epidote alteration, typical for the dacite in this immediate hangingwall position

328 m to 333.50 m (end of hole): volcanoclastic sediment (or spherulitic lava ?) ( $Ti/Zr$  from 19 to 22).

**WTDD16:** (see Figure 42 for drill hole location and Appendix 1 for geochemical data)

83 m to 121 m: footwall coherent andesite (Ti/Zr = 62)

121 m to 130.50 m: pyritic quartz-muscovite-paragonite-clinocllore- calcite assemblage  
(Na<sub>2</sub>O = 1.62%; AI = 57; CCPI = 125; S/Na<sub>2</sub>O = 3.98; Ti/Zr = 58)

130.50 m to 167 m: footwall coherent andesite (Ti/Zr = 63 to 64)

167 m to 177 m: pyritic quartz-muscovite-paragonite-clinocllore assemblage  
(Na<sub>2</sub>O = 1.85%; AI = 57; CCPI = 74; S/Na<sub>2</sub>O = 4.56; Ti/Zr = 61)

177 m to 199 m: footwall coherent andesite (Ti/Zr = 61)

199 m to 201 m: andesitic dyke with chilled margins

201 m to 211 m: footwall coherent andesite (Ti/Zr = 62)

211 m to 212 m: andesitic dyke with chilled margins (Ti/Zr = 62)

212 m to 232 m: footwall coherent andesite (Ti/Zr = 61)

232 m to 285 m: footwall "sericite" alteration zone

245 m: pyritic quartz-muscovite-pyrophyllite-dickite  
(Na<sub>2</sub>O = 0.70%; AI = 25; CCPI = 87; S/Na<sub>2</sub>O = 7.74; Ti/Zr = 47)

257 m: pyritic quartz-muscovite-pyrophyllite-dickite  
(Na<sub>2</sub>O = 0.88%; AI = 73; CCPI = 55; S/Na<sub>2</sub>O = 4.25; Ti/Zr = 41)

276 m: pyritic quartz-muscovite assemblage  
(Na<sub>2</sub>O = 0.51%; AI = 82; CCPI = 55; S/Na<sub>2</sub>O = 7.10; Ti/Zr = 48)

285 m to 293 m: "ore position" with disseminated sulphides, in part intensely weathered core

292 m: pyritic quartz-muscovite assemblage  
(Na<sub>2</sub>O = 0.47%; AI = 81; CCPI = 70; S/Na<sub>2</sub>O = 11.91; Ti/Zr = 47)

293 m to 330 m: hangingwall "sericite" alteration zone

322 m: pyritic quartz-muscovite-paragonite assemblage  
(Na<sub>2</sub>O = 1.03%; AI = 58; CCPI = 65; S/Na<sub>2</sub>O = 3.58; Ti/Zr = 44),

330 m to 358 m: volcanoclastic rocks (at 335.25 to 335.90 possibly a dyke?) (Ti/Zr from 10 to 31)

**Good massive sulphide intersections in WTDD5, WTDD9A, and WTDD27.**



Appendix 1 Whole Rock Geochemical Data Wt 16 and Wt22

Hole-depth	Lithology from field work	Alteration study	SiO <sub>2</sub>	TiO <sub>2</sub>	Al <sub>2</sub> O <sub>3</sub>	Fe <sub>2</sub> O <sub>3</sub>	MnO	MgO	CaO	Na <sub>2</sub> O	K <sub>2</sub> O	P <sub>2</sub> O <sub>5</sub>	Loss	Total	Ti/Zr	Al	CCPI	S/Na <sub>2</sub> O
WT22-100	coherent rock (andesite)		59.03	0.85	15.23	7.55	0.15	2.04	7.07	2.68	0.26	0.25	4.89	100.00	48	19	77	0.47
WT22-109	subvolcanic rock (andesite)		61.55	0.69	12.31	5.93	0.16	1.19	6.41	2.74	1.08	0.21	7.33	99.60	46	20	65	1.27
WT22-122	coherent rock (andesite)		51.61	1.14	15.89	11.08	0.16	4.14	1.75	2.78	1.86	0.27	8.75	99.43	71	57	77	2.69
WT22-132	coherent rock (andesite)		55.34	1.00	14.85	9.27	0.09	1.83	2.92	3.86	1.70	0.25	8.00	99.11	70	34	67	1.78
WT22-148	coherent rock (andesite)		55.07	1.08	15.97	9.89	0.04	0.88	2.40	5.07	1.37	0.27	7.03	99.07	71	23	63	1.51
WT22-163	intensely altered schist	FW qtz-musc-parag-chl-alb-cal	50.49	1.09	14.35	12.92	0.17	5.50	1.55	2.74	0.77	0.27	9.21	99.06	70	59	84	2.87
WT22-176	intensely altered schist	FW qtz-musc-parag-chl-alb-cal	49.75	1.41	16.25	11.89	0.15	4.88	1.39	2.93	1.15	0.36	9.19	99.35	74	58	80	2.60
WT22-190	intensely altered schist	FW qtz-musc-parag-chl-alb-cal	58.38	1.31	16.42	7.31	0.05	0.74	1.83	3.85	2.07	0.25	6.79	99.20	76	33	58	1.47
WT22-208	intensely altered schist	FW qtz-musc-parag-chl	59.43	0.71	14.88	8.79	0.11	4.32	0.39	1.23	1.39	0.16	8.08	99.49	55	78	83	4.89
WT22-222	intensely altered schist	FW qtz-musc-parag-chl	61.60	0.53	14.86	14.86	0.10	4.05	1.14	1.40	2.19	0.13	6.51	99.11	27	71	75	3.32
WT22-237	intensely altered schist	FW qtz-musc-chl	59.94	0.57	15.54	7.91	0.10	4.38	0.19	0.51	3.05	0.10	7.27	99.36	35	91	78	10.86
WT22-256	intensely altered schist	FW qtz-musc-chl	55.43	0.67	17.25	8.68	0.08	2.33	0.49	0.39	4.42	0.11	9.19	99.04	35	88	70	16.23
WT22-277	intensely altered schist	FW qtz-musc	70.25	0.49	13.14	6.30	<0.01	0.79	0.11	0.50	3.30	0.03	5.38	99.92	41	85	64	10.28
WT22-288	intensely altered schist	FW qtz-musc-parag-chl	37.00	1.02	23.57	15.26	0.01	0.17	0.32	1.04	5.98	0.08	13.07	100.86 (*)	27	83	70	11.23
WT22-295	intensely altered schist	HW qtz-musc-parag-chl-cal	55.77	0.69	17.09	6.11	0.04	1.55	2.71	1.13	3.31	0.11	7.54	99.18 (*)	28	56	63	4.18
WT22-302	coherent rock (dacite)		64.69	0.61	16.40	4.72	0.07	1.67	2.08	5.33	0.94	0.15	3.34	100.00	29	26	50	0.00
WT22-307	coherent rock (dacite)		68.66	0.52	13.03	3.84	0.02	0.28	2.67	5.48	0.68	0.15	4.47	99.80	28	11	40	0.50
WT22-314	coherent rock (dacite)		64.04	0.54	14.59	6.14	0.10	1.45	3.26	4.80	0.62	0.13	4.02	99.69	27	20	58	0.00
WT22-322	coherent rock (dacite)		64.81	0.63	14.76	6.30	0.08	1.40	2.43	5.95	0.35	0.16	3.13	100.00	30	17	55	0.00
WT22-329	volcaniclastic rock		55.86	0.69	23.42	5.05	0.06	1.56	0.74	1.81	5.22	0.13	5.00	99.54	22	73	48	0.01
WT22-332	volcaniclastic rock		65.37	0.67	16.51	5.18	0.07	2.59	0.86	1.18	3.23	0.15	3.84	99.65	19	74	64	0.05
WT16- 87	coherent rock (andesite)		55.56	0.72	17.79	9.26	0.12	3.69	6.30	2.80	0.15	0.11	3.51	100.01	63	30	81	0.00
WT16-112	coherent rock (andesite)		56.04	0.66	16.99	9.36	0.08	2.71	4.42	4.98	0.14	0.14	4.87	100.59	62	23	71	0.48
WT16-125	intensely altered schist	FW qtz-musc-parag-chl-cal	55.72	0.72	18.08	9.87	0.02	1.26	1.35	1.62	2.71	0.17	7.97	99.49	58	57	72	3.98
WT16-145	coherent rock (andesite)		56.01	0.58	16.09	9.50	0.11	3.83	3.39	4.00	0.31	0.12	5.79	99.73	64	36	76	0.59
WT16-161	coherent rock (andesite)		51.18	0.62	16.39	10.82	0.12	5.47	2.20	2.38	0.81	0.14	8.99	99.12	63	58	84	2.44
WT16-170	intensely altered schist	FW qtz-musc-parag-chl	56.52	0.73	17.21	11.13	0.01	0.59	0.34	1.85	2.34	0.14	8.59	99.45	61	57	74	4.56
WT16-186	coherent rock (andesite)		55.85	0.66	17.36	8.24	0.10	3.22	5.80	2.93	0.41	0.12	5.28	99.97	61	29	77	0.03
WT16-195	coherent rock (andesite)		54.10	0.72	18.22	9.15	0.11	3.21	6.88	2.96	0.49	0.13	3.83	99.80	61	27	78	0.19
WT16-206	coherent rock (andesite)		48.71	0.76	18.78	10.40	0.13	4.09	7.82	2.36	0.58	0.09	5.92	99.64	62	31	83	0.04
WT16-210	coherent rock (andesite)		58.22	1.01	17.16	7.01	0.09	1.10	4.69	6.88	0.02	0.27	3.07	99.52	62	9	54	0.01
WT16-223	coherent rock (andesite)		57.91	0.73	15.84	7.65	0.11	3.12	4.37	4.48	0.13	0.18	5.43	99.95	61	27	70	0.21
WT16-245	intensely altered schist	FW qtz-musc-pyroph-dick	69.28	0.75	13.50	6.79	<0.01	0.06	0.46	0.70	0.32	0.12	7.65	99.63	47	25	87	7.74
WT16-257	intensely altered schist	FW qtz-musc-pyroph-dick	60.55	1.15	21.42	4.84	<0.01	0.18	0.38	0.88	3.28	0.22	6.44	99.34	41	73	55	4.25
WT16-276	intensely altered schist	FW qtz-musc	72.58	0.71	13.47	4.52	<0.01	0.18	0.23	0.51	3.27	0.16	4.29	99.92	48	82	55	7.10
WT16-292	intensely altered schist	Ore Position qtz-musc	72.36	0.57	10.83	7.06	<0.01	0.10	0.19	0.47	2.62	0.12	5.67	99.99	50	80	70	11.91
WT16-302	intensely altered schist	HW qtz-musc-parag	74.22	0.65	11.46	4.87	<0.01	0.10	0.27	1.03	1.66	0.10	5.47	99.83	44	58	65	3.58
WT16-333	volcaniclastic rock		67.37	0.39	15.17	3.60	0.09	1.39	3.19	1.47	1.93	0.08	5.13	99.81	30	42	59	0.07
WT16-338	volcaniclastic rock		71.21	0.33	13.48	3.58	0.06	1.19	1.80	4.58	0.72	0.07	2.84	99.86	31	23	47	0.00
WT16-343	volcaniclastic rock		67.63	0.35	13.96	3.55	0.15	1.07	3.39	4.38	1.32	0.07	3.03	99.90	30	24	45	0.00
WT16-349	volcaniclastic rock		70.11	0.45	14.84	3.09	0.06	1.55	1.05	2.09	3.19	0.09	3.08	99.60	15	60	47	0.01
WT16-355	volcaniclastic rock		71.91	0.43	13.68	3.50	0.05	1.38	1.25	1.63	3.12	0.12	3.02	100.09	10	61	51	0.01

Appendix 1 Whole Rock Geochemical Data Wt 16 and Wt22

Hole-depth	Rb/Sr	S	Sc	V	Cr	Ni	Cu	Zn	As	Rb	Sr	Zr	Nb	Y	Ba	La	Ce	Nd	Pb	Bi	Th
WT22-100	0.02	1.27	26	119	3	2	37	133	26	5	292	107	7	24	124	11	24	16	12	<2	3
WT22-109	0.14	3.49	20	93	2	<1	27	203	18	23	166	89	5	21	463	9	21	14	17	<2	<1.5
WT22-122	0.46	7.47	36	240	8	4	56	313	67	40	86	96	5	26	699	8	21	11	17	<2	2
WT22-132	0.38	6.88	33	196	6	4	32	420	30	38	98	86	5	27	551	12	31	18	171	<2	2
WT22-148	0.16	7.65	35	234	7	3	73	2200	66	29	178	91	5	26	661	12	31	18	95	<2	2
WT22-163	0.15	7.87	37	230	7	5	43	470	30	16	106	93	5	23	377	15	30	19	23	<2	2
WT22-176	0.20	7.61	42	288	10	4	286	317	24	25	128	114	7	27	290	11	27	14	21	<2	3
WT22-190	0.33	5.67	41	288	10	5	27	34	46	45	138	103	6	39	563	16	36	20	21	<2	3
WT22-208	0.18	6.02	32	222	18	6	67	576	32	29	158	77	5	19	701	16	36	20	186	<2	2
WT22-222	0.63	4.65	24	110	5	1	24	753	15	47	75	117	8	17	521	9	23	10	145	<2	6
WT22-237	1.50	5.54	32	205	4	2	41	347	22	69	46	97	5	17	820	9	22	10	149	<2	4
WT22-256	2.25	6.33	37	232	4	4	53	441	27	106	47	114	6	21	834	12	28	14	95	<2	5
WT22-277	1.43	5.14	20	139	30	8	49	70	40	61	43	71	4	7	672	5	17	9	25	<2	5
WT22-286	0.57	11.68	37	144	3	3	418	234	377	133	234	223	12	18	[10400]	13	53	4	846	<2	6
WT22-295	0.08	4.72	22	86	1	3	22	265	53	78	961	148	9	16	[18400]	n.m.	n.m.	n.m.	71	<2	<1.5
WT22-302	0.11	0.01	21	85	3	2	22	218	8	26	241	128	8	27	1085	24	48	20	9	<2	5
WT22-307	0.08	2.74	18	47	4	2	15	186	10	17	207	110	6	20	380	14	32	16	29	<2	4
WT22-314	0.08	0.01	19	73	4	1	2	188	4	19	221	119	7	18	349	19	39	19	11	<2	6
WT22-322	0.06	0.01	21	64	3	2	3	109	5	12	194	127	8	22	113	18	36	18	8	<2	7
WT22-329	0.97	0.01	21	87	9	9	12	101	4	179	184	190	11	23	1903	17	44	19	5	<2	9
WT22-332	1.42	0.06	15	84	77	30	14	188	<3	115	81	213	17	35	856	36	80	34	5	<2	20
WT16-87	0.01	0.01	29	253	16	13	79	90	6	3	325	69	4	13	146	9	17	10	7	<2	3
WT16-112	0.01	2.39	29	257	15	11	76	72	5	3	288	64	3	15	118	9	18	10	9	<2	3
WT16-125	0.32	6.45	34	291	14	7	33	32	6	56	173	75	5	19	622	7	22	12	9	<2	3
WT16-145	0.06	2.35	26	220	26	11	114	117	9	7	116	54	3	15	102	6	18	11	8	<2	<1.5
WT16-161	0.10	5.80	32	278	34	12	101	356	7	17	167	59	3	15	228	6	18	11	15	<2	2
WT16-170	0.23	8.44	47	311	64	15	45	29	7	47	206	72	5	19	384	8	22	11	15	<2	3
WT16-186	0.02	0.10	29	290	14	11	69	109	4	9	349	65	4	14	248	7	18	9	8	<2	2
WT16-195	0.02	0.36	28	268	17	14	118	86	5	11	594	71	4	15	170	7	19	10	8	<2	1
WT16-206	0.02	0.09	30	255	18	14	115	94	8	12	687	73	4	14	236	8	18	10	7	<2	3
WT16-210	0.00	0.05	30	188	2	2	78	116	4	1	342	98	6	25	31	12	25	17	4	<2	2
WT16-223	0.01	0.94	27	215	9	6	61	112	3	3	259	72	5	17	43	8	19	10	12	<2	3
WT16-245	0.03	5.42	12	178	2	2	26	4	6	6	188	95	5	3	268	12	27	12	10	<2	3
WT16-257	0.33	3.74	32	187	3	2	19	9	8	60	183	169	10	17	837	21	48	26	8	<2	4
WT16-276	0.80	3.62	9	82	5	3	32	4	7	58	73	89	5	3	562	5	13	4	13	<2	<1.5
WT16-292	0.97	5.60	11	74	3	3	47	4	15	43	44	69	4	5	369	4	15	7	9	<2	<1.5
WT16-322	0.16	3.69	21	82	4	1	31	25	18	32	203	88	5	11	923	10	26	9	36	<2	2
WT16-333	0.14	0.10	11	53	6	2	3	71	4	59	430	79	6	13	778	10	31	10	11	<2	4
WT16-338	0.09	0.01	10	46	5	2	4	54	<3	22	262	63	4	11	196	10	22	10	6	<2	3
WT16-343	0.13	0.02	11	47	5	2	7	97	<3	47	352	69	4	12	309	11	27	12	6	<2	4
WT16-349	1.06	0.02	11	49	45	12	21	71	3	123	116	176	15	33	626	36	74	29	5	<2	17
WT16-355	1.43	0.01	12	37	33	13	18	73	<3	121	84	246	14	34	752	27	64	27	3	<2	16

## References

- Allen R.L., 1988. False pyroclastic textures in altered silicic lavas, with implications for volcanic-associated mineralization. *Econ. Geol.*, 83: 1424-1446.
- Allen R.L., 1994. Syn-volcanic, subseafloor replacement model for Rosebery and other massive sulfide ores. In: Cooke D.R. and Kitto P.A., *Contentious issues in Tasmania Geology*, Geol. Soc. Aust. Abstracts, 39: 107-108.
- Allen R.L. and Cas R.A.F., 1990. The Rosebery controversy: distinguishing prospective submarine ignimbrite-like units from true subaerial ignimbrites in the Rosebery-Hercules ZnCuPb massive sulphide district, Tasmania. *Geological Society of Australia, Abstracts*, 25: 31-32.
- Allen R.L. and Hunns S.R., 1990. Excursion Guide E1. The Mount Read Volcanics and related ore deposits. 10th Aust. Geol. Conv., Hobart, 15-27.
- Allen R.L., Weihed P. and Svenson S.Å., 1996b. Setting of Zn-Cu-Au-Ag massive sulfide deposits in the evolution and facies architecture of a 1.9 Ga Marine Volcanic Arc, Skellefte District, Sweden. *Econ. Geol.*, 91: 1022-1053.
- Beams S.D. and Dronseika E.V., 1995. The exploration history, geology and geochemistry of the polymetallic Reward and Highway deposits, Mt Windsor Subprovince. 17th International Geochemical Exploration Symposium. Mineral deposits of northeast Queensland: Geology and geophysics, Townsville, Queensland, Abstracts, 137-153.
- Berry R.F., 1989. Structure of the Mount Windsor Sub-province. CODES, University of Tasmania, [unpub.] Report 1: 51-73.
- Berry R.F., 1991 Structure of the Mount Windsor Sub-Province. In: Pongratz, J. and Large, R. (eds.) *Geological controls on VMS mineralisation in the Mt Windsor Volcanic Belt*. [unpub.] CODES, University of Tasmania, Australia: 1-22.
- Berry R.F., Huston D.L., Stolz A.J., Hill A.P., Beams S.D., Kuronen U. and Taube A., 1992. Stratigraphy, structure, and volcanic-hosted mineralisation of the Mount Windsor Subprovince, north Queensland, Australia. *Econ. Geol.*, 87: 739-763.
- Bodon S.B. and Valenta R.K., 1995. Primary and tectonic features of the Currawong Zn-Cu-Pb(-Au) massive sulfide deposit, Benambra, Victoria: Implications for ore genesis. *Econ. Geol.*, 90: 1694-1721.
- Brooks E.R., 1995. Palaeozoic fluidisation, folding, and peperite formation, northern Sierra Nevada, California. *Can. J. Earth Sci.*, 32: 314-324.
- Burne R.V. and Moore L.S., 1987. Microbialites: Organosedimentary deposits of benthic microbial communities. *PALAIOS*, 2: 241-254.
- Busby-Spera C.J. and White J.D.L., 1987. Variation in peperite textures associated with differing host-sediment properties. *Bull. Volc.*, 49: 765-775.
- Cas R.A.F. and Wright J.V., 1991. Subaqueous pyroclastic flows and ignimbrites: an assessment. *Bull. Volc.*, 53: 357-380.

- Davidson, G.J., 1998. Application of silica iron deposit geochemistry to exploration for VHMS deposits in the Mt Windsor Volcanic Belt. AMIRA/ARC P439 Report 6 (in prep.)
- De Rosen-Spence A.F., Provost G., Dimroth E., Gochnauer K. and Owen V., 1980. Archean subaqueous felsic flows, Rouyn-Noranda, Quebec, Canada and their Quaternary equivalents. *Precambrian Res.*, 12: 43-77.
- Demico R.V. and Hardie L.A., 1994. Sedimentary structures and early diagenetic features of shallow marine carbonate deposits. *SEPM Atlas Series*, 365 pp.
- Dimroth E., Cousineau P., Leduc M. and Sanschagrin Y., 1978. Structure and organisation of Archean basalt flows, Rouyn-Noranda area, Quebec, Canada. *Can. J. Earth Sci.*, 15: 902-918.
- Doyle M.G., 1994. Facies architecture of a submarine volcanic centre: Highway-Reward, Mount Windsor Volcanics, Cambro-Ordovician, Northern Queensland. In: Henderson, R. A. and Davis, B. K. (eds.) *New developments in geology and metallogeny: Northern Tasman Orogenic Zone*. EGRU Contribution, 50: 149-150.
- Doyle M.G., 1996. Volcanic influences in the formation of iron oxide-silica deposits in a volcanogenic-massive sulfide terrain, Mount Windsor Volcanic belt, Queensland. Australian Mineral Industries Research Association Limited - P439. 87-142.
- Doyle MG, 1997a. Alteration associated with sub-seafloor replacement style massive sulfide deposits: evidence from the Cambro-Ordovician Highway-Reward deposit, Mount Windsor Subprovince. AMIRA - P439, Studies of VHMS-related alteration: geochemical and mineralogical vectors to ore. Report 4: 231-257.
- Doyle MG, 1997b. A Cambro-Ordovician volcanic succession hosting massive sulfide mineralisation: Mount Windsor Subprovince, Queensland. [unpub. Ph.D thesis]. University of Tasmania, 264 pp.
- Doyle MG 1998b. The Ordovician Highway-Reward sub-seafloor replacement deposit, Mount Windsor Subprovince, Queensland. AMIRA - P439, Studies of VHMS-related alteration: geochemical and mineralogical vectors to ore. Report 6.
- Duffield W.A and Dalrymple G.B., 1990. The Taylor Creek Rhyolite of New Mexico: a rapidly emplaced field of lava domes and flows. *Bull. Volc.*, 52: 475-487.
- Fink J.H and Manley C.R., 1987. Origin of pumiceous and glassy textures in rhyolite flows and domes. *Geol. Soc. Am. Spec. Pap.*, 212: 77-88.
- Fisher R.V. and Schmincke H.U., 1984. *Pyroclastic rocks*. Springer-Verlag, Berlin, 472 pp.
- Frey R.W. and Pemberton S.G., 1984. Trace fossil models. In: Walker, R. G. (ed.) *Facies models*. Geoscience Canada, Toronto, 189-207 pp.
- Furnes H., Fridleifsson I.B. and Atkins F.B., 1980. Subglacial volcanics - on the formation of acid hyaloclastites. *J. Volcanol. Geotherm. Res.*, 8: 95-110.

- Galley A.G., Bailes A.H. and Kitzler G., 1993. Geological setting and hydrothermal evolution of the Chisel Lake and North Chisel Zn-Pb-Cu-Ag-Au- massive sulfide deposits, Snow Lake, Manitoba. *Explor. Mining. Geol.*, 2: 271-295.
- Galley A.G., Watkinson D.H., Jonasson I.R. and Riverin G., 1995. The subsea-floor formation of volcanic-hosted massive sulfide: Evidence from the Ansil deposit, Rouyn-Noranda, Canada. *Econ. Geol.*, 90: 2006-2017.
- Goldfarb M.S., Converse D.R., Holland H.D. and Edmond J.M., 1983. The genesis of hot spring deposits on the East Pacific Rise, 21°N. *Econ. Geol. Mon.*, 5: 184-197.
- Gregory P.W., Hartley J.S. and Wills K.J.A., 1990. Thalanga zinc-lead-copper-silver deposit. In: Hughes, F. E. (ed.) *Geology of the mineral deposits of Australia and Papua New Guinea*. Aust. Inst. Mining and Metall. Mono., 14: 1527-1537.
- Hanson R.E. and Wilson T.J., 1993. Large-scale rhyolite peperites (Jurassic, southern Chile). *J. Volcanol. Geotherm. Res.*, 54: 247-264.
- Hartley J.S., Peters S.G. and Beams S.D., 1989. Current developments in Charters Towers geology and gold mineralisation. *North Queensland Gold '89 Proceedings*, Townsville, Queensland, 7-14.
- Haymon R.M., Koski R.A. and Sinclair C., 1984. Fossils of hydrothermal vent worms from Cretaceous sulfide ores of the Samail ophiolite, Oman. *Science*, 223: 1407-1409.
- Haymon R.M., Fornari D.J., Von Damm K.L., Lilley M.D., Perfit M.R., Edmond J.M., III W.C.S., Lutz R.A., Grebmeier J.M., Carbotte S., Wright D., McLaughlin E., Smith M., Beedle N. and Olson E., 1993. Volcanic eruption of the mid-ocean ridge along the East Pacific Rise crest at 9°45-52'N: Direct submersible observations of seafloor phenomena associated with an eruption event in April, 1991. *Earth and Planetary Science Letters*, 119: 85-101.
- Hekinian R., Francheteau J., Renard V., Ballard R.D., Choukroune P., Cheminee J.L., Albarede F., Minster J.F., Charlou J.L., Marty J.C. and Boulegue J., 1983. Intense hydrothermal activity at the axis of the East Pacific Rise near 13°N: submersible witnesses the growth of sulfide chimney. *Marine Geophysical Researches*, 6: 1-14.
- Henderson R.A., 1980. Structural outline and summary geological history for northeastern Australia. In: Henserson, R. A. and Stephenson, P. J. (eds.) *The geology and geophysics of northeastern Australia*. Geol. Soc. Aust., Queensland division: 1-27.
- Henderson R.A., 1983. Early Ordovician faunas from the Mount Windsor Subprovince, northeastern Queensland. *Memoirs Association Australasian Palaeontologists*, 1: 145-175.
- Henderson R.A., 1986. Geology of the Mt Windsor Subprovince-a Lower Proterozoic volcano-sedimentary terrane in the northern Tasman Orogenic Zone. *Aust. J. Earth Sci.*, 33: 343-364.

- Herrmann, W., 1994, Immobile element geochemistry of altered Volcanics and Exhalites at the Thalanga Deposit, North Queensland: M. Econ. Geol. thesis, University of Tasmania.
- Herrmann, W., 1995, Geochemical aspects of the Thalanga massive sulphide deposit, Mt Windsor Subprovince: 17. International Geochemical Exploration Symposium. Mineral Deposits of Northeast Queensland: Geology and Geochemistry, Townsville, Australia, 1995.
- Hill A.P., 1996. Structure, volcanic setting, hydrothermal alteration and genesis of the Thalanga massive sulfide deposit [Ph.D]. University of Tasmania, 404 pp.
- Humphris S.E., Herzig P.M., Miller D.J., Alt J.C., Becker K., Brown D., Brüggmann G., Chiba H., Foquet Y., Gemmell J.B., Guerin G., Hannington M.D., Holm N.G., Honnorez J.J., Iturrino G.J., Knott R., Ludwig R., Nakamura K., Petersen S., Reysenbach A.-L., Rona P.A., Smith S., Sturz A.A., Tivey M.K. and Zhao X., 1995. The internal structure of an active sea-floor massive sulphide deposit. *Nature*, 377: 713-716.
- Huston D.L., 1991 Metal zonation and mineralogy of the Waterloo and Agincourt prospects. CODES, University of Tasmania, Mount Windsor Project Research Report, 2: 109-144
- Huston D.L., 1992. Geological and geochemical controls on mineralisation at the Reward deposit: detailed studies of the Highway pipe. [unpub.] CODES, University of Tasmania. 31 pp.
- Huston D.L. and Large R.L., 1987. Genetic and exploration significance of the zinc ratio ( $100\text{Zn}/(\text{Zn}+\text{Pb})$ ) in massive sulfide systems: *Econ. Geol.*, 82: 1521-1539.
- Huston D.L., Taylor T., Fabray J. and Patterson D.J., 1992. A comparison of the geology and mineralisation of the Balcooma and Dry River South volcanic-hosted massive sulfide deposits, northern Queensland. *Econ. Geol.*, 87: 785-811.
- Huston D.L., Kuronen U. and Stolz J., 1995. Waterloo and Arincourt prospects, northern Queensland: contrasting styles of mineralisation within the same volcanogenic hydrothermal system. *Aust. J. Earth Sci.*, 42: 203-221.
- Hutton L.J., Hartley J.S. and Riekins I.P., 1993. Geology of the Charters Towers region. In: Henderson, R. A. (ed.) Guide to the economic geology of the Charters Towers region, northeastern Queensland. *Geol. Soc. Aust., Queensland division*, 1-12.
- Jack D.J., 1989. Hellyer host rock alteration [Unpub. M.Sc. thesis]. University of Tasmania, 182 pp.
- Jones J.G., 1969. Pillow lavas as depth indicators. *Am. J. Sci.*, 267: 181-195.
- Khin Zaw and Large R.R., 1992. The precious metal-rich South Hercules mineralisation, western Tasmania: A possible subsea-floor replacement volcanic-hosted massive sulfide deposit. *Econ. Geol.*, 87: 931-952.
- Kokelaar B.P., 1982. Fluidization of wet sediments during emplacement and cooling of various igneous bodies. *J. Geol. Soc. London*, 139: 21-33.

- 
- Kurokawa A., 1992. Felsic pumiceous hyaloclastite in central Japan. 29th International Geological Congress, Kyoto, Japan, Abstracts: 499.
- Kuronen U., 1989. Report on drilling at Waterloo (ATP 3798M-Balfes Creek) and Agincourt (ATP4066M-Dione) prospects during 15.11.1998-15.7.1989: Unpub. Pancontinental Mining Ltd. Report 89/44.
- Laing W.P., 1988. Structure of the Reward deposit, north Queensland. Unpublished report to Terra Search Pty. Ltd.
- Large R.R., 1991. Ore deposit models and exploration criteria for VMS deposits in the Mt Windsor Volcanics. In: Pongratz, J. P. and Large, R. R. (eds.) Geological controls on VMS mineralisation in the Mt Windsor Volcanic Belt-research report No. 2 [unpub.], 181-198.
- Large R.R., 1992. Australian volcanic-hosted massive sulfide deposits: features, styles, and genetic models. *Econ. Geol.*, 87: 471-510.
- Large R.R. and Both R.A., 1980. The volcanogenic ores at Mount Chalmers, eastern Queensland. *Econ. Geol.*, 75: 992-1009.
- Large R.R., McGoldrick P.J., Berry R.F. and Young C.H., 1988. A tightly folded, gold-rich, massive sulfide deposit: Que River mine, Tasmania. *Econ. Geol.*, 83: 681-693.
- Letouzey J. and Kimura M., 1985. Okinawa Trough genesis: Structure and evolution of a back-arc basin developed in a continent. *Marine and Petroleum Geology*, 2: 111-130.
- Levingston K.R., 1972. Ore deposits and mines of the Charters Towers 1:25,000 Sheet area, north Queensland. *Rep. Geol. Surv. Qld.*, 57.
- Logan B.W., Rezak R. and Ginsburg R.N., 1964. Classification and environmental significance of algal stromatolites. *J. Geol.*, 72: 68-83.
- Lydon J.W., 1988b. Volcanogenic massive sulfide deposits part 2: genetic models. In: Roberts, R. G. and Sheahan, P. A. (eds.) Ore deposit models. Geoscience Canada, Reprint series 3: 155-181.
- McBirney A.R., 1963. Factors governing the nature of submarine volcanism. *Bull. Volc.*, 26: 455-469.
- McPhie J. and Allen R.L., 1992. Facies architecture of mineralised submarine volcanic sequences: Cambrian Mount Read Volcanics, western Tasmania. *Econ. Geol.*, 87: 587-596.
- McPhie J., Doyle M.G. and Allen R.L., 1993. Volcanic Textures. CODES, University of Tasmania, Hobart, 198 pp.
- Miller C.R., 1996. Geological and geochemical aspects of the Liontown VHMS deposit, NE Queensland [M. Econ. Geol.]. University of Tasmania, 90 pp.
- Murray C.G., 1986. Metallogeny and tectonic development of the Tasman Fold Belt System in Queensland. *Ore Geology Reviews*, 1: 315-400.



- Murray C.G., 1990. Tasman Fold Belt in Queensland. In: Hughes, F. E. (ed.) *Geology of the mineral deposits of Australia and Papua New Guinea*. The Australasian Institute of Mining and Metallurgy. Monograph, 14: 1431-1450.
- Nishimura A. and Murakami F., 1988. Sedimentation of the Sumisu Rift, Izu-Ogasawara Arc. *Bull. Geol. Surv. Japan*, 39: 39-61.
- Ohmoto H. and Skinner B.J., 1983. The Kuroko and related volcanogenic massive sulfide deposits: introduction and summary of new findings. *Econ. Geol. Mon.*, 5: 1-8.
- Oudin E. and Constantinou G., 1984. Black smoker chimney fragments in Cyprus sulphide deposits. *Nature*, 308: 349-353.
- Paulick, H., 1998, Alteration halo of the Thalanga VHMS deposit, north Queensland. AMIRA/ARC P439 Report 6 (in prep.)
- Perkins, C., 1993, Isotopic dating of precious and base metal deposits and their host rocks in Eastern Australia, AMIRA, project P334.
- Perkins C., McDougall I. and Walshe J.L., 1993. Isotopic dating of precious and base metal deposits and their host rocks in eastern Australia. [unpub.] AMIRA project P334.
- Pichler H., 1965. Acid hyaloclastites. *Bull. Volc.*, 28: 293-310.
- Rona P.A., Hannington M.D., Raman C.V., Thompson G., Tivey M.K., Humphris S.E., Lalou C. and Petersen S., 1993. Active and relict sea-floor hydrothermal mineralisation at the TAG hydrothermal field, Mid-Atlantic Ridge. *Econ. Geol.*, 88: 1989-2017.
- Ross C.S. and Smith R.L., 1955. Water and other volatiles in volcanic glasses. *American Mineralogist*, 40: 1071-1089.
- Scott M.R., Scott R.B., Morse J.W., Betzer P.R., Butler L.W. and Rona P.A., 1978. Metal-enriched sediments from the TAG hydrothermal field. *Nature*, 276: 811-813.
- Scott S.D., 1992. Polymetallic sulfide riches from the deep: fact or fallacy? In: Hsü, K. J. and Thiede, J. (ed.) *Use and missuse of the seafloor*. John Willey & Sons Ltd., New York, 87-115.
- Stolz A.J., 1989. Stratigraphic relationships and geochemistry of the Mount Windsor Volcanics. Mount Windsor Project-Research Report No. 1 [unpub.]. Centre for Ore Deposit and Exploration Studies, University of Tasmania, 1-50.
- Stolz A.J., 1991. Stratigraphy and geochemistry of the Mt Windsor Volcanics and associated exhalites. In: Pongratz, J. and Large, R. (eds.) *Geological controls on VMS mineralisation in the Mt Windsor Volcanic Belt-Research* [unpub.] Report No. 2. Centre for Ore Deposit and Exploration Studies, University of Tasmania, 23-83.

- 
- Stolz A.J., 1994. Geochemistry and Nd isotope character of the Mt Windsor Volcanics: implications for the tectonic setting of Cambro-Ordovician VHMS mineralisation. In: Henderson R.A. and Davis B.K. (eds.) *New developments in geology and metallogeny: Northern Tasman Orogenic Zone*, Townsville, Queensland: 13-16.
- Stolz A.J., 1995. Geochemistry of the Mount Windsor Volcanics: Implications for the Tectonic setting of the Cambro-Ordovician volcanic-hosted massive sulfide mineralisation in Northeastern Australia. *Econ. Geol.*, 90: 1080-1097.
- Taylor B., Klaus A., Brown G.R. and Moore G.F., 1991. Structural development of Sumisu Rift, Izu-Bonin arc. *J. Geophys. Res.*, 96, B10: 16113-16129.
- Van Eck M., 1994. The geology and lithogeochemistry of the Lower Palaeozoic Seventy Mile Range Group at Mt Farrenden, Charters Towers, North Queensland, Australia. [M. Econ. Geol.]. University of Tasmania, 41 pp.
- Waters J.C. and Wallace D.B., 1992. Volcanology and sedimentology of the host succession to the Hellyer and Que River volcanic-hosted massive sulfide deposits, northwestern Tasmania. *Econ. Geol.*, 87: 650-666.
- Wellman P., 1995. Tasman Orogenic System: A model for its subdivision and growth history based on gravity and magnetic anomalies. *Econ. Geol.*, 90: 1430-1442.
- Williams H. and McBirney A.R., 1979. *Volcanology*. Freeman, Cooper and Company, San Francisco, 397 pp.
- Withnall I.W., Black L.P. and Harvey K.J., 1991. Geology and geochronology of the Balcooma area: part of an early Palaeozoic magmatic belt in north Queensland. *Aust. J. Earth Sci.*, 38: 15-29.
- Wyatt D.H., Paine A.G.L, Clarke D.E., Gregory C.M. and Harding R.R., 1971. Geology of the Charters Towers 1:250,000 sheet area, Queensland. Bureau Mineral Resources, Geology and Geophysics Australia, Report 137.
- Yamagishi H., 1979. Classification and features of subaqueous volcanoclastic rocks of Neogene age in southwest Hokkaido. *Geol. Surv. Hokkaido Rep.*, 51: 1-20.
- Zierenberg R.A., Shanks III W.C., Seyfried Jr W.E., Koski R.A. and Strickler M.D., 1988. Mineralisation, alteration, and hydrothermal metamorphism of the ophiolite-hosted Turner-Albright sulfide deposit, southwestern Oregon. *J. Geophys. Res.*, 93, B5: 4657-4674.